PROPOSAL: VOLUME I

DARPA – PREEMPT (HR001118S0017)
LEAD ORGANIZATION: EcoHealth Alliance (Other Nonprofit)
OTHER TEAM MEMBERS:
Duke NUS Medical School (Other Educational)
University of North Carolina (Other Educational)
Wuhan Institute of Virology (Other Educational)
USGS National Wildlife Health Center (Other Nonprofit)
Palo Alto Research Center (Large Business)

Project DEFUSE: Defusing the Threat of Bat-borne Coronaviruses

Principal Investigator and Technical Point of Contact
Peter Daszak, Ph.D.
EcoHealth Alliance
460 West 34th Street, 17th Floor
New York, NY 10001
(p) 212-380-4474
(e) daszak@ecohealthalliance.org
(f) 212-380-4465

Administrative Point of Contact
Luke Hamel
EcoHealth Alliance
460 West 34th Street, 17th Floor
New York, NY 10001
(p) 646-868-4709
(e) hamel@ecohealthalliance.org
(f) 212-380-4465

Identifying Number: HR001118S0017-PREEMPT-PA-001
Award Instrument Requested: Grant
Places and Periods of Performance: 12/1/18 - 5/31/22; Palo Alto, CA; Kunming and Wuhan, China; Chapel Hill, NC; New York, NY; Singapore; Madison, WI
Total funds requested: $14,209,245
Proposal validity period: 6 months
Date proposal submitted: 3/27/18

24 March 2018

Dear Committee for DARPA PREventing EMerging Pathogenic Threats (PREEMPT),

Please accept the following proposal to the PREventing EMerging Pathogenic Threats (PREEMPT, HR001118S0017) program. The PI for this project is:

Dr. Peter Daszak
President, EcoHealth Alliance
460 W. 34th Street, 17th Floor
New York, NY 10001
212-380-4474
daszak@ecohealthalliance.org

Title: Project Defuse: Defusing the Threat of Bat-Borne Coronaviruses

Amount of the Requested Proposal: $14,209,245

Thank you for your time, and I look forward to hearing from you. If you have any questions, do not hesitate to call or email me.

Yours sincerely,

Aleksei Chmura
Chief of Staff, EcoHealth Alliance
460 W. 34th Street, 17th Floor
New York, NY 10001
212-380-4473
chmura@ecohealthalliance.org

**Local conservation.
Global health.**

EcoHealth Alliance
460 West 34th Street, 17th Floor
New York, NY 10001-2320
212.380.4460

EcoHealthAlliance.org

Section II   **A. EXECUTIVE SUMMARY**

<u>Technical Approach:</u> Our goal is to defuse the potential for spillover of novel bat-origin high-zoonotic risk SARS-related coronaviruses in Asia. **In TA1** we will intensively sample bats at our field sites where we have identified high spillover risk SARSr-CoVs. We will sequence their spike proteins, reverse engineer them to conduct binding assays, and insert them into bat SARSr-CoV (WIV1, SHC014) backbones (these use bat-SARSr-CoV backbones, not SARS-CoV, and are exempt from dual-use and gain of function concerns) to infect humanized mice and assess capacity to cause SARS-like disease. Our modeling team will use these data to build **machine-learning genotype-phenotype models** of viral evolution and spillover risk. We will uniquely validate these with serology from previously-collected human samples via LIPS assays that assess which spike proteins allow spillover into people. We will build **host-pathogen spatial models** to predict the bat species composition of caves across Southeast Asia, parameterized with a full inventory of host-virus distribution at our field test sites, three caves in Yunnan Province, China, and a series of unique global datasets on bat host-viral relationships. By the end of Y1, we will create a prototype app for the warfighter that identifies the likelihood of bats harboring dangerous viral pathogens at any site across Asia.

In TA2, we will evaluate two approaches to reduce SARSr-CoV shedding in cave bats: **(1) Broadscale immune boosting**, in which we will inoculate bats with immune modulators to upregulate their innate immune response and downregulate viral replication; **(2) Targeted immune boosting**, in which we will inoculate bats with novel chimeric polyvalent recombinant spike proteins plus the immune modulator to enhance innate immunity against specific, high-risk viruses. We will trial inoculum delivery methods on captive bats including a novel automated aerosolization system, transdermal nanoparticle application and edible adhesive gels. We will use stochastic simulation modeling informed by field and experimental data to characterize viral dynamics in our cave test sites, maximize timing, inoculation protocol, delivery method and efficacy of viral suppression. The most effective biologicals will be trialed in our test cave sites in Yunnan Province, with reduction in viral shedding as proof-of-concept.

<u>Management Approach:</u> Members of our collaborative group have worked together on bats and their viruses for over 15 years. The lead organization, EcoHealth Alliance, will oversee all work. EHA staff will develop models to evaluate the probability of specific SARS-related CoV spillover, and identify the most effective strategy for delivery of both immune boosting and immune targeting inocula. Specific work will be subcontracted to the following organizations:

- Prof. Baric, Univ. N. Carolina, will lead targeted immune boosting work, building on his two-decade track record of reverse-engineering CoV and other virus spike proteins.
- Prof. Wang, Duke-Natl. Univ. Singapore, will lead work on broadscale immune boosting, building on his group's pioneering work on bat immunity.
- Dr. Shi, Wuhan Institute of Virology will conduct viral testing on all collected samples, binding assays and some humanized mouse work.
- Dr. Rocke, USGS National Wildlife Health Center will optimize delivery of immune modulating biologicals, building on her vaccine delivery work in wildlife, including bats.
- Dr. Unidad, Palo Alto Research Center will lead development of novel delivery automated aerosolization mechanism for immune boosting molecules.

We are requesting $14,209,245 total funds for this project across 3.5 project years.

Section II   **C. GOALS AND IMPACT**

Overview: The overarching goals of DEFUSE are to:

- **Identify and model spillover risk** of novel SARS-related coronaviruses (SARSr-CoVs) in Asia.
- **Design and demonstrate proof-of-concept** that upregulating the naturally low innate immunity of bats (**broadscale immune boosting**) and targeting high risk SARSr-CoVs in particular (**targeted immune boosting**) will transiently reduce spillover risk.

Our strategy to reduce risk of viral emergence from bats will protect the warfighter within USPACOM, and will be scalable to other regions and viruses (Ebola, Henipaviruses, rabies).

Innovation and uniqueness:

Bats harbor more emerging zoonoses than any other group of mammals, are ubiquitous, abundant, and often overlooked. However, other than PPE, there is no available technology to reduce exposure risk to novel CoVs from bats, and no effective therapeutics or countermeasures. SARSr-CoVs are enzootic in Asian[1-3], African[4], and European bats[5,6] that roost in caves but forage widely at night, shedding virus in their feces and urine. We have now published direct evidence of spillover of novel SARSr-CoVs into people in Yunnan

Province, China, close to a cave complex where we have isolated strains that produce SARS-like disease in humanized mice but don't respond to antibody treatment or vaccination. These viruses are a clear-and-present danger to our military and to global health security because of their circulation and evolution in bats and periodic spillover into humans.

EcoHealth Alliance (EHA) leads the world in predictive models of viral emergence. We will use machine-learning models of spillover hotspots, host-pathogen spatial and genotype-phenotype mapping, and unique datasets to validate and refine hotspot risk maps of viral emergence. We have shown that dampened innate immunity in bats allows them to carry otherwise lethal viruses, likely as an adaptation to the physiologic stress of flight. We will design strategies like small molecule RIG-like receptor (RLR) or Toll-like receptor (TLR) agonists, to upregulate bat immunity, and suppress viral replication, thereby significantly reducing viral shedding and spillover (**broadscale immune boosting**). We will complement this by coupling agonist treatments with SARSr-CoV recombinant spike proteins to boost pre-existing adaptive immune response adult bats against specific, high-risk SARSr-CoVs (**targeted immune boosting**). We will design novel delivery and automated application methods, based on our previous work on wildlife vaccines, to reduce hazard during deployment.

Technical Area 1

Our strategy begins by a complete inventory of bats and their SARSr-CoVs at our intervention test site cave complex in Yunnan, China that harbors bats with high-risk SARSr-CoVs. We will collect data from three caves in that system (one is our intervention test site and two control sites) on: monthly bat abundance and diversity, viral prevalence and diversity, individual bat viral load and host physiological markers; genomic characterization of low- and high-risk SARSr-CoV strains among bat species, sexes, and age classes; satellite telemetry and mark-recapture data on bat home range and inter-cave movement; and monitoring of daily, weekly and seasonal changes in bat populations. We will use stochastic neural networks to build joint species distribution models (JSDM) to predict bat species composition of caves, and high-risk SARSr-CoV diversity across S. China, South and SE Asia. These will be parameterized with EHA's database of bat host-viral relationships and estimates of zoonotic viral richness per bat species[7]; biological inventory data on all bat caves in Southern China; the full SARSr-CoV inventory from our cave test sites in Yunnan; and species distribution data for all bats. We will test and validate viral diversity predictions using data from >10,000 previously collected bat samples from 6 Asian countries under our USAID-funded PREDICT project. We will produce a prototype app for the warfighter to identify the risk of bats harboring dangerous viruses at a site. **This 'spatial viral spillover risk' app** will be field-deployable and updated real-time with surveillance data, to ground-truth and fine-tune predictions.

To characterize spillover risk of SARSr-CoV quasispecies (QS), the Wuhan Institute of Virology team (WIV) will test bat fecal, oral, and blood samples for SARSr-CoVs by PCR. We will collect viral load data from fresh fecal pellets. SARSr-CoV spike proteins will be sequenced, viral recombination events identified, and isolates used to identify strains that can replicate in human cells. The Univ. N. Carolina (UNC) team will reverse-engineer spike proteins of a large sample of high- and low-risk viruses for further characterization. This will effectively freeze the QS we analyze at t=0. These QS_0 strain viral spike glycoproteins will be synthesized, and those binding to human cell receptor ACE2 will be inserted into SARSr-CoV backbones (non-DURC, non-GoF), and inoculated into humanized mice to assess capacity to cause SARS-like disease, efficacy of monoclonal therapies, the inhibitor GS-5734[8] or vaccines against SARS-CoV[8-12].

We will use these data to **build machine-learning genotype-to-phenotype Bayesian network models** of viral evolution and host jump risk. These will predict the capacity of QS_0 strains to infect human cells based on genetic traits and experimental assays above. Using data on diversity of spike proteins, recombinant CoVs, and flow of genes via bat movement and migration, we will estimate evolutionary rates, rates of recombination, and capacity to generate novel strains capable of human infection. Finally, virus-host relationship and bat home range data will be used to estimate spillover potential - extending models well beyond our field sites. We will **validate model predictions of host jump risk** by 1) conducting further spike
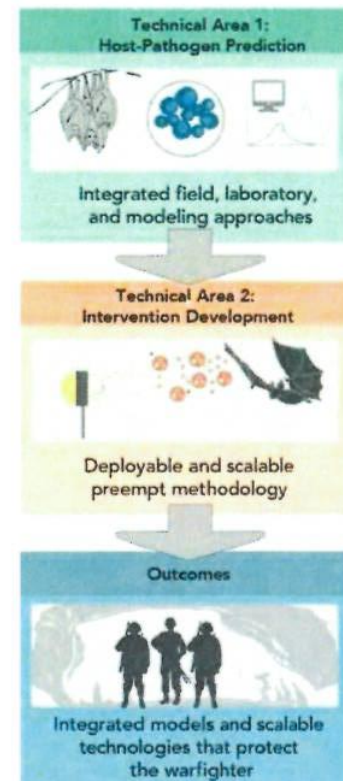
protein-based binding and cell culture experiments, and **2)** identifying whether designated high-risk SARSr-CoV strains have already spilled over into people near our bat cave sites. Our preliminary work shows ~3% seroprevalence to bat SARSr-CoVs in people at this site[13]. We will test these previously collected human sera (n>2000) <u>for presence of antibodies to the high- and low-risk SARSr-CoVs identified by our modeling</u>, using Luciferase immunoprecipitation system (LIPS) assays we design against the SARSr-CoVs identified in this project[14].

Technical Area 2
In TA2, we will **develop scalable approaches to suppress SARSr-CoVs within bat reservoir species, to reduce the likelihood of virus transmission into humans.** We will evaluate two approaches to defuse spillover potential: **1) Broadscale immune boosting:** we will apply immune modulators like bat interferon and TLR agonists to up-regulate bat innate immunity and suppress viral replication and shedding; **2) Targeted immune boosting:** we will apply polyvalent chimeric recombinant SARSr-CoV spike proteins in the presence of broadscale immune boosting treatments to boost immune memory and suppress specific SARSr-CoVs.

Both TA2 lines of work will run parallel beginning Yr 1. <u>Prof. Wang (Duke-Natl. Univ. Singapore – Duke-NUS) will lead the broadscale immune boosting work</u>, building on his pioneering work on bat immunity[15], including identifying weakened functionality of innate immunity factors like STING, a central DNA-interferon (IFN) sensing molecule, that may allow bats to maintain an effective, but not over-response to viruses[16], and IFNA, which is constitutively expressed without stimulation[17]. We will trial the following, concurrently and competitively, for efficacy and scalability: **i)** Activating TLR/RLR pathways to induce IFN induction, e.g. polyIC or 5'ppp-dsRNA. A similar strategy has been demonstrated in a mouse model for SARS-CoV[18,19]; **ii)** Universal bat interferon. Interferon has been used clinically in people, e.g. against filoviruses[20], and replication of SARSr-CoV is sensitive to interferon[21]; **iii)** Boosting bat IFN by blocking negative regulators. Bat IFNα is constitutively expressed but cannot be induced to a high level[17]. We will use CRISPRi to identify potential negative regulators and screen for compounds targeting this gene; **iv)** Activating dampened IFN production pathways via DNA-STING-dependent and ssRNA-TLR7-dependent pathways. Mutant bat STING restores antiviral functionality, suggesting these pathways are important in bat-viral coexistence[16]. We will directly activate the pathways downstream of STING/TLR7, to promote viral clearance; **v)** Inoculating crude CoV fragments to upregulate innate immune responses to specific CoVs – a partial step towards the targeted immune boosting work below.

<u>Prof. Baric (UNC) will lead the targeted immune boosting work.</u> We will develop recombinant chimeric spike-proteins[22] from known SARSr-CoVs, and those characterized by DEFUSE. Using details of SARS S protein structure and host cell binding[23] we will sequence, reconstruct and characterize spike trimers and receptor binding domains of SARSr-CoVs, incorporate them into nanoparticles or raccoon poxvirus-vectors for delivery to bats[10,24-27]. In combination with immune-boosting small molecules, we will use these to boost immune memory in adult bats previously exposed to SARSr-CoVs, taking the best candidate forward for field-testing. Recombinant S glycoprotein-based constructs with immunogenic blocks from across group 2B SARSr-CoVs should induce broadscale adaptive immune responses that reduce heterogeneous virus burdens in bats and transmission risk to people[28,29]. Innate immune damping is highly conserved in all bat species tested so far. We will use the unique Duke-NUS

Asian cave bat (*Eonycteris spelaea*) breeding colony to conduct initial proof-of-concept tests, extended to small groups of wild-caught *Rhinolophus sinicus* bats at WIV.

A novel delivery method for our immune boosting molecules will be developed and implemented by Dr. Rocke at the USGS National Wildlife Health Center (NWHC) who has previously developed animal vaccines through to licensure[30]. Using locally acquired insectivorous bats[31,32], we will assess delivery vehicles and methods including: 1) transdermally applied nanoparticles; 2) sticky edible gels that bats mutually groom and consume; 3) aerosolization via prototype sprayers (Dr. Unidad, PARC) designed for cave settings; and 4) automated sprays triggered by timers and movement detectors at critical cave entry points We have extensive preliminary data on these techniques for wildlife, including vaccinating bats against rabiesin the lab[31], successful delivery, consumption and spread in wild vampire bats. We will use the NWHC captive bat colony and wild bats in US caves to trial delivery vehicles using the biomarker rhodamine B (which fluorescently marks hair on consumption) to assess uptake. **The most optimal deployment approaches will be tested on wild bats at our test cave sites in Yunnan, using the most effective immune modulation preparations.** Bat populations from experimental and control caves will be surveyed longitudinally for viral load before and after deployment trials. EHA has had unique access to these sites for ~10 years. In DEFUSE Yr1, we will seek permission for experimental trials from collaborators at the Yunnan Forestry Department and Center for Disease Control, following our proven track record of rapidly obtaining IACUC and DoD ACURO approval for animal research. We will **model optimal strategies to maximize treatment efficacy** for TA2, using stochastic simulation modeling of viral circulation dynamics at our sites, informed by field and experimental data. We will estimate frequency and population coverage required for our intervention, and model the time period of viral suppression, until re-colonization or evolution leads to return of a high-risk SARSr-CoV.

Deliverables:
- Open source models and App identifying geographical and host-specific risk of spillover for novel SARSr-CoVs
- Experimentally validated genotype-phenotype models of spillover for viral strains.
- Proven technology to modulating bat innate immunity to reduce viral shedding
- Tested and validated delivery mechanism for bat cave usage including vaccines in other bat host-pathogen systems (e.g. rabies, WNS).
- Proof-of-concept approach to transiently reducing viral shedding in wild bats that can be adapted for other systems including Ebola virus.

Section II   **D. TECHNICAL PLAN**

Technical Area I:
Choice of site and model host-virus system. For the past 14 years, our team has conducted CoV surveillance in bat populations across S. China, resulting in >180 unique SARSr-CoVs in ~10,000 samples (>5% prevalence, including multiple individuals harboring the same viral strains)[2,21,33] and a per-bat species prevalence up to 10.9%. Bat SARSr-CoVs are genetically diverse, especially in the S gene, and most are highly divergent from SARS-CoV. However, our test cave site in Yunnan Province, harbors a quasispecies (QS) population assemblage that contains all the genetic components of epidemic SARS-CoV[34]. We have isolated three strains there (WIV1,

WIV16 and SHC014) that unlike other SARSr-CoVs, do not contain two deletions in the receptor-binding domain (RBD) of the spike, have far higher sequence identity to SARS-CoV (**Fig. 1**), use human ACE2 receptor for cell entry, as SARS-CoV does (**Fig. 2**), and replicate efficiently in various animal and human cells[2,3,33-35], including primary human lung airway cells, similar to epidemic SARS-CoV[11,12]. Chimeras (recombinants) with these SARSr-CoV S genes inserted into a SARS-CoV backbone, and synthetically reconstructed full length SHC014 and WIV1 cause SARS-like illness in humanized mice (mice expressing human ACE2), with clinical signs that are not reduced by SARS-CoV monoclonal antibody therapy or vaccination[11,12]. People living up to 6 kilometers from our test cave have SARSr-CoV antibodies (~3% seroprevalence)[13], suggesting active spillover. These data, phylogeography of SARSr-CoVs, and coevoutionary analysis of bats and their CoVs (unpubl.), suggest that bat caves in SW China, and *Rhinolophus* spp. bats are the likely origin of the SARS-CoV clade, and are a **clear-and-present danger for the emergence of a SARSr-CoV from the current QS**. The *Rhinolophus* spp. bats that harbor these viruses occur across Asia, Europe, and Africa. **Thus, while DEFUSE fieldwork will focus on high-risk sites in S. China, our approach to reduce the risk of these viruses spilling over is broadly applicable across four combatant command regions (PACOM, CENTCOM, EUCOM, AFRICOM).**
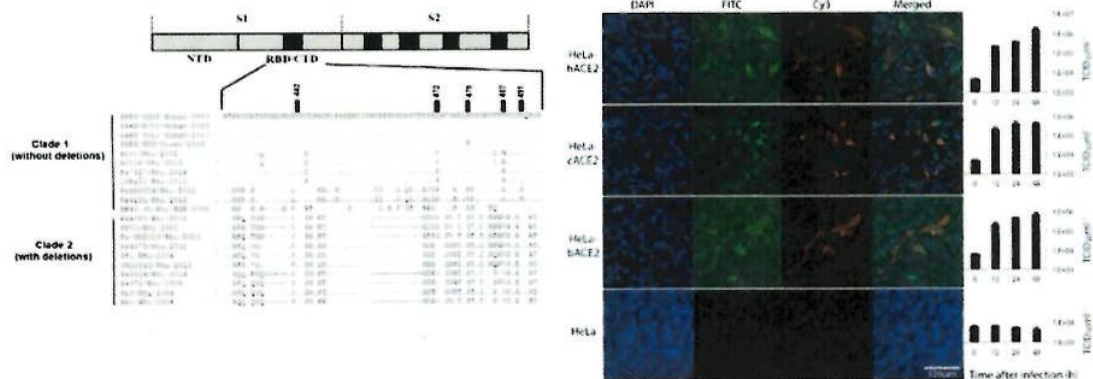

Fig. 1 (top left): Alignment of amino acid sequences of the spike protein receptor-binding motif of SARSr-CoVs and SARS-CoV[34]. Numbered amino acid residues are responsible for interaction with human ACE2[36]. Fig. 2 (top right): Bat SARSr-CoV WIV1 replicates efficiently in HeLa cells expressing human, civet and bat ACE2[2].

Full inventory of bat SARSr-CoV QS at our test cave sites, Yunnan, China. To provide data to train and validate our modeling, and as baseline for our immune modulation trial (TA2), DEFUSE fieldwork will target the high-risk cave site in Yunnan Province, SW China (**Fig. 4, red triangle**) where we will conduct our field trial, and where we have previously identified and isolated high-risk SARSr-CoVs[2,11,33,34]. At three cave sites (one designated for our trial, two as controls), we will determine the baseline QS_0 risk of SARSr-CoV spillover. We will conduct longitudinal surveillance of bat populations to detect and isolate SARSr-CoVs, determine changes in viral prevalence over time, and measure bat population demographics and movement, definitively characterizing their SARSr-CoV host-viral dynamics. Field data will allow us to test the accuracy of our model predictions and compare efficacy of lab animal models with field trials. Our preliminary data (**Table 1**) demonstrate that *R. sinicus*, *R. ferrumequinum*, and *R. affinis* (which co-roost at our test site) are primary reservoirs of SARSr-CoV and the only reservoirs of three high-risk strains (WIV1, WIV16, SHC014), with *Hipposideros* and *Myotis* spp. playing an

insignificant (<1% prevalence) role in viral dynamics. We will capture *Rhinolophus spp.* bats using harp traps and mist nets during evening flyout, collect rectal, oral, and whole blood samples (×2 per bat) using sterile technique to avoid cross-contamination, and take 2-mm wing tissue punch biopsies for host DNA bar-coding, host ACE2 receptor gene sequencing (interface site – 3 individuals per species), and cophylogeny analyses. Bats will be subcutaneously microchipped (PIT tag), and morphological and physiological data (age class, body weight, reproductive status etc.).

Species	n	SARSr-CoV prevalence
Rhinolophus sinicus	1036	10.9%
R. ferrumequinum	191	6.3%
R. affinius	518	1.2%

In Phase I we will **sample 60 bats each of** *R. sinicus, R. ferrumequinum,* and *R. affinis,* (**180** bats per cave) **every three months** non-destructively for **18 months** from our three cave sites. Given ~6-9% prevalence (n=3,304) of SARSr-CoVs in *Rhinolophus* spp. at our sites, this sample size would allow detection of 10% fluctuation in viral prevalence among sampling periods and caves. During the 2 months per quarter without physical bat trapping we will collect fresh fecal pellets by placing clean 2m^2 polyethylene sheets beneath roosting bats[37]. *Rhinolophus* spp. have a 7-week gestation period, spring birthing, and aggregate during mating periods. Our monthly sampling strategy will collect adequate data to parameterize stochastic simulation models, and cover two mating and gestation periods to assess life-history driven changes in viral prevalence and immune marker (e.g. interferon) levels. We will conduct **pre- and post-intervention sampling** (biweekly fecal pellet sampling for 4 months, and 10 male and 10 female bats per species tested every 2 weeks post-intervention for 4 months, prior to- and post-deployment) **to monitor SARSr-CoV QS and bat immune status changes in test and control site bats during Phase II (TA2)**. Immune status can be followed in individual bats due to the relatively small roost sizes in these caves and our individual marking of captured bats. We will be assess immune status using nanostring immune profiling panels validated during captive bat studies at Duke NUS. We will use infrared spotlights and digital infrared imaging to record the number and species of bats above each plastic sheet and fecal pellets will be genetically barcoded to confirm species identification[38]. Samples will be preserved in viral transport medium, immediately frozen in liquid nitrogen dry shippers, and transported to partner laboratories with maintained cold chain and under strict biosafety protocols. PIT tag readers and weatherproof thermal imaging IR cameras mounted at each cave entrance will passively monitor temporal roost site fidelity, rates of inter-cave movement, and daily fluctuation in bat population[39]. ICARUS satellite transmitters (1g) will be attached to 12 *Rhinolophus* spp. bats from each study roost (36 bats total) to determine nightly foraging dispersal patterns (https://icarusinitiative.org). Telemetry and PIT tag data will be used to calculate home range, degree of mixing among roosts, and parameterize dynamic models. **Study caves will be surveyed using portable LiDAR technology**[40-42], to give a 3-D image of roost

areas and data on species composition for targeting of immune modulation treatments in TA2 (**Fig. 3**). Sampling quotas will be adjusted based on lab and model results to optimize viral detection.
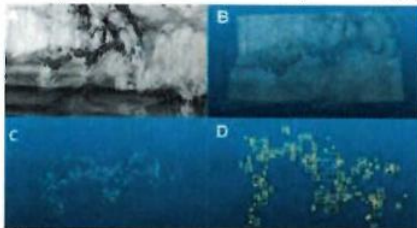
Fig. 3: Light Detection and Ranging (LiDAR) scanning to characterize caves and quantify number of individual bats roosting in clusters: A) LiDAR system takes a 360° omnidirectional photo of clustered bats, B)

photo converted to 3-D point cloud, C) non-bat points, based on laser return intensity removed, D) automated counting algorithm counts individual bats. Figure from[41].

Our team has more than 50 years collective experience in safe and humane handling of bats for biological sampling. This project will operate under appropriate IACUC/ACURO and PPE guidelines. EHA has several ongoing DTRA-supported projects, has obtained ACURO approval for animal research from the DoD, and currently maintains IACUC protocols through Tufts University (EHA staff are adjunct faculty), which we will use for DEFUSE IACUCs. IACUCs already approved for lab/field work at Duke-NUS, UNC, NWHC, and WIV, will be modified for DEFUSE.

Predictive models of high-risk sites and bat species across Asia. We will build models that predict bat and viral diversity and spillover risk across Asia to enable warfighters and planners to assess risk and necessity for intervention deployment (TA2). We will combine regional-scale joint species distribution models (JSDM), machine-learning host-virus association models, and non-parametric viral richness estimators to respectively predict the composition of bat communities in caves across Asia, host range for key viral clades, and as-of-yet unsampled viral diversity. We will use a stochastic feedforward neural network to implement JSDMs that are effective at multiple scales with incomplete observations (as occurs for bats and their viruses), and that account for bat species co-occurrence driven by environment or evolution[43]. We will fit our JSDM to biological inventory data on over 200 caves in the region[44], to physiologically relevant bioclimatic variables (BIOCLIM)[45], open source topographic data, and proxies for subterranean habitat such as ruggedness and habitat heterogeneity. As in previous work[46], we will refine these models with regional-scale environmental variables (land-use, distance to roads, etc.) and cave-specific variables (cave length, availability of roosting area, entrance dimensions, cave complexity etc.). We will validate them using independent bat occurrence estimates and observations[47,48], and use EHA's unique database of all known host-virus relationships[7] (**Fig. 4**). We will use generalized additive host trait predictive models and machine-learning algorithms (BRT, random forest)[49] with non-parametric estimators to predict SARSr-CoV diversity in the QS of each bat species[50], and assess viral discovery rates in real time through sampling (**Fig. 5**).
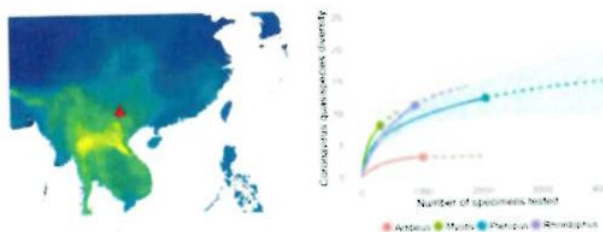

*Fig. 4: Predictive map of zoonotic viral diversity in bats for China and SE Asia (yellow=more viruses), based on all known mammal host-viral relationships[7]. Our Yunnan test cave site is labeled (red asterisk). **Fig. 5**: CoV QS diversity estimates (dashed line with 95% confidence intervals) based on PREDICT sampling data (solid line) for four bat genera.*

To extend the geographic scope of predictive models, we will include data from >1800 viral detections (CoVs and others) from >10,000 individual bat samples in 6 Asian countries (NIAID- and USAID PREDICT-funded). For species composition and viral presence predictions, we will validate models against a 20% validation subset of data, and field data.

Prototype app for the warfighter. Drawing on experience building applications for data collection and analysis for DoD (e.g. https://flirt.eha.io/, https://eidr-connect.eha.io/, https://mantle.io/grrs), we will produce a prototype 'spatial viral spillover risk' app for the

warfighter that identifies probability of dangerous viral pathogens spilling over from bats at a site. We will use outputs from our spatial risk modeling, observed and predicted host-viral associations, open-source species and pathogen ontologies, and app-directed crowd-sourced echolocation data to ground-truth and fine-tune its predictive capacity. This app will be updated in Y2 and Y3 to incorporate additional risk data from host-virus binding assays and SARSr-CoV surveys. We will use EHA's risk-ranking algorithms (https://ibis.eha.io/) to display critical areas of high risk based on geolocation features, recency of information, host and pathogen characteristics. The app will collect user GPS location data and preload bat species distribution and community composition estimates from our JSDMs. These will be refined with real-time surveillance data collected without the need to enter cave sites using mobile phone-enabled high-frequency microphones for bat detection[51], validated and trained with reference acoustic calls using convolutional neural networks[52]. Identified bat species will be automatically linked with viral diversity data from EHA's host-pathogen database and SARSr-CoV data from DEFUSE to deliver high-risk pathogen lists, displayed as pathogen-centric, bat-centric, or map-centric views, with proactive alerts when critical information is received. All code modules will be available and documented on GitHub (https://github.com/ecohealthalliance/). This technology will improve overall situational awareness of existing and novel infectious agents found in bats, allowing DoD personnel to quickly identify areas high spillover risk sites and rapidly deploy resources to respond to and mitigate their impact preemptively when necessary.

SARSr-CoV QS detection, sequencing, and recovery. We will screen samples for SARSr-CoV nucleic acid using our pan-CoV consensus one-step hemi-nested RT-PCR assay targeting a 440-nt fragment in the RNA-dependent RNA polymerase gene (RdRp) of all known α- and β-CoVs[1,53], and specific assays for known SARSr-CoVs[2,21,33,34]. PCR products will be gel purified, sequenced and qPCR performed on SARSr-CoV-positive samples to determine viral load. Full-length genomes or S genes of all SARSr-CoVs will be high-throughput sequenced followed by genome walking[2,3,34]. We will analyze the S gene for its ability to bind human ACE2 by Biocore or virus entry assay. *Synthesis of Chimeric Novel SARSr-CoV QS:* We will commercially synthesize SARSr-CoV S glycoprotein genes, designed for insertion into SHC014 or WIV16 molecular clone backbones (88% and 97% S-protein identity to epidemic SARS-Urbani). These are BSL-3, not select agents or subject to P3CO (they use bat SARSr-CoV backbones which are exempt) and are pathogenic to hACE2 transgenic mice. Different backbone strains increase recovery of viable viruses identification of barriers for RNA recombination-mediated gene transfer between strains[34]. Recombinant viruses will be recovered in Vero cells, or in mouse cells over-expressing human, bat or civet ACE2 receptors to support cultivation of viruses with a weaker RBD-human ACE2 interface. *Recovery of Full length SARSr-CoV:* We will compile sequence/RNAseq data from a panel of closely related strains (<5% nucleotide variation) and compare full length genomes, scanning for unique SNPs representing sequencing errors[54-56]. Consensus candidates genomes will be synthesized commercially (e.g. BioBasic), using established techniques and genome-length RNA and electroporation to recover recombinant viruses[28,57].

Predicting strain-specific SARSr-CoV spillover risk. We will <u>combine detailed experimental</u> <u>characterization of QS₀ at our test cave sites with state-of-</u> <u>the-art genotype-phenotype Bayesian network models.</u> This will enable us to predict the jump probability of future QS that emerge with unique genetic recombinations. Our models will be parameterized with experimental data from a series of assays on the S genes of bat SARSr-CoVs (**Fig. 6, right**), with experimental and modeling work flowing together in iterative steps. Our prior data will act as baseline to parameterize spillover risk modeling[11,12,29,58]. This will be supplemented by characterization of isolated viruses under DEFUSE (at WIV), **approximately 15-20 bat SARSr-CoV spike proteins/year** (at UNC, WIV), and >180 bat SARSr-CoV strains sequenced in our prior work and not yet examined for spillover potential. All experiments will be performed in triplicate <u>and data fed to models in real time</u>:


Predicting SARSr-CoV QS jump potential
Screen and isolate SARSr-CoV QS₀

Select QS₀ with human infection potential

% spike similarity

spike trimer structure   ACE2 interaction

Construct chimeric viruses

Evaluate expression in vitro and vivo

Input data for predictive modeling

Experimental assays of SARSr-CoV QS jump potential (Fig. 6, right). *Pre-screening via structural protein modeling,* *mutation identification, and pseudovirus assays:* Viral entry is the major species restriction preventing spillover of SARSr-CoVs[29,58]. To select QS for further characterization we will first use structural modeling of SARSr-CoV S protein binding to ACE2 receptors[59,60]. Mutations in the RBD[29,58,61,62], and host protease proteolytic processing of the S glycoprotein[63-65], regulate SARSr-CoV cell entry and cross-species infectivity. Mismatches in the S-RBD-ACE2 molecules or S proteolytic processing will prevent cell entry of SARS-CoV[29,58] and QS with these mismatches will be deprioritized. Single amino acid variations could dramatically alter these phenotypes and we will evaluate the impact of low abundant, high consequence micro-variation in the RBD using RNAseq to identify low abundant QS variants encoding mutations relevant to ACE2 binding. We will conduct *in vitro* pseudovirus binding assays, using established techniques[2], and live virus binding assays (at WIV to prevent delays and unnecessary dissemination of viral cultures) for isolated strains. Initial model predictions based on these data inputs will be used to guide strain selection for further characterization. *In vitro testing of* *chimeric viruses:* All chimeric viruses will be sequence verified and evaluated for: **i)** ACE2 receptor usage across species *in vitro,* **ii)** growth in primary HAE, **iii)** sensitivity to broadly cross neutralizing human monoclonal antibodies that recognize unique epitopes in the RBD[66,67]. Should some isolates prove highly resistant to our mAB panel, we will evaluate cross neutralization against a limited number of human SARS-CoV serum samples from the Toronto outbreak. Chimeric viruses that encode novel S genes with spillover potential will be used to identify SARSr-CoV strains for recovery as full genome length viable viruses. *In vivo* *pathogenesis:* Groups of 10 animals will be infected intranasally with 1.0 x 10⁴ PFU of each vSARSr-CoV, clinical signs (weight loss, respiratory function, mortality, etc.) followed for 6 days
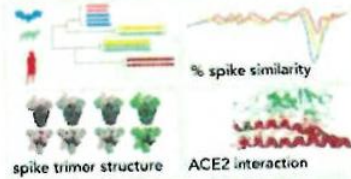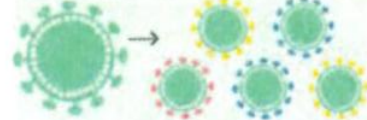
p.i., and sacrificed at day 2 or 6 p.i. for virologic analysis, histopathology and immunohistochemistry of the lung and for 22-parameter complete blood count (CBC) and bronchiolar alveolar lavage (BAL). *Validation with full-length genome QS:* We will validate results from chimeric viruses by re-characterizing full-length genome versions, testing whether backbone genome sequence alters full length SARSr-CoV spillover potential. QS for full-genome characterization will be selected to reflect strain differences in antigenicity, receptor usage, growth in human cells and pathogenesis. We will test growth in primary HAE cultures and *in vivo* in hACE2 transgenic mice. We anticipate recovering ~3-5 full length genome viruses/yr. *Testing Synthetic Modifications:* We will synthesize QS with novel combinations of mutations to determine the effects of specific genetic traits and the jump potential of future and unknown recombinants. *RBD deletions:* Small deletions at specific sites in the SARSr-CoV RBD alter risk of human infection. We will analyze the functional consequences of these RBD deletions on SARSr-CoV hACE2 receptor usage, growth in HAE cultures and *in vivo* pathogenesis. First, we will delete these regions, sequentially and in combination, in SHC014 and SARS-CoV Urbani, anticipating that the introduction of deletions will prevent virus growth in Vero cells and HAE[58]. In parallel, we will evaluate whether RBD deletion repair restores the ability of low risk strains to use human ACE2 and grow in human cells. *S2 Proteolytic Cleavage and Glycosylation Sites:* After receptor binding, a variety of cell surface or endosomal proteases[68-71] cleave the SARS-CoV S glycoprotein causing massive changes in S structure [72] and activating fusion-mediated entry[64,73]. We will analyze all SARSr-CoV S gene sequences for appropriately conserved proteolytic cleavage sites in S2 and for the presence of potential furin cleavage sites[74,75]. SARSr-CoV S with mismatches in proteolytic cleavage sites can be activated by exogenous trypsin or cathepsin L. Where clear mismatches occur, we will introduce appropriate human-specific cleavage sites and evaluate growth potential in Vero cells and HAE cultures. In SARS-CoV, we will ablate several of these sites based on pseudotyped particle studies and evaluate the impact of select SARSr-CoV S changes on virus replication and pathogenesis. We will also review deep sequence data for low abundant high risk SARSr-CoV that encode functional proteolytic cleavage sites, and if so, introduce these changes into the appropriate high abundant, low risk parental strain. *N-linked glycosylation:* Some glycosylation events regulate SARS-CoV particle binding DC-SIGN/L-SIGN, alternative receptors for SARS-CoV entry into macrophages or monocytes[76,77]. Mutations that introduced two new N-linked glycosylation sites may have been involved in the emergence of human SARS-CoV from civet and raccoon dogs[77]. While the sites are absent from civet and raccoon dog strains and clade 2 SARSr-CoV, they are present in WIV1, WIV16 and SHC014, supporting a potential role for these sites in host jumping. To evaluate this, we will sequentially introduce clade 2 disrupting residues of SARS-CoV and SHC014 and evaluate virus growth in Vero cells, nonpermissive cells ectopically expressing DC-SIGN, and in human monocytes and macrophages anticipating reduced virus growth efficiency. We will introduce the clade I mutations that result in N-linked glycosylation in rs4237 RBD deletion repaired strains, evaluating virus growth efficiency in HAE, Vero cells, or nonpermissive cells ± ectopic DC-SIGN expression[77]. *In vivo*, we will evaluate pathogenesis in transgenic hACE2 mice. *Low abundance micro-variations:* We will structurally model and identify highly variable residue changes in the SARSr-CoV S RBD, use commercial gene blocks to introduce these changes singly and in combination into the S glycoprotein gene of the low risk, parental strain and test ACE2 receptor usage, growth in HAE and *in vivo* pathogenesis.
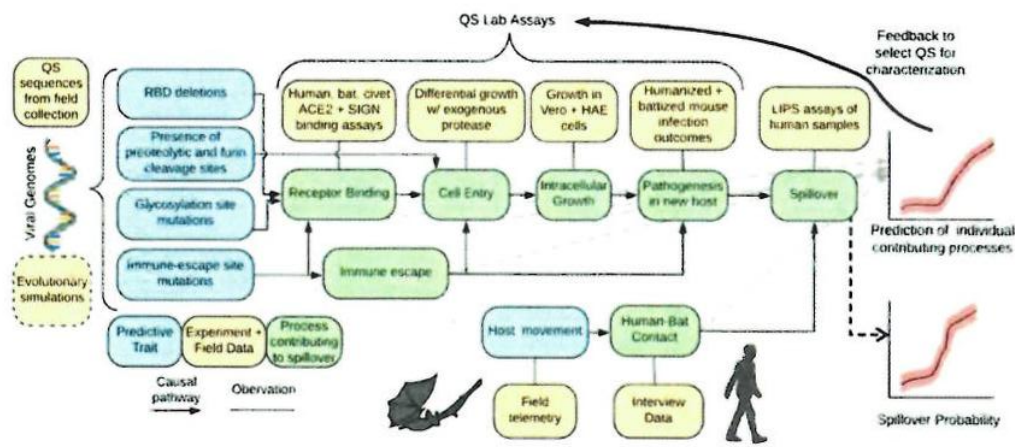
Fig. 7: *A simplified directed graph of a Bayesian network model representing the causal relationships between input data, modeled processes, and outputs.*

Network machine-learning to predict spillover potential of high-risk SARSr-CoV strains. We will use experimental data from above to **build genotype-phenotype models of bat SARSr-CoV spillover potential.** We will use Bayesian Network Models (BNM), fit via MCMC methods[78] to predict spillover risk based on bat SARSr-CoVs genotype data (presence of deletions in RBD, proteolytic binding and glycosylation sites etc.) and the ecological traits of hosts - integrating data on multiple, interacting processes and QS spillover potential to generate overall spillover probabilities. The Bayesian approach will allow us to update our models iteratively as new data is acquired, and use interim model predictions to guide which experiments to prioritize to maximize predictive ability[79]. We will control for experimental conditions (assays on live viral isolates, full-genome or synthetic chimeric viruses, and the molecular backbone of the latter). Traits will be used as inputs to BNM's causal graph, to predict latent variables representing interconnected processes that contribute to SARSr-CoV QS infection in new hosts : receptor binding, cell entry, immune system interaction, and intracellular growth, all measured by our lab assays. These, in turn will **act as predictors for the ultimate outcomes of host pathogenesis and host jumping potential (Fig. 7)**. We will use published work on these genetic traits to put informative priors on strength and direction of interactions in the causal graph. We will use **prior-knowledge model simulations to select target sequences from our sampling for characterization and genome-sequencing,** to collect data that maximally enhances the predictive power of our model, and update these simulations iteratively throughout the experimental phase to continually guide QS selection. We will use regularizing priors to reduce over-fitting and select the most predictive variables in the final model.

Model validation using SARSr-CoV serology from previously-collected human samples and surveillance data. Active spillover of SARSr-CoV in our study region enables us to measure actual spillover risk to validate our models of QS jump potential. We will gather data on viral QS antibodies found in the local human population using LIPS assays on >2,000 previously-collected human sera (NIAID, Daszak PI) from people living close to our test cave sites in Yunnan Province, a sub-sample of which showed 2.7% seropositivity to bat SARSr-CoVs[13]. The IRB for

this work is current and covers proposed DEFUSE testing. We will design LIPS assays targeting high- and low-spillover risk SARSr-CoV QS, as done previously for SARSr-CoVs[13,80,81] and the novel SADS-CoV[24]. We will: **1)** insert different high- and low-risk SARSr-CoV N genes into pREN-2 vector (LIPS vector), first assessing N gene similarity to determination their potential cross-reactivity in a LIPS assay; **2)** determine LIPS assay specificity by producing polyclonal sera via injection of recombinant protein or attenuated virus into rabbits; **3)** validate LIPS assays by incubating antigens with their respective positive serum samples and the antigen antibody complex eluted using protein A/G beads; **4)** validate LIPS positive sera results by spike protein based LIPS and viral neutralization assay. As a confirmatory test, the positive samples from LIPS will be validated by virus neutralization assay. We will use these LIPS assays to test serum samples for presence of antibodies to high- and low-risk SARSr-CoV QS. We will validate predictions of jump potential and extend the BNMs to predict actual spillover probabilities by modeling bat-human contact rates with bats. We will use ecological data on bat hosts and human behavioral survey data collected previously from these individuals to estimate wildlife contact in predicting exposure measured by our LIPS assays.

Evolutionary modeling and simulation to predict potential strains. Our Bayesian network modeling will generate predictions of the spillover risk of QS sequences we identify. To examine risk associated with the total viral population, we will model and simulate evolutionary processes **to identify likely viral QS that our sampling has not captured, and viral QS likely to arise in the future ("QS$_x$").** We will use a large dataset of S protein sequences and full-length genomes generated from prior work and DEFUSE fieldwork to estimate SARSr-CoV substitution rate and its genome-wide variation using coalescent and molecular clock models within a Bayesian MCMC framework[82]. We will estimate SARSr-CoV recombination rates at the cave population level using these data and Bayesian inference[83,84]. We will apply RDP[85], similarity plots, and bootscan to identify recombination breakpoints and hotspots within the SARSr-CoV genome as done previously[34], now extended to the full genome. Using these estimates we will simulate the evolution of the SARSr-CoV QS virome using a forward-time approach implemented in simulators that model specific RNA virus functions (e.g. VIRAPOPS[86]). We will predict the rate at which new combinations of genetic traits can spread in viral populations and compare recombination rates among caves and bat communities. Our forward-simulated results **will provide a pool of likely unknown and future QS$_x$ species.** Using these and our SEM model for spillover risk, **we will predict the QS$_x$ most likely to arise *and* have spillover and pathogenic potential.** We will use evolutionary simulation results to iteratively improve our Bayesian network model. The number of genetic traits with potential for prediction of pathogenicity is large, so we will perform variable reduction using tree-based clustering, treating highly co-occurring traits as joint clusters for prediction. We will generate these clusters from all SARSr-COV sequences from DEFUSE fieldwork and prior work. As trait clusters may be modified through recombination, we will use our forward-evolutionary modeling to predict how well trait clusters will be conserved, retaining only those unlikely to arise in unknown or QS$_x$ genomes. This will enable a trade-off between increased predictive power based on current samples and generalizability to future strains that have not yet evolved.

Technical Area 2

Immune modulation approach to reducing bat SARSr-CoV spillover risk. Our work shows that the following unique immunological features of bats may explain their capacity to harbor high viral loads with minimal clinical signs: a) bats maintain constitutively high expression of IFNα that may respond to and restrict viral infection[17]; b) several interferon activation pathways are dampened, e.g. STING (a central cytosolic DNA-sensor molecule to induce interferon) dependent and TLR7 dependent pathways[16]; c) the NLRP3 dependent inflammasome pathway is dampened, and key inflammation response genes like AIM2 are not present in bats[87,88]. These traits may be due to bat immune-sensing pathway adaptation as a fitness cost of flight[15]. We hypothesize that bat virus replication will likely be restricted quickly by constitutively expressed IFNα in bats, resulting in lower B/T cell stimulation due to lower viral stimuli. Second, dampened interferon and inflammasome responses will result in lower cytokine responses that are required to trigger T/B cell dependent adaptive immunity (e.g. antibody response), ultimately resulting in suppression of viral replication and shedding. **We and others have demonstrated proof-of-concept of this phenomenon:** Experimental Marburg virus infection of Egyptian fruits bats, a natural reservoir host, resulted in widespread tissue distribution with low viral load, brief viremia, low seroconversion and a low antibody titer that waned quickly, suggesting no long-term protection is established[89-91]. Poor neutralizing antibody responses occur after experimental infection of bats with Tacaribe virus[92] and in our studies of experimental infection of bats with SARS-CoV (Wang, unpubl.). We also successfully showed that bat interferon can inhibit bat SARSr-CoVs[21]. We hypothesize that use of immune modulators that upregulate the naturally low innate immunity of bats to their viruses, will transiently suppress viral replication and shedding, reducing the host jump risk. We further hypothesize that because *Rhinolophus* bats are long-lived (20+ yrs in the wild), most bats in a population will have been exposed to a range of SARSr-CoV QS at our sites. Specifically targeting upregulation of their adaptive immunity (immune memory) to high-risk viral strains may lead to heightened clearance of high-risk strains. We will evaluate two immune modulation approaches to defuse spillover of SARSr-CoVs from bats to humans: **1) Broadscale Immune Boosting strategies (Wang, Duke-NUS):** we will apply immune modulators like TLR-ligands, small molecule RIG-like receptor (RLR) agonists or bat interferon in live bats, to up-regulate their innate immunity and suppress viral replication and shedding; **2) Targeted Immune Boosting (Baric, UNC):** the broadscale immune boosting approach will be applied in the presence of chimeric immunogens to activate immune memory in adult bats and boost clearance of high-risk SARSr-CoVs. We will use novel chimeric polyvalent recombinant S proteins in microparticle encapsidated gels for oral delivery and/or virus adjuvanted immune boosting strategies where chimeric recombinant SARSr-CoV S are expressed by raccoon poxvirus. Both lines of work will begin in Year 1 and run parallel, be assessed competitively for efficiency, cost, and scalability, and successful candidates from captive animal trials will be used in live bat trials at our test cave in Yunnan. The finding of low innate immunity across bats suggest that immune boosting could be broadly applicable to bat genera and viral families.

Broadscale immune boosting (Duke-NUS). We will work on the following key leads to identify the most effective approach to up-regulate innate immunity and suppress viral loads. *Toll-like receptor (TLR)/RIG-I Like Receptor (RLR) ligands:* Our work indicates a robust response in live bats to TLR-stimuli like polyI:C as measured by transcriptomics on spleen tissue (**Fig. 8**), liver, lung and lymph node, with matched proteomics to characterize immune activation *in vivo*. These activation profiles will be used to assess bat immune response to different stimuli and identify those which lower viral load in our experimental system at Duke-NUS (below).

Fig. 8: Pathway analyses from Ingenuity Pathway Analysis (IPA) of whole spleen NGS after stimulation with either LPS or polyI:C. Z-score increase over control bats is indicated as per scale, and suggests strong activation of many pathways.

We will also stimulate the RIG-I pathway with 5'pppDSRNA, a mimetic of the natural RIG-I stimulant that will activate functional bat IFN production pathways, as shown in a mouse model that cleared SARS-CoV, IAV and HBV[18,19].

Universal bat interferon: We will design a conserved universal bat interferon protein sequence with artificial gene synthesis and produce recombinant protein by cleavable-affinity-tagged purification of supernatant from over-expressing bat cells, as used previously for recombinant *Pteropus alecto* IFNα[17,93] and CSF-1/IL-4. Utilization of a universal IFN for bats will overcome species-dependent response to the ligand, allowing the use of IFN throughout broad geographical and ecological environments and across many bat species. We have already produced recombinant non-universal, tagged, bat IFN that induce appropriate immune activation (**Fig. 9**). This ligand has been shown to reduce viral titers in humans, ferrets and mouse models intranasally and orally[18,19,94]. Interferon has been used clinically in humans as an effective countermeasure when antiviral drugs are unavailable, e.g. against filoviruses[20]. Interferon is known to be toxic, therefore we will carefully examine dose tolerance in bats and assess clinical effects of the treatment. We have shown that replication of SARSr-CoV is sensitive to IFN treatments[21]. The successful delivery, immune activation and outcome on the host will be characterized thoroughly to optimize rapid immune activation.
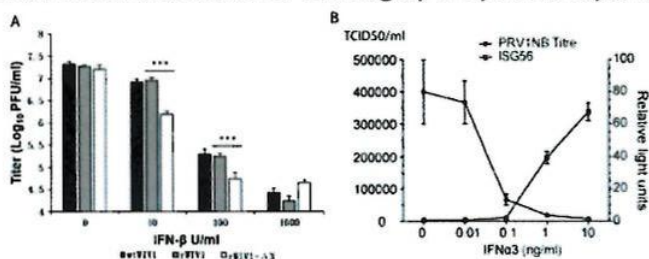

Fig. 9: Bat viruses are sensitive to IFN treatments. A) Recombinant bat SARS-related coronavirus WIV1 replication was inhibited by human IFN-β in a dose dependent manner in Vero cells. B) Bat reovirus PRV1NB replication was inhibited by recombinant bat IFNα3 in a dose dependent manner in bat PakiT03 cells.

Boosting bat IFN by blocking bat-specific IFN negative regulators: Uniquely, bat IFNα is naturally constitutively expressed but cannot be induced to a high level, indicating a negative regulatory factor in the bat interferon production pathway[17,95]. We will use a *Pteropus alecto* CRISPRi library pool that we have created covering multiple RNA targets in every gene in the *P. alecto* genome (Wang, unpubl.

data). Genes affecting influenza replication in bat cells have already been identified using this library. Using CRISPRi we will identify negative regulator genes and screen for compounds targeting them to boost the inducibility of the IFN system in a shorter time-frame. Based on previous work[96-98], it is highly likely this will be a conserved pathway across all bats. _Activating dampened bat-specific innate immune pathways which include DNA-STING-dependent and TLR-dependent pathways:_ We have shown that mutant bat STING or reconstitution of AIM2 and functional NLRP3 homologs restores antiviral functionality, suggesting these pathways are important in bat-viral coexistence. By identifying small molecules to directly activate pathways downstream of STING or TLR/RLRs, such as TBK1 activation, we will activate bat innate defense by interferons, promote viral clearance and, we hypothesize, significantly reduce viral load in bats. _Validation in a bat-mouse model._ Various CoVs show efficient infection and replication inside the human host but exhibit defective entry and replication using mouse as a host due in part to differences in DPP4 and ACE2 receptors.
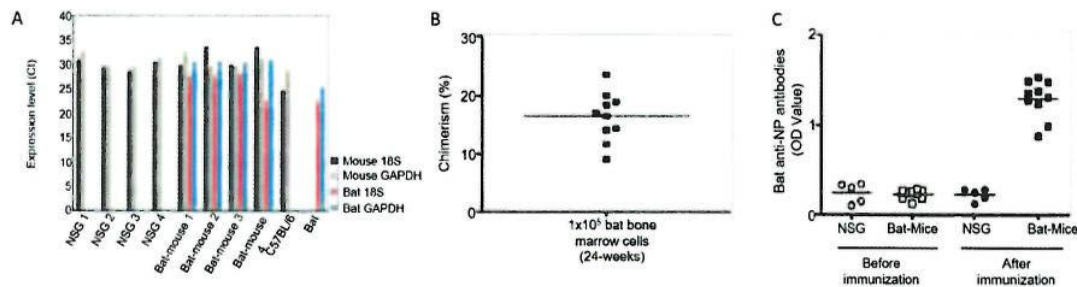

Fig. 10: _A) Presence of at-specific qPCR in reconstituted mice after 12 weeks. B) chimeric ratio of bat-mouse cells in circulation after 24 weeks. C) Specific antibody response to a KLH-tetanus antigen generated by bat-reconstituted mice._

We have shown efficient reconstitution of irradiated mice using bat bone marrow from multiple species, including _E. spelaea_ (**Fig. 10**), including reconstitution of bat PBMC's in the mouse, presence of circulating bat cells and generation of bat-specific antibodies in mice incapable of producing an antibody response. **This 'batified' mouse model** can be utilized for both circulating infection of SARS-CoV (in the immune compartment only) and as a model for generating bat-specific antibodies against CoV proteins. Efficient validation of infection into bat cells will be used to validate the infectivity of the viruses and generation of bat antibodies will facilitate validation of the best proteins/peptide to elicit an effective immune response.

Targeted immune boosting (UNC). To boost targeted adaptive immunity (immune memory) in wild bats chronically exposed to circulating SARSr-CoV QS, we will inoculate with chimeric S glycoproteins in the presence of the broadscale immune boosting agonists above. We have developed novel group 2b SARSr-CoV chimeric S glycoproteins that encode neutralizing domains from phylogenetically distant strains (e.g. Urbani, HKU3, BtCoV 279, ~25% diversity). The chimeric S programs efficient expression when introduced in the HKU3 backbone full length genome, and elicits protective immunity against multiple group 2b strains. We will develop robust expression systems for SARSr-CoV chimeric S using ectopic expression _in vitro_. We will work with Dr. Ainslie (UNC-Pharmacy) who has developed **novel microparticle delivery systems and dry powders for aerosol release** that encapsidate recombinant proteins and adjuvants (innate immune agonists) that we will use for **parallel broadscale immune boosting strategies**

± chimeric immungens. Simultaneously, we will introduce chimeric and wildtype S in raccoon poxvirus (RCN), in collaboration with Dr. Rocke and confirm recombinant protein expression, first *in vitro* and in the Duke-NUS bat colony, prior to any field trial. The goal is to develop a suite of reagents to remotely reduce exposure risk in high risk environmental settings. *Chimeric SARSr-CoV S Immunogens:* CoVs evolve quickly by mutation and RNA recombination[34,99], and encode neutralizing epitopes in the amino terminal domain (NTD), RBD and S2 portion of the S glycoprotein[66,100,101], providing a strategy to build chimeric immunogens that induce broadly cross reactive neutralizing antibodies. Given the breadth of SARSr-CoV circulating in natural settings, chimeric immunogens will be designed to increase the breadth of neutralizing epitopes across the group 2b phylogenetic subgroup[48]. Using synthetic genomes and structure guided design, we fused the NTD of HKU3 with the SARS-CoV RBD with the remaining BtCoV 279/04 S glycoprotein molecule, introduced the chimeric S glycoprotein gene into the HKU3 genome backbone (25% different than SARS-CoV, clade 2 virus) and recovered viable viruses (HKU3-S_{mix}) that could replicate in Vero cells. We inserted HKU3$_{mix}$ S glycoprotein gene into VEE virus replicon vectors (VRP-$S_{chimera}$) and demonstrated that VRP vaccines protect against lethal SARS-CoV challenge and virus growth. VRP-S_{HKU3} and VRP-S_{279} both protect against HKU3$_{mix}$ challenge and growth *in vivo*, demonstrating that neutralizing epitopes in the HKU3$_{mix}$ S glycoprotein provide broad cross protection against multiple SARSr-CoV strains. In addition to using these immunogens as a targeted broad-based boosting strategy in bats, we will produce other chimeras for more focused immune targeting of known high risk strains. We will use the Protein Expression Core at UNC (https://www.med.unc.edu/csb/pep) to produce codon optimized, stabilized and purified prefusion SARS-CoV glycoprotein ectodomains[23]. Purified recombinant protein will be used for inclusion in delivery matrices (e.g. purified powders, dextran beads, gels – see below) with broadscale immune agonists (adjuvants, Duke-NUS). *2nd Generation Chimeric S glycoprotein Immunogen Design and Testing:* We will produce a chimeric SHC014 NTD/SARS-CoV-RBD/HKU3 S C terminal recombinant S immunogen (HKU3-S_{S014}), for more focused immune targeting on known high and low risk strains designated from our experimental and modeling analyses. The recombinant HKU3-S_{S014} S genes will be sent to Dr. Rocke for insertion into the raccoon poxvirus vaccine vector. Using established techniques, we will characterize S expression and provide virus vectors to Prof. Wang for immune boosting trials at Duke-NUS, and if successful in the field (Prof. Shi). The human codon optimized HKU3-S_{S014}, and HKU3-S_{mix} recombinant chimeric spike glycoproteins will be expressed and purified by the UNC proteomics core, producing mg quantities for inclusion in nanoparticle and microparticle carriers in collaboration with Dr. Ainslie. We will produce WIV-S_{S014} and HKU3-S_{mix} glycoprotein expression will be validated by Western blot and by vaccination of mice, allowing us to determine if the recombinant protein elicits neutralizing antibodies that protect against lethal SARS-CoV and SHC014 challenge. We will produce enough material for *in vivo* testing in mice and in bats. We will validate recombinant virus glycoprotein expression by Western blot and by vaccination of mice, to determine if the recombinant protein elicits neutralizing antibodies that protect against lethal SARS-CoV, HKU3-Smix and SHC014 challenge. We will survey the RNAseq data for evidence of complex S glycoprotein gene RNA recombinants in the SARSr-CoV population genetic structure. If present, we will synthesize 2-3 potentially effective recombinant S genes, insert these genes into SHC014 or HKU3 genome backbones and VRP, and characterize their

viability and replicative properties in cell culture and in mice. We will produce immunogens and evaluate their ability to protect against infection.
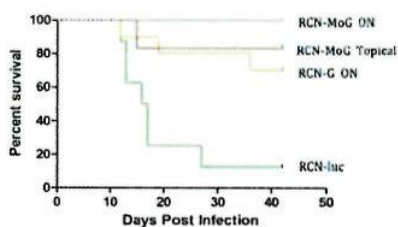
Adjuvant and Immunogen Delivery Vehicles. Dr. Ainslie (UNC) has developed the biodegradable polymer acetalated dextran (Ac-DEX) for the delivery of antigens and adjuvants in vaccine applications. Ac-DEX has advantages over other polymers for vaccine development: it is easily synthesized and scalable using an FDA-approved one-step method to move from water-soluble to insoluble[102-104]; it is acid sensitive which improves antigen presentation; microparticles (MPs) are small (5-8μm) so can be phagocytosed by DCs and traffic to the lymph node for efficient molecule delivery[105]; MPs are pH-neutral, safe[106], stable outside the cold-chain[107], can be aerosolized or delivered in sprays or gels[102,108]; and we have previously encapsulated Poly (I:C)(1), resiquimod[105], and a STING agonist into our novel MPs[109], providing proof-of-concept that this significantly enhances the activity of the TLR agonist. We have displayed better efficacy than state-of-the-art FDA-approved inactivated flu virus (Fluarix) in a ferret model of influenza[110], using HA with encapsulated STING cyclic [G(3',5')pA(3',5')p][111]. *Microparticle Performance Metrics in vitro and in Rodents and Bats:* We will encapsulate Poly (I:C), resiquimod (TLR 7) or other innate immune agonists to enhance type I interferon production in in consultation with Prof. Wang. Agonist laden particles will be made separately or in combination with recombinant SARS-CoV chimeric spike proteins, encapsulated into our aerodynamic MPs and nanoparticles. *Viral infection models in* Eonycteris spp. *(Duke-NUS) and wild-caught* Rhinolophus spp. *(Wuhan Inst. Virol.) bats:* To test and compare the efficacy of the immune modulating approaches above, we will use our cave-nectar bat (*Eonycteris spelaea*) breeding colony infected with Melaka virus (family *Reoviridae*) which infects this species[112,113]. First, we will take wing punch biopsies from 3 individuals to sequence their ACE2 receptor gene. This will be inserted into human cell lines to pre-screen viral strains for binding. Those that bind will be used for *in vivo* expts. We will use two coronaviruses (SARSr-CoV WIV1 and MERS-CoV) in ABSL3. SARS and MERS infection studies are already underway in *Eonycteris* and *Pteropus* cell lines and primary immune cells. Our *E. spelaea* colony has now reached a sustainable population for infection experiments and the ABSL3 facility has been outfitted with bat-specific cages. The planned pilot *in vivo* infection of *Eonycteris* bats with Melaka Virus and MERS will be completed by July 2018. Previous infection studies were completed in *Pteropus* and *Rhinolophus* bats in Australia by L-F Wang at CSIRO, AAHL and an additional *Pteropus* infection trial is currently planned through the University of Queensland in Australia. At WIV, 20 adult wild *Rhinolophus* spp. bats (10 of each sex) will be captured at our test cave site, housed within ABSL3, ACE2 receptor genes sequenced and used to pre-screen spikes as above, then bats will be tested using PCR and serology for current and prior exposure to SARSr-CoVs, and inoculated with WIV1, WIV16 or SHC014. For all experiments, viral loads will be measured by qPCR, titration of produced virus, NGS transcriptomics and viral-specific nanostring probes added to the immunoprofiling panel. Antibody responses will be measured by LIPS assay, as described previously. In addition to direct *in vivo* delivery of ligands, aerosolized and liquid-phase deployment methods suitable for a cave-like environment will be tested, in collaboration with UNC, NWHC and PARC. This approach allows us to test our immune-boosting strategies, in a safe and controlled environment, prior to expanding to field-based evaluation. The experimental protocols and analytical methods used for the *E. spelaea* colony, with a focus on

internal-normalization and small amounts of sample materials (including nanostring analysis from whole blood-droplets), will be replicated to analyze experimental infection of wild-caught *Rhinolophus* spp. bats at WIV and in the test cave trail in TA2.

Delivery system development (NWHC). We have previously developed, safety- and efficacy-tested, and registered oral vaccines and delivery methods to manage disease in free-ranging wildlife including a plague vaccine for prairie dogs[30], a rabies vaccine for bats[31] and strategies for white-nose syndrome (unpubl. data)[114]. As previously shown for rabies vaccine in bats, we will trial sticky edible gels that bats groom among each other to deliver immune modulators and recombinant SARSr-CoV spike proteins to *Rhinolophus* bats, including trials of them combined with poxvirus vectors and nanoparticles/nanoemulsions that enhance uptake through transdermally. Poxviruses are effective viral vectors for delivering vaccines to wildlife [30,115,116], and can replicate safely at high levels in bats after oronasal administration[32]. We have demonstrated proof-of-concept and safety in bats with modified vaccinia Ankara (MVA) and raccoon poxvirus (RCN) vectors using *in vivo* biophotonic imaging[31]. RCN replicated to higher levels in bats than MVA, even via the oral route, and was found to be safe. We used raccoon poxvirus-vectored novel rabies glycoprotein (mosaic or MoG) and demonstrated protective efficacy in bats after oronasal and topical administration[31] (**Fig. 11**).

Fig. 11: Vaccine efficacy, rabies challenge in Epstesicus fuscus immunized with raccoon poxvirus expressing a mosaic G protein (RCN-MoG) oronasally (ON) or topically in comparison to RCN expressing typical G protein or luciferase (negative control).

Poxviruses are safe in a wide variety of wild and domestic animals, and allow for large inserts of foreign DNA. We have previously used a raccoon poxvirus vectored vaccine expressing plague antigens to manage plague caused by *Yersinia pestis* in prairie dogs. We incorporated the biomarker Rhodamine B (RB) into baits to assess uptake by target and non-target species [114,117] (**Fig. 12**). RB is visible under a UV microscope until the hair grows out (~50 days in prairie dogs). We have since conducted a large field trial that demonstrated vaccine efficacy in four species of prairie dogs in seven western states[30].
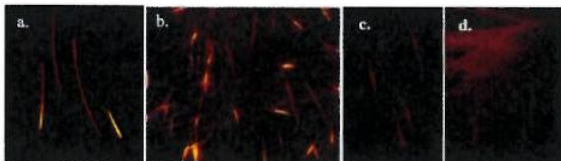

Fig. 12: Prairie dog hair and whisker samples under fluorescence microscope to determine uptake of baits containing Rhodamine B. a) 20 days after bait distribution, b) 16 days after bait distribution, c) and d) controls (note natural dull fluorescence).

Transcutaneous delivery: To trial a strategy that avoids use of live agents, we will use nanoparticles to increase transcutaneous delivery efficiency[118]. We will use poly lactic-co-glycolic acid (PLGA) to encapsulate immune modulators as a method of transcutaneous delivery of vaccine to bats via dendritic cell uptake[119], as has been shown for delivery of TLR agonists and antigens simultaneously to mice[120]. This approach will be competitively trialed against ac-DEX, with and without adjuvants[121] which enhance the immune response in mice to SARS-CoV spike proteins[24]. Initial trials will be conducted in the USA with locally acquired insectivorous big brown bats (*Eptesicus fuscus*) which we have maintained and housed for several experiments previously[31,32]. We will treat bats via topical application with various test formulations that include the biomarker Rhodamine B (RB), co-

house them with untreated bats, and monitor transfer between bats by collecting hair and whiskers for biomarker analysis. _Initial field trials:_ High rates of grooming within bat colonies allow effective transfer or products among a colony. In biomarker trials in Peru, RB-labeled glycerin jelly yielded a rate of transfer from 1.3 – 2.8 bats for every bat marked. We will conduct initial trials with each of the delivery vehicles in local US insectivorous bats in their natural setting. Within one week of application of varying doses, bats will be trapped at the cave entrance using mist nets or Harp traps and hair will be collected to assess the rate of uptake via biomarker analysis, then released. After we have determined optimal approaches for mass delivery, we will test them on wild-caught captive _Rhinolophus_ bats (WIV), then in our three cave sites in Yunnan Province. Biomarker will be used to assess rates of uptake (and non-target species contamination) and these data used in modeling studies to help determine the optimal rates of application of immunomodulating agents. _Innovative Aerosol Approach to Bat Inoculation:_ Once we have confirmed uptake in laboratory studies, we will assess scalable delivery methods in local caves and hibernacula using biomarker-labeled mediums without immunomodulatory substances. In collaboration with Dr. Jerome Unidad of Palo Alto Research Center (PARC), we will use an innovative aerosol platform technology unique to PARC to design a field-deployable prototype for use in cave settings. The Filament Extension Atomization (FEA)[122] technology can spray fluids with a wide-range of viscosities ranging from 1mPa-s (the viscosity of saliva and most aqueous vaccine formulations) up to 600Pa-s (the viscosity of creams and gels for topical delivery) using a roll-to-roll misting process (https://www.parc.com/services/focus-area/amds/) that results in narrowly-dispersed droplets with tunable sizes from 5-500 microns. FEA technology is compatible with all the formulations of interest to project DEFUSE, including aqueous formulations intended for conventional spraying and the edible gels and creams for topical delivery, with no limit on bioactive ingredient loading. FEA can be a universal delivery platform for direct spraying onto bats with the formulation geared towards bio-efficacy. Potential form factors for a prototype cave-based spray system are shown in **Fig. 13**.
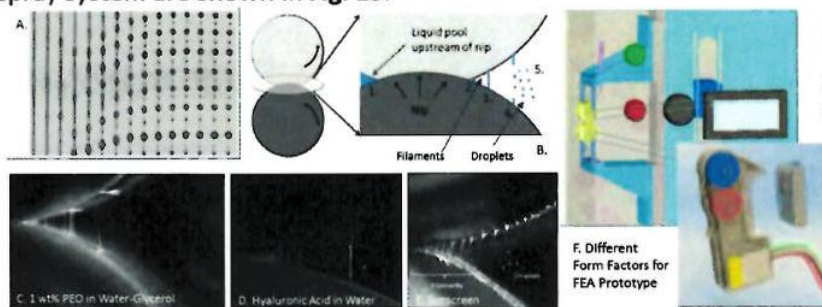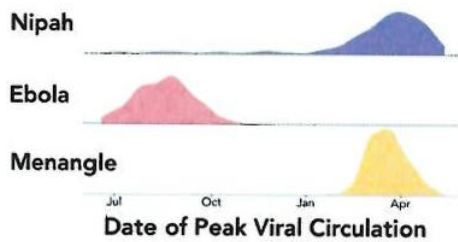

Fig. 13: PARC FEA Technology – A. Beads-on-a-string structures in viscoelastic fluids[123], B. Parallelization of filament formation and droplet break-up in an FEA roller system, C.-E. Images from high speed videos of representative fluids sprayed with FEA, F.

Potential field-deployable prototype for Project DEFUSE (benchtop, handheld).

PARC and NWHC will conduct initial prototype trials on US cave bats. PARC will then develop the prototype to a form that will be used for the proof-of-concept demonstration at the test sites in the Kunming bat caves, Yunnan, China. The field-deployable system will be motion-actuated, and on a timer so that bats will be targeted at fly-in and fly-out to avoid non-target species (e.g. cave swiftlets).

Dynamic circulation modeling to optimize deployment strategy. To select immune boosting,

and multiple delivery options and schedules, we will simulate deployment using a model of viral circulation in cave bat populations. The model will be fit to data from our three-cave test system but designed to be robust and generalizable to other cases. We will simulate outcomes under a variety of different deployment scenarios to produce conservative estimates of optimal application under real-world conditions. *Fit stochastic viral circulation models to longitudinal sampling data:* We will use longitudinal viral prevalence, mark-recapture data, telemetry and infrared camera data collected during our field sampling to parameterize and construct models of bat population dynamics and viral circulation in our test caves. **Fig. 14**: *Modeled seasonal circulation of viruses modeled from longitudinal sampling of viruses in bat colonies in Bangladesh.*

Nipah

Ebola

Menangle

Jul   Oct   Jan   Apr

Date of Peak Viral Circulation

We will modify existing models that extract temporal dynamics developed for multiviral systems based on longitudinal studies in Bangladesh[124] (**Fig. 14**). We will use a simple but robust stochastic SIR process model with immigration and emigration and flexible, nonlinear contact rates between bats[125] to capture a wide range of viral dynamics from intermittent viral outbreaks to regular, endemic circulation with a relatively small number of parameters. We will fit these models to our sampling data using the **partially observable markov process (pomp)** framework[126], allowing estimates of the underlying latent dynamic disease transmission process, accounting for and separating natural stochasticity of viral circulation and observation error in sampling. We will validate our models via temporal cross-validation and by testing the results of a fit from two cave sites on data from a third. *Simulate circulation under a set of plausible deployment scenarios.* Using the top performing sets of immune boosting molecules from captive trials, and the most effective delivery media and methods from cave studies, we will use the stochastic SIR model to generate simulations of viral circulation under a series of deployment scenarios in our test caves. These scenarios will cover a range of plausible intensities, frequencies, and combinations of suppression strategies and will incorporate uncertainty in the efficacy of each treatment strategy. From these simulations, we will estimate the expected degree and time period of suppression of viral circulation and shedding and determine the optimal scenario for deployment in our focal study caves. *Test robustness of deployment strategies under broader conditions:* We anticipate deployment is likely to occur under highly varied species population and compositions, with uncertain estimates based on rough observations, with varied uptake and efficacy of treatment due to different environmental conditions, and with limited time and resources. We will simulate deployment under many potential conditions to determine optimal deployment under each, and strategies that are conservative and robust to uncertainties and limitations.

Proof-of-concept deployment of immune modulation molecules in test caves in Yunnan Province, China. We will deploy the most successful immune modulation molecules at our three test-caves in Yunnan Province, China. We will identify the primary entry/exit points and traffic patterns for each cavern used by bats during flyout by LiDAR mapping and infrared video surveillance, and position two PARC spray nozzles around the top (10 and 2 o'clock position, pointing down) of the primary opening. Depending on the size of the cave opening, we will

mount the nozzles on extendable booms to position them at the top of the cave mouth. Spray will be activated by bat movement to spray continuously or in a staggered manner during flyout and flyin to create an aqueous curtain that bats will fly through. We will determine the optimal duration of spraying using <u>stochastic viral circulation models and real-time population size data</u>. We assume a rate of glycerin gel transfer of 2.0, through grooming activity from preliminary data. Initial trials will use RB to assess coverage. Then, at the test cave, immune-modulation biologicals and biomarkers will be deployed, with biomarker only sprayed at two other control caves. The 4 months pre-deployment sampling will be followed by 4 months post deployment surveillance (**see sampling strategy**) commencing the day following deployment through which we will assess 1) nature and duration of individual bat immune response to the treatment and 2) population level SARSr-CoV viral shedding rates in the test and control caves based on fecal pellet screening. We will also screen for the biomarker to assess coverage achieved. This approach can be **scaled up** for a larger network of bat roosts by using our app to model bat roost connectivity (mixing patterns among local caves based on our recapture and telemetry data) and identify caves with the highest connectivity so that bats transfer the biological treatment to other caves at a rate that will dampen viral shedding over a much larger area.

Section 1.03   **MANAGEMENT PLAN**
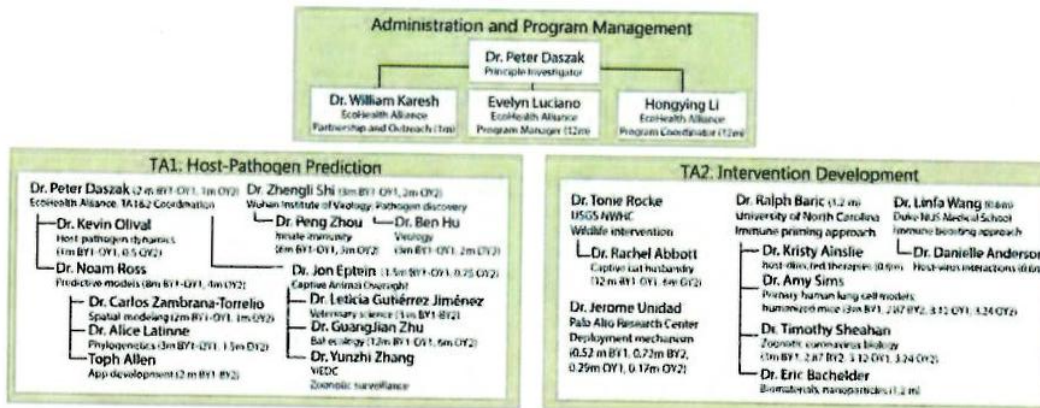
Project DEFUSE lead institution is EcoHealth Alliance, New York, an international research organization focused on emerging zoonotic diseases. The PI, Dr. Daszak, has 25+ years' experience managing lab, field and modeling research projects on emerging zoonoses. Dr. Daszak will commit 2 months annually (one funded by DEFUSE, one funded by core EHA funds) to oversee and coordinate all project activities, with emphasis on modeling and fieldwork in TA1. Dr. Karesh has 40+ years' experience leading zoonotic and wildlife disease projects, and will commit 1 month annually to manage partnership activities and outreach. Dr. Epstein, with 20 years' experience working emerging bat zoonoses will coordinate animal trials across partners. Drs. Olival and Ross will manage modeling approaches for this project. Support staff includes a field surveillance team, modeling analysts, developers, data managers, and field consultants in Yunnan Province, China. The EHA team has worked extensively with other collaborators: Prof. Wang (15+ yrs); Dr. Shi (15+ yrs); Prof. Baric (5+ yrs) and Dr. Rocke (15+ yrs). **Subcontracts: #1** to Prof. Baric, UNC, to oversee reverse engineering of SARSr-CoVs, BSL-3 humanized mouse experimental infections, design and testing of targeted immune boosting

treatments; **#2** to Prof. Wang, Duke-NUS, to oversee broadscale immune boosting, captive bat experiments, and analyze immunological and virological responses to immune modulators; **#3** to Dr. Shi, Wuhan Inst. Virol., to conduct PCR testing, viral discovery and isolation from bat samples collected in China, spike protein binding assays, humanized mouse work, and experimental trials on *Rhinolophus* bats; **#4** to Dr. Rocke, USGS NWHC, to refine delivery mechanisms for immune boosting treatments. Dr. Rocke will use a captive colony of bats at NWHC for initial trials, and oversee cave experiments in the US and China. **#5** to Dr. Unidad, PARC, to develop innovative aerosal platform into a field-deployable device for large-scale inoculation of the bats. Dr. Unidad will collaborate closely with Dr. Rocke in developing a field deployable prototype for both initial trails and cave experiments in China.

Collaborator Coordination: All key personnel will join regularly-scheduled web conferencing and conference calls in addition to frequent ad hoc email and telephone interactions between individuals and groups of investigators. Regular calls will include:

- Weekly meetings between the PI and Program Manager (on project and task status)
- Weekly web/phone meetings between Program Manager and subawardee admin. staff
- Monthly web/phone conferences between EHA PIs and all subawardee PIs.
- Monthly web conferences between key personnel (research presentations/coordination)
- Four in-person partner meetings annually with key personnel at EHA and two in-person partner meetings annually between subawardees.
- Annual in-person meeting among all key personnel

Evaluation metrics will include the generation of high-quality data, successful achievement of milestones and timelines, scientific interaction and collaboration, the generation of high quality publications, and effective budget management. The PI and subawardee PIs will attend a kickoff meeting and the PI will meet regularly with DAPRA at headquarters and at site visits.

Data Management and Sharing: EcoHealth Alliance will maintain a central database of data collected and generated via all project field, laboratory, and modeling work. The database will use secure cloud hosting services and enable export to archival and platform-independent formats. It will ensure data and metadata compatibility between project components, track data versioning and annotations, and enable compliance with DARPA data requests and disclosure requirements. All archived human sample data will be de-identified. Partners will provide raw and processed data to the central database throughout the course of the project. Project partners will have access to the data they generate in the database at all times, and maintain control over local copies. Release of any data from the database to non-DARPA outside parties or for public release or publication will occur only after consultations with all project partners. EHA has extensive experience in managing data for multi-partner partner projects (PREDICT, USAID IDEEAL, the Global Ranavirus Reporting System).

Problem identification and resolution: Regular planning, monitoring, and evaluation meetings will be the primary mechanisms for problem identification. Minor problems (e.g. delays in sample availability or test results) will be dealt with internally through appropriate action and resolution monitored by Dr. Daszak and the Project Manager. In the event of significant problems, such as prolonged poor productivity, inadequate scientific collaboration, or major disputes regarding research direction or resource allocation, EHA will assist with resolving the

problem through negotiation. Should a resolution not be forthcoming, consultation with our technical advisors and DARPA Program staff may be warranted.

Risk management: Maintaining a timeline and meeting milestones will require strict and continuous oversight of all project phases, frequent and regularly scheduled communication, and the ability to make decisions and implement strategies. A project of this nature requires a different mindset from that typically associated with basic research activities that move at an incremental pace with investigators gradually optimizing experimental systems, refining data, or waiting for additional data before moving ahead with an analysis approach. To maintain our timeline, we will continually evaluate these trade-offs to make decisions about when iteration is appropriate and when necessary to move forward with current information.

Biographies:
Dr. Peter Daszak is President and Chief Scientist of EcoHealth Alliance, Chair of the NASEM Forum on Microbial Threats, member of the Executive Committee and the EHA institutional lead for the $130 million USAID-EPT-PREDICT. His >300 scientific papers include the first global map of EID hotspots[49,127], estimates of unknown viral diversity[50], predictive models of virus-host relationships[7], and evidence of the bat origin of SARS-CoV[2] and other emerging viruses [128-131].
Prof. Ralph Baric is a Professor in the UNC-Chapel Hill Dept. of Epidemiology and Dept. of Microbiology & Immunology. His work focuses on coronaviruses as models to study RNA virus transcription, replication, persistence, cross species transmission and pathogenesis. His group has developed a platform strategy to assess and evaluate countermeasures of the potential "pre-epidemic" risk associated with zoonotic virus cross species transmission[10-12,29,57,64].
Prof. Linfa Wang is the Emerging Infectious Diseases Programme Director at Duke-NUS Medical School. His research focuses on emerging bat viruses, including SARS-CoV, SADS-CoV, henipaviruses, and others[2,14,60,80,124] and genetic work linking bat immunology, flight, and viral tolerance[15,16,75,93]. A 2014 recipient of the Eureka Prize for Research in Infectious Diseases, he currently heads a Singapore Nat. Res. Foundation grant "Learning from bats" ($9.7M SGD).
Prof. Zhengli Shi is director of the Center for Emerging Infectious Diseases of the Wuhan Institute of Virology, Chinese Academy of Sciences and BSL3 and BSL4 lead. Her research focuses on traditional and high-throughput sequencing techniques for viral pathogen discovery. Since 2004, she has studied bat-borne viruses, leading the SARSr-CoV group discovery[2,3,34,67].
Dr. Tonie Rocke is a research scientist at the USGS National Wildlife Health Center. Her research focuses on the ecology and management of diseases in wild mammals (e.g. plague, monkeypox, rabies and white-nose syndrome). She leads a large-scale field trial of oral plague vaccination of wild praire dogs in the western U.S. [30-32,114,117].
Dr. Jerome Unidad is a Member of Research Staff at the Hardware Systems Laboratory at PARC. His research focuses on novel fluid delivery systems including aerosol delivery for high viscosity fluids, polymers and biomacromolecules. He is the technical lead in developing the FEA spray technology for consumer and biomedical applications, and additive manufacturing.

Section II	CAPABILITIES

EcoHealth Alliance (EHA) is an international non-profit researching emerging zoonoses in >20 countries Asia, Africa and South America. EHA has pioneered modeling and analyses of the origins and drivers of emerging diseases, of the bat origins of emerging viruses, and the

dynamics of SARSr-CoVs, henipaviruses and other high-profile emerging pathogens. EHA is major consortium partner in the USAID-EPT-PREDICT program that has tested over 35,000 animals and discovered 200 new viruses to date.

University of North Carolina Medical School (UNC). The Baric Laboratory in University of North Carolina at Chapel Hill comprise biosafety level two facilities equipped to perform basic virology, immunology, and molecular biology as well as university space for breeding mice for the proposed studies. The Baric BSL-3 laboratories are approved and have the required equipment to perform all of the chimeric virus recovery and characterization and ventilated rodent caging to examine the bat coronaviruses within this proposal.

The National Wildlife Center (NWHC) contains specialized research laboratories and support areas, staff offices, and BSL-3 biocontainment animal research areas. Two, fully equipped laboratories in the research building are available at all times for the proposed work. NWHC's BSL-3 biocontainment animal research area is equipped with pathology incineration, steam sterilization equipment, and an ultraviolet radiation chamber so that all materials can be treated before leaving the biological containment area, and is maintained under negative air pressure. Trained animal care staff and a Veterinary Medical Officer are available to maintain, monitor and handle animals. The NWHC is fully equipped for animal medical procedures.

Palo Alto Research Center (PARC) is composed of 140+ professional full time researchers from physics, materials science, chemistry, biology, engineering, computer science, controls and ethnography fields. Facilities comprise two general purpose labs for conducting spray experiments and fluid mechanics measurements, a cell culture lab, chemistry labs, laser patterning and 3D printing facilities, a professional staffed model shop and electronics labs.

Wuhan Institute of Virology: includes BSL2, BSL-3, and BSL-4 laboratories, animal feeding rooms and other supporting facilities. The Biosafety Laboratory will carry out CoV research, sample testing, sequencing, binding assays, *in vitro* and *in vivo* work.

Duke-NUS Medical School; Singapore: The Duke NUS Animal BSL-3 facility is co-located with the SingHealth Animal Husbandry and Hospital in Northern Singapore. The Facility is a state-of-the-art modular laboratory equipped to safely carry out infectious diseases research. The Animal BSL-3 lab is equipped with virology, basic immunology, and molecular biology capacity, and is equipped for handling caged animals including rodents, nonhuman primates and bats.

Intellectual property rights: PARC asserts restrictions on the following noncommercial item: An Efficient Method for Collecting Droplets of Strain Hardening Viscoelastic Fluids in a Spray Device, to be used in device development towards Project DEFUSE. PARC will develop the technology exclusively at private expense, and asserts that the USG has limited rights on technical data associated with the device. PARC is willing to negotiate in good faith with the government or technology transition partner for relevant background intellectual property to support transition. There are no restrictions on Commercial property rights.

Related research:

Daszak, PI on subcontract, USAID-EPT1&2, PREDICT: Consortium partner lead, Exec. Board member, Modeling & Analytics lead for two 5-year contracts ($75 million; $138 million) to conduct surveillance for novel viruses in wildlife in >25 countries globally, capacity build, assess behavioral risk, and manage databases. EHA subcontracts >$35 million. >1000 viruses discovered, 10,000 samples collected. Papers published in *Science, Nature, Lancet.*

Daszak, PI, NIAID: Understanding the Risk of Bat Coronavirus Emergence: 5-year grant to research spillover risk of novel SARSr-CoVs in China. $2.8 million, 5 subawards. Published work in *Science, Nature, PNAS.*

Daszak, Chief-of-Party, USAID: Infectious Disease Emergence & Economics of Altered Landscapes: PI on 3-year $2.5 million contract to analyze economics of land use change and disease emergence in Malaysia.

Section II	STATEMENT OF WORK

PHASE 1

PI-TA-01 Task 1: Conduct longitudinal bat sampling and ecological data collection from field sites in Southern China to obtain data for experimental studies and modeling (EHA)
Sub-Task 1.1 Apply for and obtain IACUC and ACURO approval and appropriate permits in China for bat sample collection and field intervention pilot (EHA). *Sub-Task 1.2* Collect monthly specimens from bats at cave sites in Yunnan, China for SARSr-CoV screening and sequencing. Oral, fecal, and blood sample collected from 360 *Rhinolophus spp.* bats per month using live-capture and non-invasive sampling. Specimens shipped to laboratory for analysis. Associated morphological, demographic, and physiological data for individual bats collected (EHA, consultant Zhu). *Sub-Task 1.3* PIT tagging to assess bat connectivity and roost fidelity. All sampled bats marked with Passive Integrated Transponder tags. Radio frequency identification data loggers installed at each cave entrance for remote capture-recapture monitoring. (EHA, consultant Zhu). *Sub-Task 1.4* Satellite telemetry to assess bat home range size and connectivity. Mark 36 *Rhinolophus sp.* bats with 1g ICARUS satellite tags. (EHA, consultant Zhu). *Sub-Task 1.5* Real-time monitoring of bat populations. Conduct LiDAR cave surveys and establish remote IR thermal cameras at roost entrances for population size monitoring. Optimize algorithms for image recognition. (EHA, consultant Zhu). *Sub-Task 1.6* Develop and maintain project-wide database. Secure, cloud-hosted database will store all data collected and generated from field, lab, and experimental work, including code and generated data from modeling. (EHA)

Milestone(s): 1.1 Animal care and use approval and wildlife sampling permits obtained; 1.2 monthly collection of bat specimens and associate host data completed; 1.3 dataloggers and 1.5 IR cameras installed; 1.4 bat transmitters launched and data collection successful; 1.6 database built and tested; 1.6 field data entered into database monthly.

Deliverables: Specimens from 3,240 bats and fecal pellets collected from high-risk reservoir populations which have been obtained with all proper permits and permissions and shipped to WIV for analysis; real-time telemetry and mark-recapture data uploaded and made available to DARPA collaborators; completed database maintained.

PI-TA-01 Task 2: Construct models to predict bat species distributions and locations of greatest viral spillover risk (EHA).
Sub-Task 2.1 Construct joint species distribution models to predict bat community in caves across S. and SE Asia and identify high-risk geographic hotspots for viral spillover (EHA). *Sub-Task 2.2* Machine learning models using host and ecological traits to predict presence of viruses with zoonotic potential in bats (EHA) *Sub-Task 2.3* Non-parametric viral richness estimators to predict as-of-yet unsampled viral diversity. *Sub-Task 2.4* Develop prototype 'spatial viral spillover risk' app for the warfighter (EHA)

Milestone(s): 2.1 Joint species distribution model fit for Asian Bats, Cave-level predictions of bat community composition and viral diversity, 2.2 and 2.3 predictions of viral diversity and jump potential per bat spp. Prediction validation for 2.1-2.3; 2.4 Prototype app produce for β-testing, prototype app successfully field tested.
Deliverables: Deployable models of bat community composition and per-species viral diversity and zoonotic jump potential. Development of fully functional and user-friendly application.

PI-TA-01 Task 3: Screen, characterize and isolate SARSr-CoV QS_0 from bat samples (WIV)
Subtask 3.1 PCR screening of longitudinal specimens from target bat species (WIV). ***Subtask 3.2*** Genetically sequence SARSr-CoV spike proteins from PCR-positive samples (WIV). ***Subtask 3.3*** Develop and recover recombinant viruses with spike proteins from novel SARSr-CoVs (Duke-NUS). ***Subtask 3.4*** Identify the presence of low abundant, high risk SARSr-CoV, based on deep sequencing data (UNC)
Milestone(s): CoV prevalence and genetic diversity quantified; full genomes recovered
Deliverables: Library of PCR-positive specimens. Full sequencing of spike proteins. Creation of recombinant viruses to be used in task 4. List of potential higher risk SARSr-CoV QS.

PI-TA-01 Task 4: Experimental assays of SARSr-CoV QS jump potential (UNC)
Sub-Task 4.1 Conduct pre-screening via structural protein modeling, mutation identification, pseudovirus assays. (UNC). ***Subtask 4.2*** Conduct *in vitro* testing of chimeric viruses against host cell lines (UNC). ***Subtask 4.3*** Assess *in vivo* pathogenesis in hACE2 transgenic mice (UNC). ***Subtask 4.4*** Validate results from chimeric viruses with full-genome QS (UNC). ***Subtask 4.5*** Test synthetic modifications to viral spike proteins including RBD deletions, S2 Proteolytic Cleavage and Glycosylation Sites, N-linked glycosylation (UNC). ***Subtask 4.6*** Test effects of low-abundance, high-consequence micro-variations on jump potential. (UNC)
Milestone(s): Initiation and completion of each experimental sub-task.
Deliverables: Laboratory confirmed list of higher risk SARSr-CoV QS with zoonotic capability. Candidate SARSr-CoV for animal experiments. Data made available.

PI-TA-01 Task 5: Build and test Bayesian network models to predict genotype-phenotype spillover potential of high-risk SARSr-CoV strains. (EHA).
Subtask 5.1 Make predictions using prior data to guide QS selection for characterization (EHA). ***Subtask 5.2*** Update model predictions based on real-time data from viral *in vitro* and *in vivo* testing (EHA).
Milestone(s): Completion of preliminary model using prior data, tested and refined model using real-time data from the project.
Deliverables: Source code and model outputs from functional Bayesian predictive model for the risk of spillover of high-risk SARSr-CoV strains.

PI-TA-01 Task 6: Validate model predictions using SARSr-CoV serology from previously-collected human samples and surveillance data (EHA, WIV, Duke-NUS).
Subtask 6.1 Design Luciferase immunoprecipitation system (LIPS) assays to high- and low- jump risk SARSr-CoV QS_0 we have characterized (WIV). ***Subtask 6.2*** Determine specificity of LIPS assays by recombinant protein or attenuated virus inoculation into rabbits (WIV). ***Subtask 6.3*** Validate LIPS assays using positive serum samples; spike protein based LIPS and viral neutralization. (WIV). ***Subtask 6.4*** Test previously-collected human sera from Yunnan Province

to assess SARSr-CoV QS spillover (WIV). **Subtask 6.5** Validate BNM predictions of QS_0 jump potential and identify actual spillover probabilities using bat-human contact data (EHA).
Milestone(s): LIPS assays developed and validated; sera screened; Bayesian model validated
Deliverables: Data from serological assay validation and testing; New LIPS serology assays for specific SARSr-CoV QSs; Source code for validated model based on spillover evidence.

PI-TA-02 Task 7: Experimental testing of 'Broadscale Immune Boosting' using batified mice and captive bat colonies (Duke-NUS)
Subtask 7.1 Boost bat interferon (IFN) by blocking bat-specific IFN negative regulators (Duke-NUS). **Subtask 7.2** Activate dampened bat-specific innate immune pathways including DNA-STING-dependent and TLR-dependent pathways (Duke-NUS). **Subtask 7.3** Validate broadscale immune boosting in a bat-mouse model (Duke-NUS). **Subtask 7.4** Test immune modulation in captive *Eonycteris* sp. colony, using Malaka virus and SARSr-CoV infections. (Duke-NUS).
Subtask 7.5 Test targeted immune boosting in wild-caught captive *Rhinolophus* spp. (WIV)
Milestone(s): Initiation and completion of each experimental sub-task.
Deliverables: Experimental data; whole animal profiling of immune stimulants and associated response kinetics. Selection of one primary and two secondary ligands for use in subsequent viral challenge studies. Demonstrated animal models for broadscale immune boosting.

PI-TA-02 Task 8: Experimental testing of 'targeted immune boosting' using humanized mice and experimental bat colonies (UNC, NWHC, Duke-NUS, WIV)
Subtask 8.1 Develop chimeric SARSr-CoV S immunogens (UNC) **Subtask 8.2** Design and test 2nd generation chimeric S glycoprotein immunogens in humanized mice (UNC). **Subtask 8.3** Create raccoon poxvirus-vectored targeted immune boosting approach to be tested in captive bats at Duke-NUS (NWHC). **Subtask 8.4** Test targeted immune boosting in captive *Eonycteris* sp. colony, using Malaka virus and SARSr-CoV infections (Duke-NUS). **Subtask 8.5** Test targeted immune boosting in wild-caught captive *Rhinolophus* spp. (WIV)
Milestone(s): Initiation and completion of each subtask.
Deliverables: Chimeric SARSr-CoV S immunogens and poxvirus-vectored immune boosting molecules available for use. Proof-of-concept for targeted immune boosting approach in humanized mice and captive bats.

PI-TA-02 Task 9: Develop and assess transcutaneous delivery methods for immune boosting molecules (UNC, Duke-NUS, NWHC)
Subtask 9.1 Synthesize polymer acetalated dextran (Ac-DEX) microparticles (MPs) containing candidate broadscale and targeted immune boosting molecules (UNC, Duke-NUS). **Subtask 9.2** Test MP metrics *in vitro* and in rodents (UNC). **Subtask 9.3** Test MP safety in bats in Wisconsin and in Singapore (NWHC, Duke-NUS).
Milestone(s): Initiation and completion of each subtask.
Deliverables: Ac-DEX MPs that contain broadscale or targeted immune boosting molecules available for use. Data from MP efficacy and safety trials.

PI-TA-02 Task 10: Develop and assess delivery systems to deploy immune boosting molecules (NWHC, PARC)
Subtask 10.1 Test transcutaneous delivery methods using the biomarker Rhodamine (RB) on captive US bats (NWHC). **Subtask 10.2** Conduct field trials of RB-marked delivery substances on

wild US bats (NWHC). *Subtask 10.3* Develop prototype filament extension atomization (FEA) device (PARC). *Subtask 10.4* Trial FEA device using RB on US captive bats (NWHC)
Milestone(s): Initiation and completion of each subtask.
Deliverables: Data from transcutaneous delivery experiments in captive and wild bats. Prototype of FEA device. Proof-of-concept of FEA device delivery system.

<u>PHASE II:</u>
PII-TA-01 Task 1 (continued from PI-TA-01 Task 2): Updated 'spatial viral spillover risk' app based on laboratory and field experiments (EHA).
Subtask 1.1 Incorporate information on bat species risk from laboratory and field results (EHA).
Subtask 1.2 Incorporate risk-ranking algorithmns using geolocation features and host-pathogen characteristics (EHA). *Subtask 1.3* Link host species with viral diversity data from the project and previous data (EHA).
Milestone(s): Initiation and completion of each subtask.
Deliverables: Working prototype app that displays information by pathogen ranking, bat species ranking, and geographical ranking.

PII-TA-01 Task 2 (continued from PI-TA-01 Task 5): Build and test Bayesian network models to predict genotype-phenotype spillover potential of high-risk SARSr-CoV strains. (EHA).
Subtask 2.1 Estimate intra- and inter-species mutation and recombination rates in SARSr-CoV population (EHA). *Subtask 2.2* Simulate forward evolution to predict future and unsampled QS (EHA). *Subtask 2.3* Make predictions of likely future high-risk QS spillover (EHA)
Milestone(s): Initiation and completion of each subtask.
Deliverables: Source code and model outputs from functional model. Prediction of future QS variants. Identification of high-risk SARSr-CoV QS by network machine-learning model.

PII-TA-02 Task 3 (continued from PI-TA-02-10): Develop and assess delivery systems to deploy immune boosting molecules (NWHC, PARC)
Subtask 3.1 Design and optimize motion- and time- actuated facility for FEA prototype (PARC).
Subtask 3.2 Conduct field trials of RB-marked delivery substances using FEA motion-actuated prototype on wild bats in Wisconsin (PARC, NWHC).
Milestone(s): FEA deployment prototype designed; field trials completed.
Deliverables: Optimized FEA prototype with motion- and time- actuated facility. Proof-of-concept FEA delivery of RB-marked substances in wild bats.

PII-TA-02 Task 4: Build and test dynamic circulation models to optimize deployment strategy
Subtask 4.1 Develop robust stochastic SIR process model with immigration/emigration and flexible nonlinear contact rates among bats (EHA). *Subtask 4.2* Fit SIR model to sampling data from Yunnan test cave using partially observable markov process framework and validate via temporal cross-validation (EHA). *Subtask 4.3* Simulate viral circulation under series of plausible deployment scenarios to determine optimal scenario for deployment at test cave sites (EHA). *Subtask 4.4* Test robustness of deployment strategies under broader conditions.
Milestone(s): Initiation and completion of each subtask.
Deliverables: Source code and outputs from dynamic circulation models; Optimized scenario for deployment.

PH-TA-02 Task 5: Demonstrate accuracy of risk/pre-emption models then deploy most effective molecule delivery methods to suppress viral shedding in multispecies bat colonies of Yunnan Province caves (EHA, PARC, NWHC, Duke-NUS, UNC)

Subtask 5.1 Identify specific sites (entry, exit points), identify FEA automatic aerosolization points, fine-tune deployment plan. (EHA, WIV, NWHC, Duke-NUS, PARC, UNC). **Subtask 5.2** Conduct bat viral surveillance of one test-site cave and two control caves at our cave complex to assess baseline data for 4 months before deployment proof-of-concept experiment (EHA Consultant Zhu, WIV). **Subtask 5.3** Run deployment experiment of most effective immune boosting molecules and delivery techniques via FEA aerosolization mechanism at one test and two control bat cave sites in Yunnan, China (PARC, EHA, WIV) **Subtask 5.4** Conduct bat viral surveillance of one test-site cave and two control caves for 4 months after deployment. (EHA Consultant Zhu, WIV). **Subtask 5.5** Assess efficacy of proof-of-concept trial (EHA, UNC, DNUS). **Milestone(s):** Specific sites identified; Initiation and completion of trial under subtask 5.2-5.5. **Deliverables:** Baseline immunology and viral shedding data from study populations. Proof-of-concept of deploying biological intervention. Post-deployment metrics for immune modulation and viral shedding in study populations. Report on proof-of-concept efficacy.

Section II	H. SCHEDULE AND MILESTONES

See Table 2 Schedules and Milestones.

Section II	I. PREEMPT TRANSITION PLAN

Technology from this project will be transitioned to multiple potential users throughout both phases. Partners PARC and the USGS National Wildlife Health Center will initiate planning for transition of aerosol deployment equipment within 12 months of Phase 1 including government customers such as DoD and USGS (for bat-related disease control) and possible manufacturers. IP rights for these efforts will be negotiated with DARPA. Prior to the completion of Phase 1, panels of fully sequence new viruses, in-silico models for pandemic prediction, and animal models that could be used to evaluate therapeutics will be shared with DARPA and collaboratively agreed upon for early distribution to DoD users such as DoD medical community, other UGS agencies, and ultimately made publically available. We have no plans to patent or otherwise restrict IP on this information unless requested by DARPA or requested by a project partner and approved by DARPA. Proposed technology to be experimentally deployed and evaluated in Phase 2 will be shared with DARPA and collaboratively agreed upon for early distribution to DoD users such as DoD medical community, other UGS agencies. We have no plans to patent or otherwise restrict IP on this information unless requested by DARPA or requested by a project partner and approved by DARPA.

PARC as a private industry partner (large business) is a fully-owned subsidiary of Xerox Corporation and is committed to commercializing the FEA technology through IP licensing for different applications spaces to different commercial partners. PARC has been and will continue to engage potential licensees (OEMs) in the biotechnology and biomedical fields for eventual transitioning of targeted delivery technology potentially developed in DEFUSE. PARC already has existing networks of business relations in the biotechnology and biomedical space, both large companies (Fortune 500, Fortune 1000) and small businesses and start-ups who could be transition partners for FEA as a wide-scale, large-area drug delivery device. In addition, in

Table 2. Schedule & Milestones

	Task #	Task Name/Milestones	Organization	Phase I Y1				Phase I Y2				Phase II OY1				OY2	
				Q1	Q2	Q3	Q4	Q1	Q2	Q3	Q4	Q1	Q2	Q3	Q4	Q1	Q2
	PI-Task 1	**Longitudinal sampling and surveillance**	EHA														
	1.1	IACUC and ACURO approval / Permits obtained	EHA														
	1.2	Invasive and non-invasive monthly specimen collection / >3,000 specimens collected	EHA (Zhu)														
	1.3	Bat connectivity and roost fidelity study / All bats PIT tagged	EHA (Zhu)														
	1.4	Assess bat home ranges / Bat transmitters launched; data collected	EHA (Zhu)														
	1.5	Real-time bat population monitoring / IR cameras installed; data collected	EHA (Zhu)														
	1.6	Develop and maintain project database / Database built & secure; field data entered	EHA														
	PI-Task 2	**Construct spillover risk models**	EHA														
	2.1	Joint species distribution models / Models fit for Asian bat spp.; cave-level predictions	EHA														
	2.2	Host and ecological machine learning models / Models developed; per-species spillover risk	EHA														
	2.3	Viral richness estimator model / Models developed and refined w longitudinal surveillance data	EHA														
	2.4	Prototype of 'spatial viral spillover risk' app / Prototype app developed and beta-tested	EHA														
	PI-Task 3	**Laboratory analysis of SARSr-CoV QS**	WIV														
	3.1	PCR screening of bat specimens / Prevalance estimates; initial CoV seq data generated	WIV														
	3.2	Sequence SARSr-CoV spike proteins / Genetic sequences generated and made available	WIV														
	3.3	Develop recombinant SARSr-CoV viruses / Novel recombinants developed and recovered	DNUS														
	3.4	Assess SARSr-CoV via deep sequencing / Full genome data generated and made available	UNC														
	PI-Task 4	**Experimental assays of SARSr-CoV QS**	UNC														
	4.1	Pre-screen SARSr-CoV via viral traits / List of pre-screened QS using protein models and mutations	UNC														
	4.2	SARSr-CoV chimeric virus testing in cell lines / In vitro cell line experiments completed; data available	UNC														
	4.3	In vivo pathogenesis in hACE2 transgenic mice / Mouse experiments completed; data available	UNC														
	4.4	Validate chimeric viruses by with full-genome QS / Full genomes sequenced and made available	UNC														
	4.5	Test synthetic modifications of spike proteins / Experimental tests completed; data available	UNC														
	4.6	Test effects of low-abundance, high consequence micro-variations on jump potential / Variants quantified	UNC														
	PI-Task 5	**Build and test Bayesian genotype-phenotype network models**	EHA														
	5.1	Use prior data to guide GS selection for characterization / Prelim model developed; source code available	EHA														
	5.2	Update model predictions using real-time data / Model refined and validated w experimental data	EHA														
	PI-Task 6	**Validate model predictions using human spillover evidence**	WIV														
	6.1	Design LIPS assays to SARS-CoV we have characterized / Novel LIPS assays developed	WIV														
	6.2	Determine LIPS assays specificity / Specificity tested in rabbit model and data made available	WIV														
	6.3	Validate LIPS assays using positive laboratory samples / Assays validated and data made available	WIV														
	6.4	Test previously-collected human sera for SARS-CoV spillover / Previous-collected human sera screened	WIV														
	6.5	Validate BNM predictions using bat-human contact data / Bayesian network model externally validated	EHA														
	PI-Task 7	**Testing of broadscale immune boosting approach**	DNUS														
	7.1	Block bat-specific IFN negative regulators / Experiments completed; data made available	DNUS														
	7.2	Activate dampened bat-specific innate immune pathways / Experiments and immune profiling completed	DNUS														
	7.3	Test broadscale immune boosting in bat-mouse model / Experiments completed; data made available	DNUS														
	7.4	Test broadscale immune boosting in Eonycteris sp. / Experiments completed; data made available	DNUS														
	7.5	Test broadscale immune boosting in Rhinolophus sp. / Experiments completed; data made available	WIV														
	PI-Task 8	**Testing of targeted immune boosting approach**	UNC														

Left row groupings:
- **TA1 Phase I** — spans PI-Task 1 through PI-Task 6
- **TA2 Phase I** — spans PI-Task 7 through PI-Task 8

	ID	Milestone / Deliverable	Lead
TA2 Phase I	8.1	Develop chimeric SARSr-CoV S immunogens / Chimeras developed and made available for experiments	UNC
	8.2	Test chimeric immunogens in humanized mice / Experiments completed; data made available	UNC
	8.3	Create raccoon poxvirus vectored immune boosting approach / Experimental validation complete	NWHC
	8.4	Test targeted immune boosting in Eonycteris sp. / Experiments completed; data made available	DNUS
	8.5	Test targeted immune boosting in Rhinolophus spp. / Experiments completed; data made available	WIV
	PI-Task 9	**Develop transcutaneous delivery methods**	
	9.1	Synthesize Ac-DEX MPs / Microparticles synthesized w immune boosting molecules	UNC, DNUS, NWHC
	9.2	Test MP metrics in vitro and in rodents / Experiments completed in rodents; data made available	UNC, DNUS
	9.3	Test MB safety in bats in WI and Singapore / Safety experiments completed in bats; data made available	UNC, DNUS
	PI-Task 10	**Develop delivery systems for immune boosting molecules**	NWHC, DNUS
	10.1	Trial RB-marked substances on captive bats / Experiments completed in captive bats; data available	NWHC, PARC
	10.2	Trial RB-marked substances on wild bats / Experiments completed in wild bats; data available	NWHC
	10.3	Develop prototype FEA device / Prototype FEA device developed to deploy immune boosting molecules	PARC
	10.4	Trial FEA device using RB on US captive bats / Prototype FEA device tested on captive bats	NWHC
TA1 Phase II	**PII-Task 1**	**Update 'spatial viral spillover risk' app**	EHA
	1.1	Incorporate laboratory and field results / Bat species risk metrics from lab and field incoporated to model	EHA
	1.2	Incorporate spatial and host-pathogen characteristics to risk ranking / Models and source code updated	EHA
	1.3	Link host species to viral diversity data / Viral data integrated into host-pathogen spillover models	EHA
PII-Task 2	**PII-Task 2**	**Build and test Bayesian genotype-phenotype network models**	EHA
	2.1	Estimate intra- and inter-species mutation and recombination rates / Recombination analyses completed	EHA
	2.2	Simulate forward evolution to predict future and unsampled QS / List of predicted future QS variants	EHA
	2.3	Make predictions of likely future high-risk QS spillover / High-risk SARSr-CoV QSs identified by model	EHA
	PII-Task 3	**Develop delivery systems for immune boosting molecules**	PARC, NWHC
	3.1	Design and optimize facility for FEA prototype / Develop motion- and time- actuated delivery system	PARC
	3.2	Conduct field trials of RB on US wild bats / Field trials completed on wild bats; data available	PARC, NWHC
PII-Task 4	**PII-Task 4**	**Build and test models to optimize deployment strategy**	EHA
	4.1	Develop robust stochastic SIR process model / Model developed including bat contact rates	EHA
	4.2	Fit SIR model to sampling data / Fit SIR model using markov process; temporal cross-validation	EHA
	4.3	Simulate deployment scenarios / Develop scenario model simulations to optimize deployment	EHA
	4.4	Test robustness of deployment strategies / Various deployment scenarios tested w cave-specific data	EHA
TA2 Phase II	**PII-Task 5**	**Demonstrate accuracy of delivery models and deploy methods**	All Orgs
	5.1	Identify specific sites and fine tune deployment plan / Identify specific sites within caves for deployment	All Orgs
	5.2	Conduct baseline viral surveillance pre deployment / Complete 4 month pre-deployment surveillance	EHA, WIV
	5.3	Run deployment experiment / Deploy immune boosting intervention at one test cave site and two controls	EHA (Zhu), NHWC, PARC
	5.4	Conduct viral surveillance post deployment / Complete 4 month post-deployment surveillance	EHA, WIV
	5.5	Assess efficacy of proof-of-concept trial / Data analyzed; including pre- and post- lab screening data	EHA, UNC, DNUS

collaboration with our extended network of DEFUSE partners and with DARPA, we will further identify existing government needs for our delivery technology, particularly in wildlife health management (in collaboration with EHA and USGS-NWHC) and in suppression of emerging threats (in collaboration with government agencies such as the CDC). PARC will leverage this knowledge in developing a needs-based commercialization plan with potential partners.

Project DEFUSE partners come from academic, government, private industry, private non-profit institutions and will develop a coherent transition plan for research findings, data and any technology developed in this work.

Section II	J. PREEMPT RISK MITIGATION PLAN

Risks: Personnel safety, biosafety, mitigation of risks to public health and animal safety

Animal Use & safety: All work with wild bats will be conducted in China by EcoHealth Alliance staff and Wuhan Institute of Virology. Capture and sampling techniques have been previously approved by Tufts University School of Veterinary Medicine IACUC under our NIH NIAID award (Daszak, PI). Experimental work using bats and or transgenic mice will be conducted at the BSL-3 lab in WIV, Duke-NUS, UNC, or NWHC. Each partner institute will apply for and procure animal research approval from its respective IACUC. All animal work conducted by EcoHealth Alliance in China will be overseen by both the IACUC at WIV and the IACUC at Tufts. Each partner institute will be responsible for ensuring the training and safety of its laboratory personnel, which will be documented by EcoHealth Alliance, and each partner has extensive experience and a record of safety with the techniques and procedures for lab animal experiments described in this protocol. *Field safety:* Free-ranging bats will be captured using either a mist net or harp trap. The net system is manned by two people during the entire capture period, and bats are removed from the net as soon as they become entangled to minimize stress and prevent injury. In our experience, a maximum of 20-30 bats can be safely held and processed by a team of three people per trapping period. Duration of trapping will depend on the capture rate. Bats are placed into a small cloth bag and hung from a branch or post until samples are collected. Bats are held for a maximum of six hours. Field personnel will be required to conduct a hazard assessment prior to each field sampling period and at each location. *Biosafety and Personal Protective Equipment:* Dedicated clothing will be worn in the field which provides protection against injury from bites or scratches as well as nitrile gloves (double layer), an N95 respirator, and safety glasses or a face shield when removing bats from a net or trap, and when sampling bats. External clothing and all equipment will be decontaminated at the field site using virkon, and biohazardous waste will be contained in biohazard bags and sharps containers and incinerated at WIV or Yunnan CDC facilities. Personnel will wear water-impermeable Tyvek suits, rubber boots, and powered air purifying respirators (PAPRs) when entering a cave for sample collection or image collection (e.g. LiDAR) and will doff and dispose of PPE and disinfect PAPRs on exiting the cave. **All field personnel will be immunized against rabies and demonstrate a current (within 6 months) protective titer according to CDC guidelines[132].** Personnel without PPE training and complete rabies immunization will not be permitted to work with bats or enter the study caves. Use of LiDAR to map study caves will be conducted by trained personnel with caving experience.

Risks to general public: The proposed work has minimal risk to the general public, as sampling will be done near the cave sites and not in populous areas. Our team has extensive experience

Section II   K. ETHICAL, LEGAL, SOCIETAL IMPLICATIONS

All activities in this project will be done with strict adherence to US and Chinese law, with permission from the Chinese government and local authorities to conduct field work. We will conduct educational outreach to local wildlife authorities and cultural leaders so that there is a public understanding of what we are doing and why we are doing it, particularly because of the common practice of bat consumption in the region (**see also Risk Mitigation Strategy**). These agents have not been tested on humans, but they have been shown to be safe in a variety of lab animal models. There is minimal risk associated with human exposure to the fluid containing MPs. We will explain the risk mitigation strategies and safety data that were considered when developing this study, and how this could be of benefit to local communities. There is also a potential benefit to local communities if the agents are effective in reducing viral shedding. The broader societal impact of this project could be significant, as wildlife immunization against viral zoonoses has been limited to date. However, this may open up a field where animal reservoirs for known high-risk agents could be "immunized" at high risk times of year which could reduce the number or magnitude of human outbreaks. This would add a valuable countermeasure to ecological studies that have elucidated the timing of viral spillover from animal reservoirs to human or livestock populations. We will develop a plan to ensure that the details of technologies developed and tested for deploying biological immune modulating agents are made available publicly so that they can be adapted to other types of medical interventions and pathogens. There may be conservation benefits, where wildlife reservoirs are considered less threatening to public health and therefore there may be less impetus to exterminate or extirpate local populations as a public health measure – particularly if an option to reduce the risk of spillover through a wildlife vaccination effort is available.

Section III   **BIBLIOGRAPHY**

1   Anthony, S. J. *et al.* Global patterns in coronavirus diversity. *Virus Evolution* **3**, doi:10.1093/ve/vex012 (2017).

2   Ge, X. Y. *et al.* Isolation and characterization of a bat SARS-like coronavirus that uses the ACE2 receptor. *Nature* **503**, 535-538, doi:10.1038/nature12711 (2013).

3   Li, W. D. *et al.* Bats are natural reservoirs of SARS-like coronaviruses. *Science* **310**, 676-679, doi:10.1126/science.1118391 (2005).

4   Quan, P.-L. *et al.* Identification of a severe acute respiratory syndrome coronavirus-like virus in a leaf-nosed bat in Nigeria. *MBio* **1**, e00208-00210 (2010).

5   Ar Gouilh, M. *et al.* SARS-CoV related Betacoronavirus and diverse Alphacoronavirus members found in western old-world. *Virology* **517**, 88-97, doi:https://doi.org/10.1016/j.virol.2018.01.014 (2018).

6   Drexler, J. F. *et al.* Genomic characterization of severe acute respiratory syndrome-related coronavirus in European bats and classification of coronaviruses based on partial RNA-dependent RNA polymerase gene sequences. *J Virol* **84**, 11336-11349, doi:10.1128/JVI.00650-10 (2010).

7   Olival, K. J. *et al.* Host and viral traits predict zoonotic spillover from mammals. *Nature* **546**, 646-650 (2017).

8   Sheahan, T. P. *et al.* Broad-spectrum antiviral GS-5734 inhibits both epidemic and zoonotic coronaviruses. *Science translational medicine* **9**, eaal3653 (2017).

9   Anthony, S. *et al.* Further evidence for bats as the evolutionary source of Middle East respiratory syndrome coronavirus. *MBio* **8**, e00373-00317 (2017).

10   Cockrell, A. S. *et al.* A mouse model for MERS coronavirus-induced acute respiratory distress syndrome. *Nature microbiology* **2**, 16226 (2017).

11   Menachery, V. D. *et al.* SARS-like WIV1-CoV poised for human emergence. *Proceedings of the National Academy of Sciences of the United States of America* **113**, 3048-3053, doi:10.1073/pnas.1517719113 (2016).

12   Menachery, V. D. *et al.* A SARS-like cluster of circulating bat coronaviruses shows potential for human emergence. *Nature Medicine* **21**, 1508-1513, doi:10.1038/nm.3985 (2015).

13   Wang, N. *et al.* Serological Evidence of Bat SARS-Related Coronavirus Infection in Humans, China. *Virologica Sinica*, doi:10.1007/s12250-018-0012-7 (2018).

14   Zhou, P. *et al.* Fatal swine acute diarrhea syndrome caused by an HKU2-related coronavirus of bat origin. *Nature* **In press** (2018).

15   Zhang, G. *et al.* Comparative analysis of bat genomes provides insight into the evolution of flight and immunity. *Science* **339**, 456-460, doi:10.1126/science.1230835 (2013).

16   Xie, J. *et al.* Dampened STING-Dependent Interferon Activation in Bats. *Cell host & microbe* (2018).

17   Zhou, P. *et al.* Contraction of the type I IFN locus and unusual constitutive expression of IFN-α in bats. *Proceedings of the National Academy of Sciences* **113**, 2696-2701 (2016).

18   Kugel, D. *et al.* Intranasal Administration of Alpha Interferon Reduces Seasonal Influenza A Virus Morbidity in Ferrets. *Journal of Virology* **83**, 3843-3851, doi:10.1128/jvi.02453-08 (2009).

19   Zhao, J. *et al.* Intranasal treatment with poly (I· C) protects aged mice from lethal respiratory virus infections. *Journal of virology* **86**, 11416-11424 (2012).

20   Smith, L. M. *et al.* Interferon-β therapy prolongs survival in rhesus macaque models of Ebola and Marburg hemorrhagic fever. *The Journal of infectious diseases* **208**, 310-318 (2013).

21   Zeng, L.-P. *et al.* Bat Severe Acute Respiratory Syndrome-Like Coronavirus WIV1 Encodes an Extra Accessory Protein, ORFX, Involved in Modulation of the Host Immune Response. *Journal of Virology* **90**, 6573-6582, doi:10.1128/jvi.03079-15 (2016).

22   Deng, X. *et al.* A chimeric virus-mouse model system for evaluating the function and inhibition of papain-like proteases of emerging coronaviruses. *Journal of virology* **88**, 11825-11833 (2014).

23   Pallesen, J. *et al.* Immunogenicity and structures of a rationally designed prefusion MERS-CoV spike antigen. *Proceedings of the National Academy of Sciences* **114**, E7348-E7357 (2017).

24   Coleman, C. M. *et al.* Purified coronavirus spike protein nanoparticles induce coronavirus neutralizing antibodies in mice. *Vaccine* **32**, 3169-3174 (2014).

25   Coleman, C. M. *et al.* MERS-CoV spike nanoparticles protect mice from MERS-CoV infection. *Vaccine* **35**, 1586-1589, doi:10.1016/j.vaccine.2017.02.012 (2017).

26   Du, L. *et al.* A 219-mer CHO-expressing receptor-binding domain of SARS-CoV S protein induces potent immune responses and protective immunity. *Viral immunology* **23**, 211-219 (2010).

27   Sheahan, T. *et al.* Successful vaccination strategies that protect aged mice from lethal challenge from influenza virus and heterologous severe acute respiratory syndrome coronavirus. *Journal of virology* **85**, 217-230 (2011).

28   Agnihothram, S. *et al.* A mouse model for Betacoronavirus subgroup 2c using a bat coronavirus strain HKU5 variant. *MBio* **5**, e00047-00014 (2014).

29   Becker, M. M. *et al.* Synthetic recombinant bat SARS-like coronavirus is infectious in cultured cells and in mice. *Proc Natl Acad Sci U S A* **105**, 19944-19949 (2008).

30   Rocke, T. E. *et al.* Sylvatic plague vaccine partially protects prairie dogs (Cynomys spp.) in field trials. *Ecohealth* **14**, 438-450 (2017).

31   Stading, B. *et al.* Protection of bats (*Eptesicus fuscus*) against rabies following topical or oronasal exposure to a recombinant raccoon poxvirus vaccine. *Plos Neglect. Trop. Dis.* **11**, doi:10.1371/journal.pntd.0005958 (2017).

32   Stading, B. R. *et al.* Infectivity of attenuated poxvirus vaccine vectors and immunogenicity of a raccoonpox vectored rabies vaccine in the Brazilian Free-tailed bat (Tadarida brasiliensis). *Vaccine* **34**, 5352-5358, doi:10.1016/j.vaccine.2016.08.088 (2016).

33   Yang, X. L. *et al.* Isolation and Characterization of a Novel Bat Coronavirus Closely Related to the Direct Progenitor of Severe Acute Respiratory Syndrome Coronavirus. *Journal of Virology* **90**, 3253-3256, doi:10.1128/jvi.02582-15 (2016).

34   Hu, B. *et al.* Discovery of a rich gene pool of bat SARS-related coronaviruses provides new insights into the origin of SARS coronavirus. *PLoS pathogens* **13**, e1006698, doi:10.1371/journal.ppat.1006698 (2017).

35   Yuan, J. *et al.* Intraspecies diversity of SARS-like coronaviruses in Rhinolophus sinicus and its implications for the origin of SARS coronaviruses in humans. *Journal of general virology* **91**, 1058-1062 (2010).

36   Li, W. *et al.* Angiotensin-converting enzyme 2 is a functional receptor for the SARS coronavirus. *Nature* **426**, 450 (2003).

37   Memish, Z. A. *et al.* Middle East Respiratory Syndrome Coronavirus in Bats, Saudi Arabia. *Emerging Infectious Diseases* **19**, 1819-1823, doi:10.3201/eid1911.131172 (2013).

38   Walker, F. M., Williamson, C. H., Sanchez, D. E., Sobek, C. J. & Chambers, C. L. Species from feces: order-wide identification of Chiroptera from guano and other non-invasive genetic samples. *PloS one* **11**, e0162342 (2016).

39   Hayman, D. T. S., Cryan, P. M., Fricker, P. D., Dannemiller, N. G. & Freckleton, R. Long-term video surveillance and automated analyses reveal arousal patterns in groups of hibernating bats. *Methods in Ecology and Evolution* **8**, 1813-1821, doi:doi:10.1111/2041-210X.12823 (2017).

40   Azmy, S. N. *et al.* Counting in the dark: Non-intrusive laser scanning for population counting and identifying roosting bats. *Scientific reports* **2**, 524 (2012).

41   Shazali, N. *et al.* Assessing Bat Roosts Using the LiDAR System at Wind Cave Nature Reserve in Sarawak, Malaysian Borneo. *Acta Chiropterologica* **19**, 199-210 (2017).

42   McFarlane, D. A. *et al.* Terrestrial LiDAR-based automated counting of swiftlet nests in the caves of Gomantong, Sabah, Borneo. *International Journal of Speleology* **44**, 191 (2015).

43   Harris, D. J. Generating realistic assemblages with a joint species distribution model. *Methods in Ecology and Evolution* **6**, 465-473 (2015).

44   Luo, J. *et al.* Bat conservation in China: should protection of subterranean habitats be a priority? *Oryx* **47**, 526-531 (2013).

45   Karger, D. N. *et al.* Climatologies at high resolution for the earth's land surface areas. *Scientific data* **4**, 170122 (2017).

46   Phelps, K., Jose, R., Labonite, M. & Kingston, T. Correlates of cave-roosting bat diversity as an effective tool to identify priority caves. *Biological Conservation* **201**, 201-209 (2016).

47   IUCN. Vol. 2017-1 (2017).

48   GBIF.org. GBIF Occurrence Download.

49   Allen, T. *et al.* Global hotspots and correlates of emerging zoonotic diseases. *Nature Communications* **8**, 1124 (2017).

50   Anthony, S. J. *et al.* A strategy to estimate unknown viral diversity in mammals. *mBio* **4**, e00598-00513 (2013).

51   Wildlife Acoustics. *Wildlife Acoustics Bioacoustic Monitoring System*, <https://www.wildlifeacoustics.com/products/echo-meter-touch-2?gclid=EAIaIQobChMI3qnOmK_o2QIVDlcNCh1KRwZuEAAYASAAEgJvVPD_BwE> (2018).

52   Mac Aodha, O. *et al.* Bat Detective-Deep Learning Tools for Bat Acoustic Signal Detection. *bioRxiv*, 156869 (2017).

53   Anthony, S. J. *et al.* Coronaviruses in bats from Mexico. *Journal of General Virology* **94**, 1028-1038 (2013).

54   Huynh, J. *et al.* Evidence Supporting a Zoonotic Origin of Human Coronavirus Strain NL63. *Journal of Virology* **86**, 12816-12825, doi:10.1128/jvi.00906-12 (2012).

55   Donaldson, E. F. *et al.* Systematic Assembly of a Full-Length Infectious Clone of Human Coronavirus NL63. *Journal of Virology* **82**, 11948-11957, doi:10.1128/jvi.01804-08 (2008).

56   Scobey, T. *et al.* Reverse genetics with a full-length infectious cDNA of the Middle East respiratory syndrome coronavirus. *Proceedings of the National Academy of Sciences of the United States of America* **110**, 16157-16162, doi:10.1073/pnas.1311542110 (2013).

57   Yount, B. *et al.* Reverse genetics with a full-length infectious cDNA of severe acute respiratory syndrome coronavirus. *Proceedings of the National Academy of Sciences of the United States of America* **100**, 12995-13000, doi:10.1073/pnas.1735582100 (2003).

58   Sheahan, T. *et al.* Mechanisms of zoonotic severe acute respiratory syndrome coronavirus host range expansion in human airway epithelium. *Journal of Virology* **82**, 2274-2285, doi:10.1128/jvi.02041-07 (2008).

59   Kirchdoerfer, R. N. *et al.* Pre-fusion structure of a human coronavirus spike protein. *Nature* **531**, 118-121, doi:10.1038/nature17200 (2016).

60   Gui, M. *et al.* Cryo-electron microscopy structures of the SARS-CoV spike glycoprotein reveal a prerequisite conformational state for receptor binding. *Cell Res.* **27**, 119-129, doi:10.1038/cr.2016.152 (2017).

61   Li, F. Structural analysis of major species barriers between humans and palm civets for severe acute respiratory syndrome coronavirus infections. *Journal of Virology* **82**, 6984-6991, doi:10.1128/jvi.00442-08 (2008).

62   Li, F., Li, W. H., Farzan, M. & Harrison, S. C. Structure of SARS coronavirus spike receptor-binding domain complexed with receptor. *Science* **309**, 1864-1868, doi:10.1126/science.1116480 (2005).

63   Huang, I. C. *et al.* SARS coronavirus, but not human coronavirus NL63, utilizes cathepsin L to infect ACE2-expressing cells. *Journal of Biological Chemistry* **281**, 3198-3203, doi:10.1074/jbc.M508381200 (2006).

64   Yang, Y. *et al.* Receptor usage and cell entry of bat coronavirus HKU4 provide insight into bat-to-human transmission of MERS coronavirus. *Proceedings of the National Academy of Sciences of the United States of America* **111**, 12516-12521, doi:10.1073/pnas.1405889111 (2014).

65   Earnest, J. T. *et al.* The tetraspanin CD9 facilitates MERS-coronavirus entry by scaffolding host cell receptors and proteases. *PLoS pathogens* **13**, doi:10.1371/journal.ppat.1006546 (2017).

66   Rockx, B. *et al.* Escape from Human Monoclonal Antibody Neutralization Affects In Vitro and In Vivo Fitness of Severe Acute Respiratory Syndrome Coronavirus. *Journal of Infectious Diseases* **201**, 946-955, doi:10.1086/651022 (2010).

67   Zeng, L. P. *et al.* Cross-neutralization of SARS coronavirus-specific antibodies against bat SARS-like coronaviruses. *Science China-Life Sciences* **60**, 1399-1402, doi:10.1007/s11427-017-9189-3 (2017).

68   Bertram, S. *et al.* Cleavage and Activation of the Severe Acute Respiratory Syndrome
        Coronavirus Spike Protein by Human Airway Trypsin-Like Protease. *Journal of
        Virology* **85**, 13363-13372, doi:10.1128/JVI.05300-11 (2011).

69   Simmons, G., Zmora, P., Gierer, S., Heurich, A. & Pöhlmann, S. Proteolytic activation
        of the SARS-coronavirus spike protein: Cutting enzymes at the cutting edge of
        antiviral research. *Antiviral research* **100**, 605-614,
        doi:10.1016/j.antiviral.2013.09.028 (2013).

70   Reinke, L. M. *et al.* Different residues in the SARS-CoV spike protein determine
        cleavage and activation by the host cell protease TMPRSS2. *PLoS ONE* **12**, e0179177,
        doi:10.1371/journal.pone.0179177 (2017).

71   Lu, G. W., Wang, Q. H. & Gao, G. F. Bat-to-human: spike features determining 'host
        jump' of coronaviruses SARS-CoV, MERS-CoV, and beyond. *Trends in Microbiology*
        23, 468-478, doi:10.1016/j.tim.2015.06.003 (2015).

72   Walls, A. C. *et al.* Tectonic conformational changes of a coronavirus spike
        glycoprotein promote membrane fusion. *Proceedings of the National Academy of
        Sciences of the United States of America* **114**, 11157-11162,
        doi:10.1073/pnas.1708727114 (2017).

73   Li, F. Structure, Function, and Evolution of Coronavirus Spike Proteins. *Annual
        review of virology* **3**, 237-261, doi:10.1146/annurev-virology-110615-042301
        (2016).

74   Duckert, P., Brunak, S. & Blom, N. Prediction of proprotein convertase cleavage sites.
        Protein Engineering Design & Selection **17**, 107-112, doi:10.1093/protein/gzh013
        (2004).

75   Tian, S., Huajun, W. & Wu, J. Computational prediction of furin cleavage sites by a
        hybrid method and understanding mechanism underlying diseases. *Scientific
        Reports* **2**, 261, doi:10.1038/srep00261 (2012).

76   Shih, Y.-P. *et al.* Identifying Epitopes Responsible for Neutralizing Antibody and DC-
        SIGN Binding on the Spike Glycoprotein of the Severe Acute Respiratory Syndrome
        Coronavirus. *Journal of Virology* **80**, 10315-10324, doi:10.1128/JVI.01138-06
        (2006).

77   Han, D. P., Lohani, M. & Cho, M. W. Specific Asparagine-Linked Glycosylation Sites
        Are Critical for DC-SIGN- and L-SIGN-Mediated Severe Acute Respiratory Syndrome
        Coronavirus Entry. *Journal of Virology* **81**, 12029-12039, doi:10.1128/JVI.00315-07
        (2007).

78   Nagarajan, R., Scutari, M. & Lèbre, S. *Bayesian Networks in R*. (Springer, 2013).

79   Landuyt, D. *et al.* A review of Bayesian belief networks in ecosystem service
        modelling. *Environmental Modelling & Software* **46**, 1-11,
        doi:https://doi.org/10.1016/j.envsoft.2013.03.011 (2013).

80   Li, W. *et al.* Bats are natural reservoirs of SARS-like coronaviruses. *Science* **310**, 676-
        679, doi:10.1126/science.1118391 (2005).

81   Li, Y. *et al.* Antibodies to Nipah or Nipah-like viruses in bats, China. *Emerg Infect Dis*
        14, 1974-1976, doi:10.3201/eid1412.080359 (2008).

82   Drummond, A. J. & Rambaut, A. BEAST: Bayesian evolutionary analysis by sampling
        trees. *BMC Evolutionary Biology* **7**, 214 (2007).

83   McVean, G., Awadalla, P. & Fearnhead, P. A coalescent-based method for detecting and estimating recombination from gene sequences. *Genetics* **160**, 1231-1241 (2002).

84   Wilson, D. J. & McVean, G. Estimating diversifying selection and functional constraint in the presence of recombination. *Genetics* **172**, 1411-1425 (2006).

85   Martin, D. P., Murrell, B., Golden, M., Khoosal, A. & Muhire, B. RDP4: Detection and analysis of recombination patterns in virus genomes. *Virus evolution* **1** (2015).

86   Petitjean, M. & Vanet, A. VIRAPOPS: a forward simulator dedicated to rapidly evolved viral populations. *Bioinformatics* **30**, 578-580 (2013).

87   Ahn, M., Cui, J., Irving, A. T. & Wang, L.-F. Unique Loss of the PYHIN Gene Family in Bats Amongst Mammals: Implications for Inflammasome Sensing. *Scientific Reports* **6**, doi:10.1038/srep21722 (2016).

88   Ahn, M., Irving, A. T. & Wang, L. F. Unusual regulation of inflammasome signaling in bats. *Cytokine* **87**, 156-156 (2016).

89   Paweska, J. T. *et al.* Lack of Marburg virus transmission from experimentally infected to susceptible in-contact Egyptian fruit bats. *The Journal of infectious diseases* **212**, S109-S118 (2015).

90   Paweska, J. T. *et al.* Virological and serological findings in Rousettus aegyptiacus experimentally inoculated with vero cells-adapted hogan strain of Marburg virus. *PloS one* **7**, e45479 (2012).

91   Schuh, A. J. *et al.* Modelling filovirus maintenance in nature by experimental transmission of Marburg virus between Egyptian rousette bats. *Nature communications* **8**, 14446 (2017).

92   Cogswell-Hawkinson, A. *et al.* Tacaribe virus causes fatal infection of an ostensible reservoir host, the Jamaican fruit bat. *J Virol* **86**, 5791-5799, doi:10.1128/JVI.00201-12 (2012).

93   Zhou, P. *et al.* Unlocking bat immunology: establishment of Pteropus alecto bone marrow-derived dendritic cells and macrophages. *Scientific Reports* **6**, 38597, doi:10.1038/srep38597 https://www.nature.com/articles/srep38597#supplementary-information (2016).

94   Farr, B., Gwaltney, J., Adams, K. & Hayden, F. Intranasal interferon-alpha 2 for prevention of natural rhinovirus colds. *Antimicrobial agents and chemotherapy* **26**, 31-34 (2009).

95   Zhang, Q. *et al.* IFNAR2-dependent gene expression profile induced by IFN-α in Pteropus alecto bat cells and impact of IFNAR2 knockout on virus infection. *PLoS ONE* **12**, e0182866, doi:10.1371/journal.pone.0182866 (2017).

96   Fuchs, J. *et al.* Evolution and Antiviral Specificities of Interferon-Induced Mx Proteins of Bats against Ebola, Influenza, and Other RNA Viruses. *Journal of Virology* **91**, e00361-00317, doi:10.1128/JVI.00361-17 (2017).

97   Kuzmin, I. V. *et al.* Innate Immune Responses of Bat and Human Cells to Filoviruses: Commonalities and Distinctions. *Journal of Virology* **91**, e02471-02416, doi:10.1128/JVI.02471-16 (2017).

98   Liang, Y.-Z. *et al.* Cloning, expression, and antiviral activity of interferon β from the Chinese microbat, Myotis davidii. *Virologica Sinica* **30**, 425-432, doi:10.1007/s12250-015-3668-2 (2015).

99　Fu, K. & Baric, R. S. Map locations of mouse hepatitis virus temperature-sensitive mutants: confirmation of variable rates of recombination. *Journal of Virology* **68**, 7458-7466 (1994).

100　Rockx, B. *et al.* Structural Basis for Potent Cross-Neutralizing Human Monoclonal Antibody Protection against Lethal Human and Zoonotic Severe Acute Respiratory Syndrome Coronavirus Challenge. *Journal of Virology* **82**, 3220-3235, doi:10.1128/JVI.02377-07 (2008).

101　Coughlin, M. M. & Prabhakar, B. S. Neutralizing Human Monoclonal Antibodies to Severe Acute Respiratory Syndrome Coronavirus: Target, Mechanism of Action and Therapeutic Potential. *Reviews in Medical Virology* **22**, 2-17, doi:10.1002/rmv.706 (2012).

102　Bachelder, E. M., Beaudette, T. T., Broaders, K. E., Dashe, J. & Fréchet, J. M. Acetal-derivatized dextran: an acid-responsive biodegradable material for therapeutic applications. *Journal of the American Chemical Society* **130**, 10494-10495 (2008).

103　Broaders, K. E., Cohen, J. A., Beaudette, T. T., Bachelder, E. M. & Fréchet, J. M. Acetalated dextran is a chemically and biologically tunable material for particulate immunotherapy. *Proceedings of the National Academy of Sciences* **106**, 5497-5502 (2009).

104　Kauffman, K. J. *et al.* Synthesis and characterization of acetalated dextran polymer and microparticles with ethanol as a degradation product. *ACS applied materials & interfaces* **4**, 4149-4155 (2012).

105　Chen, N. *et al.* Degradation of acetalated dextran can be broadly tuned based on cyclic acetal coverage and molecular weight. *International journal of pharmaceutics* **512**, 147-157 (2016).

106　Jiang, W., Gupta, R. K., Deshpande, M. C. & Schwendeman, S. P. Biodegradable poly (lactic-co-glycolic acid) microparticles for injectable delivery of vaccine antigens. *Advanced drug delivery reviews* **57**, 391-410 (2005).

107　Kanthamneni, N. *et al.* Enhanced stability of horseradish peroxidase encapsulated in acetalated dextran microparticles stored outside cold chain conditions. *International journal of pharmaceutics* **431**, 101-110 (2012).

108　Hoang, K. V. *et al.* Acetalated Dextran Encapsulated AR-12 as a Host-directed Therapy to Control Salmonella Infection. *International journal of pharmaceutics* **477**, 334-343, doi:10.1016/j.ijpharm.2014.10.022 (2014).

109　Junkins, R. D. *et al.* A robust microparticle platform for a STING-targeted adjuvant that enhances both humoral and cellular immunity during vaccination. *Journal of Controlled Release* **270**, 1-13 (2018).

110　Belser, J. A., Katz, J. M. & Tumpey, T. M. The ferret as a model organism to study influenza A virus infection. *Disease models & mechanisms* **4**, 575-579 (2011).

111　Davies, Bryan W., Bogard, Ryan W., Young, Travis S. & Mekalanos, John J. Coordinated Regulation of Accessory Genetic Elements Produces Cyclic Di-Nucleotides for V. cholerae Virulence. *Cell* **149**, 358-370, doi:https://doi.org/10.1016/j.cell.2012.01.053 (2012).

112　Chua, K. B. *et al.* A previously unknown reovirus of bat origin is associated with an acute respiratory disease in humans. *Proc Natl Acad Sci U S A* **104**, 11424-11429, doi:10.1073/pnas.0701372104 (2007).

113 Chua, K. B. et al. Investigation of a Potential Zoonotic Transmission of Orthoreovirus Associated with Acute Influenza-Like Illness in an Adult Patient. *Plos One* 6, doi:10.1371/journal.pone.0025434 (2011).

114 Tripp, D. W. et al. Apparent field safety of a raccoon poxvirus-vectored plague vaccine in free-ranging prairie dogs (Cynomys spp.), Colorado, USA. *Journal of wildlife diseases* 51, 401-410 (2015).

115 Slate, D. et al. Oral rabies vaccination in North America: opportunities, complexities, and challenges. *Plos Neglect. Trop. Dis.* 3, e549 (2009).

116 Freuling, C. M. et al. The elimination of fox rabies from Europe: determinants of success and lessons for the future. *Phil. Trans. R. Soc. B* 368, 20120142 (2013).

117 Tripp, D. W. et al. Season and application rates affect vaccine bait consumption by prairie dogs in Colorado and Utah, USA. *Journal of wildlife diseases* 50, 224-234 (2014).

118 Roberts, M. et al. Topical and cutaneous delivery using nanosystems. *Journal of Controlled Release* 247, 86-105 (2017).

119 Mishra, D. K., Dhote, V. & Mishra, P. K. Transdermal immunization: biological framework and translational perspectives. *Expert opinion on drug delivery* 10, 183-200 (2013).

120 Ebrahimian, M. et al. Co-delivery of Dual Toll-Like Receptor Agonists and Antigen in Poly (Lactic-Co-Glycolic) Acid/Polyethylenimine Cationic Hybrid Nanoparticles Promote Efficient In Vivo Immune Responses. *Frontiers in immunology* 8, 1077 (2017).

121 Karande, P. & Mitragotri, S. Transcutaneous immunization: an overview of advantages, disease targets, vaccines, and delivery technologies. *Annual review of chemical and biomolecular engineering* 1, 175-201 (2010).

122 Unidad, J., Karatay, E., Neelakantan, R., Jose, A. & Johnson, D. M. in *33rd International Conference of the Polymer Processing Society*.

123 Oliveira, M. S. N. & McKinley, G. H. Iterated stretching and multiple beads-on-a-string phenomena in dilute solutions of highly extensible flexible polymers. *Physics of Fluids* 17, 071704, doi:10.1063/1.1949197 (2005).

124 Epstein, J. H. et al. Nipah virus ecology and infection dynamics in its bat reservoir, Pteropus medius, in Bangladesh. *International Journal of Infectious Diseases* 53, 20-21, doi:10.1016/j.ijid.2016.11.056.

125 Borremans, B. et al.   (Dryad Data Repository, 2016).

126 Ionides, E. L., Nguyen, D., Atchadé, Y., Stoev, S. & King, A. A. Inference for dynamic and latent variable models via iterated, perturbed Bayes maps. *Proceedings of the National Academy of Sciences* 112, 719-724 (2015).

127 Jones, K. E. et al. Global trends in emerging infectious diseases. *Nature* 451, 990-993, doi:10.1038/nature06536 (2008).

128 Alagaili, A. N. et al. Middle East respiratory syndrome coronavirus infection in dromedary camels in saudi arabia. *MBio* 5, doi:10.1128/mBio.00884-14 (2014).

129 Homaira, N. et al. Nipah virus outbreak with person-to-person transmission in a district of Bangladesh, 2007. *Epidemiology and Infection* 138, 1630-1636, doi:10.1017/s0950268810000695 (2010).

130   Islam, M. S. *et al.* Nipah Virus Transmission from Bats to Humans Associated with Drinking Traditional Liquor Made from Date Palm Sap, Bangladesh, 2011–2014. *Emerging Infectious Disease journal* 22, 664, doi:10.3201/eid2204.151747 (2016).

131   Olival, K. J. *et al.* Ebola Virus Antibodies in Fruit Bats, Bangladesh. *Emerging Infectious Diseases* 19, 270-273, doi:10.3201/eid1902.120524 (2013).

132   Manning, S. E. *et al.* Human rabies prevention-United states, 2008. *MMWR Recomm Rep* 57, 1-28 (2008).

133   (National Institutes of Health, 2014).

Section III	RELEVANT PAPERS

We are attaching three relevant papers:

- Ge et al. (2017). Isolation and characterization of a bat SARS-like coronavirus that uses the ACE2 Receptor. *Nature.*
- Menachery et al. (2016). SARS-like WIV-CoV poised for human emergence. *PNAS.*
- Zhou et al. (*In Press*). Fatal swine acute diarrhoea syndrome caused by an HKU2-related coronavirus of bat origin. *Nature.*

LETTER

Isolation and characterization of a bat SARS–like coronavirus that uses the ACE2 receptor

Xing-Yi Ge[1]*, Jia-Lu Li[1]*, Xing-Lou Yang[1]*, Aleksei A. Chmura[2], Guangjian Zhu[2], Jonathan H. Epstein[2], Jonna K. Mazet[3], Ben Hu[1], Wei Zhang[1], Cheng Peng[1], Yu-Ji Zhang[1], Chu-Ming Luo[1], Bing Tan[1], Ning Wang[1], Yan Zhu[1], Gary Crameri[4], Shu-Yi Zhang[5], Lin-Fa Wang[4,6], Peter Daszak[2] & Zheng-Li Shi[1]

The 2002–3 pandemic caused by severe acute respiratory syndrome coronavirus (SARS-CoV) was one of the most significant public health events in recent history[1]. An ongoing outbreak of Middle East respiratory syndrome coronavirus[2] suggests that this group of viruses remains a key threat and that their distribution is wider than previously recognized. Although bats have been suggested to be the natural reservoirs of both viruses[3–5], attempts to isolate the progenitor virus of SARS-CoV from bats have been unsuccessful. Diverse SARS-like coronaviruses (SL-CoVs) have now been reported from bats in China, Europe and Africa[5–8], but none is considered a direct progenitor of SARS-CoV because of their phylogenetic disparity from this virus and the inability of their spike proteins to use the SARS-CoV cellular receptor molecule, the human angiotensin converting enzyme II (ACE2)[9,10]. Here we report whole-genome sequences of two novel bat coronaviruses from Chinese horseshoe bats (family: Rhinolophidae) in Yunnan, China: RsSHC014 and Rs3367. These viruses are far more closely related to SARS-CoV than any previously identified bat coronaviruses, particularly in the receptor binding domain of the spike protein. Most importantly, we report the first recorded isolation of a live SL-CoV (bat SL-CoV-WIV1) from bat faecal samples in Vero E6 cells, which has typical coronavirus morphology, 99.9% sequence identity to Rs3367 and uses ACE2 from humans, civets and Chinese horseshoe bats for cell entry. Preliminary *in vitro* testing indicates that WIV1 also has a broad species tropism. Our results provide the strongest evidence to date that Chinese horseshoe bats are natural reservoirs of SARS-CoV, and that intermediate hosts may not be necessary for direct human infection by some bat SL-CoVs. They also highlight the importance of pathogen-discovery programs targeting high-risk wildlife groups in emerging disease hotspots as a strategy for pandemic preparedness.

The 2002–3 pandemic of SARS[1] and the ongoing emergence of the Middle East respiratory syndrome coronavirus (MERS-CoV)[2] demonstrate that CoVs are a significant public health threat. SARS-CoV was shown to use the human ACE2 molecule as its entry receptor, and this is considered a hallmark of its cross-species transmissibility[11]. The receptor binding domain (RBD) located in the amino-terminal region (amino acids 318–510) of the SARS-CoV spike (S) protein is directly involved in binding to ACE2 (ref. 12). However, despite phylogenetic evidence that SARS-CoV evolved from bat SL-CoVs, all previously identified SL-CoVs have major sequence differences from SARS-CoV in the RBD of their S proteins, including one or two deletions[6,9]. Replacing the RBD of one SL-CoV S protein with SARS-CoV S conferred the ability to use human ACE2 and replicate efficiently in mice[9,13]. However, to date, no SL-CoVs have been isolated from bats, and no wild-type SL-CoV of bat origin has been shown to use ACE2.

We conducted a 12-month longitudinal survey (April 2011–September 2012) of SL-CoVs in a colony of *Rhinolophus sinicus* at a single location in Kunming, Yunnan Province, China (Extended Data Table 1). A total of 117 anal swabs or faecal samples were collected from individual bats using a previously published method[5,14]. A one-step reverse transcription (RT)-nested PCR was conducted to amplify the RNA-dependent RNA polymerase (RdRP) motifs A and C, which are conserved among alphacoronaviruses and betacoronaviruses[15].

Twenty-seven of the 117 samples (23%) were classed as positive by PCR and subsequently confirmed by sequencing. The species origin of all positive samples was confirmed to be *R. sinicus* by cytochrome b sequence analysis, as described previously[16]. A higher prevalence was observed in samples collected in October (30% in 2011 and 48.7% in 2012) than those in April (7.1% in 2011) or May (7.4% in 2012) (Extended Data Table 1). Analysis of the S protein RBD sequences indicated the presence of seven different strains of SL-CoVs (Fig. 1a and Extended Data Figs 1 and 2). In addition to RBD sequences, which closely matched previously described SL-CoVs (Rs672, Rf1 and HKU3)[5,8,17,18], two novel strains (designated SL-CoV RsSHC014 and Rs3367) were discovered. Their full-length genome sequences were determined, and both were found to be 29,787 base pairs in size (excluding the poly(A) tail). The overall nucleotide sequence identity of these two genomes with human SARS-CoV (Tor2 strain) is 95%, higher than that observed previously for bat SL-CoVs in China (88–92%)[5,8,17,18] or Europe (76%)[6] (Extended Data Table 2 and Extended Data Figs 3 and 4). Higher sequence identities were observed at the protein level between these new SL-CoVs and SARS-CoVs (Extended Data Tables 3 and 4). To understand the evolutionary origin of these two novel SL-CoV strains, we conducted recombination analysis with the Recombination Detection Program 4.0 package[19] using available genome sequences of bat SL-CoV strains (Rf1, Rp3, Rs672, Rm1, HKU3 and BM48-31) and human and civet representative SARS-CoV strains (BJ01, SZ3, Tor2 and GZ02). Three breakpoints were detected with strong *P* values ($<10^{-20}$) and supported by similarity plot and bootscan analysis (Extended Data Fig. 5a, b). Breakpoints were located at nucleotides 20,827, 26,553 and 28,685 in the Rs3367 (and RsSHC014) genome, and generated recombination fragments covering nucleotides 20,827–26,533 (5,727 nucleotides) (including partial open reading frame (ORF) 1b, full-length S, ORF3, E and partial M gene) and nucleotides 26,534–28,685 (2,133 nucleotides) (including partial ORF M, full-length ORF6, ORF7, ORF8 and partial N gene). Phylogenetic analysis using the major and minor parental regions suggested that Rs3367, or RsSHC014, is the descendent of a recombination of lineages that ultimately lead to SARS-CoV and SL-CoV Rs672 (Fig. 1b).

The most notable sequence differences between these two new SL-CoVs and previously identified SL-CoVs is in the RBD regions of their S proteins. First, they have higher amino acid sequence identity to SARS-CoV (85% and 96% for RsSHC014 and Rs3367, respectively). Second, there are no deletions and they have perfect sequence alignment with the SARS-CoV RBD region (Extended Data Figs 1 and 2). Structural

[1]Center for Emerging Infectious Diseases, State Key Laboratory of Virology, Wuhan Institute of Virology of the Chinese Academy of Sciences, Wuhan 430071, China. [2]EcoHealth Alliance, New York, New York 10001, USA. [3]One Health Institute, School of Veterinary Medicine, University of California, Davis, California 95616, USA. [4]CSIRO Australian Animal Health Laboratory, Geelong, Victoria 3220, Australia. [5]College of Life Sciences, East China Normal University, Shanghai 200062, China. [6]Emerging Infectious Diseases Program, Duke-NUS Graduate Medical School, Singapore 169857.
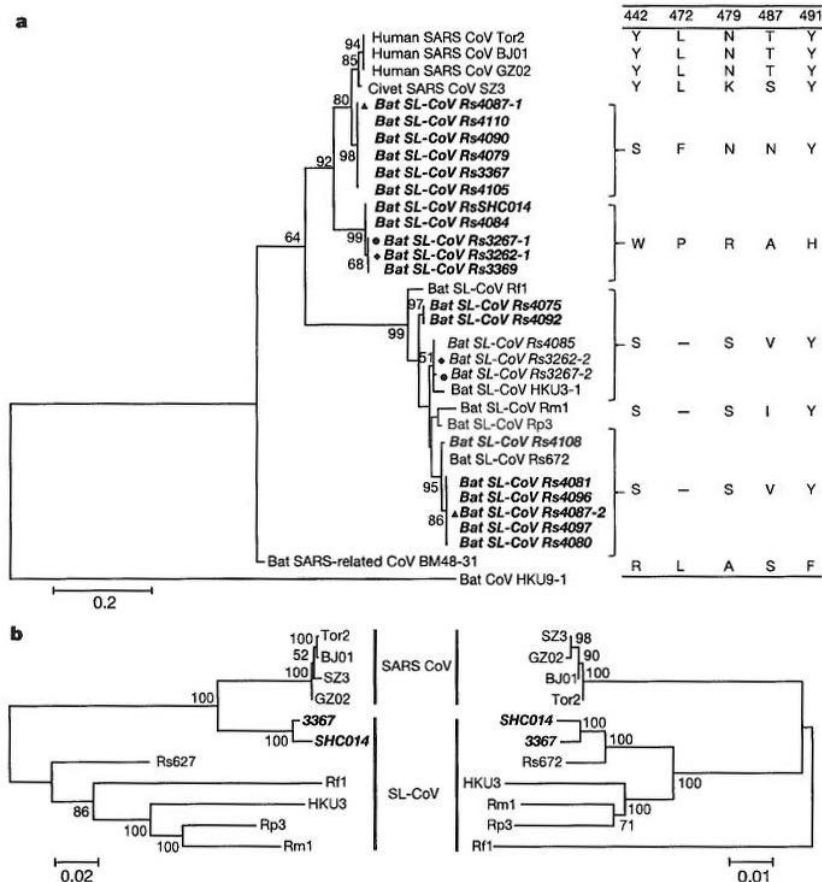*These authors contributed equally to this work.

a

	442	472	479	487	491
Human SARS CoV Tor2	Y	L	N	T	Y
Human SARS CoV BJ01	Y	L	N	T	Y
Human SARS CoV GZ02	Y	L	N	T	Y
Civet SARS CoV SZ3	Y	L	K	S	Y
Bat SL-CoV Rs4087-1 ▲					
Bat SL-CoV Rs4110					
Bat SL-CoV Rs4090	S	F	N	N	Y
Bat SL-CoV Rs4079					
Bat SL-CoV Rs3367					
Bat SL-CoV Rs4105					
Bat SL-CoV RsSHC014					
Bat SL-CoV Rs4084					
Bat SL-CoV Rs3267-1 ●	W	P	R	A	H
Bat SL-CoV Rs3262-1 ●					
Bat SL-CoV Rs3369					
Bat SL-CoV Rf1					
Bat SL-CoV Rs4075					
Bat SL-CoV Rs4092					
Bat SL-CoV Rs4085	S	–	S	V	Y
Bat SL-CoV Rs3262-2 ●					
Bat SL-CoV Rs3267-2 ●					
Bat SL-CoV HKU3-1					
Bat SL-CoV Rm1	S	–	S	I	Y
Bat SL-CoV Rp3					
Bat SL-CoV Rs4108					
Bat SL-CoV Rs672					
Bat SL-CoV Rs4081	S	–	S	V	Y
Bat SL-CoV Rs4096					
Bat SL-CoV Rs4087-2 ▲					
Bat SL-CoV Rs4097					
Bat SL-CoV Rs4080					
Bat SARS-related CoV BM48-31	R	L	A	S	F
Bat CoV HKU9-1					

0.2

b

Figure 1 | Phylogenetic tree based on amino acid sequences of the S RBD region and the two parental regions of bat SL-CoV Rs3367 or RsSHC014. a, SARS-CoV S protein amino acid residues 310–520 were aligned with homologous regions of bat SL-CoVs using the ClustalW software. A maximum-likelihood phylogenetic tree was constructed using a Poisson model with bootstrap values determined by 1,000 replicates in the MEGA5 software package. The RBD sequences identified in this study are in bold and named by the sample numbers. The key amino acid residues involved in interacting with the human ACE2 molecule are indicated on the right of the tree. SARS-CoV GZ02, BJ01 and Tor2 were isolated from patients in the early, middle and late phase, respectively, of the SARS outbreak in 2003. SARS-CoV SZ3 was identified from *Paguma larvata* in 2003 collected in Guangdong, China. SL-CoV Rp3, Rs672 and HKU3-1 were identified from *R. sinicus* collected in China (respectively: Guangxi, 2004; Guizhou, 2006; Hong Kong, 2005). Rf1 and Rm1 were identified from

R. ferrumequinum and *R. macrotis*, respectively, collected in Hubei, China, in 2004. Bat SARS-related CoV BM48-31 was identified from *R. blasii* collected in Bulgaria in 2008. Bat CoV HKU9-1 was identified from *Rousettus leschenaultii* collected in Guangdong, China in 2005/2006 and used as an outgroup. All sequences in bold and italics were identified in the current study. Filled triangles, circles and diamonds indicate samples with co-infection by two different SL-CoVs. '–' indicates the amino acid deletion. **b**, Phylogenetic origins of the two parental regions of Rs3367 or RsSHC014. Maximum likelihood phylogenetic trees were constructed from alignments of two fragments covering nucleotides 20,827–26,533 (5,727 nucleotides) and 26,534 –28,685 (2,133 nucleotides) of the Rs3367 genome, respectively. For display purposes, the trees were midpoint rooted. The taxa were annotated according to strain names: SARS-CoV, SARS coronavirus; SARS-like CoV, bat SARS-like coronavirus. The two novel SL-CoVs, Rs3367 and RsSHC014, are in bold and italics.

and mutagenesis studies have previously identified five key residues (amino acids 442, 472, 479, 487 and 491) in the RBD of the SARS-CoV S protein that have a pivotal role in receptor binding[20,21]. Although all five residues in the RsSHC014 S protein were found to be different from those of SARS-CoV, two of the five residues in the Rs3367 RBD were conserved (Fig. 1 and Extended Data Fig. 1).

Despite the rapid accumulation of bat CoV sequences in the last decade, there has been no report of successful virus isolation[6,22,23]. We attempted isolation from SL-CoV PCR-positive samples. Using an optimized protocol and Vero E6 cells, we obtained one isolate which caused cytopathic effect during the second blind passage. Purified virions displayed typical coronavirus morphology under electron microscopy (Fig. 2). Sequence analysis using a sequence-independent amplification method[14] to avoid PCR-introduced contamination indicated that the isolate was almost identical to Rs3367, with 99.9% nucleotide genome sequence identity and 100% amino acid sequence identity for the S1 region. The new isolate was named SL-CoV-WIV1.

To determine whether WIV1 can use ACE2 as a cellular entry receptor, we conducted virus infectivity studies using HeLa cells expressing or not expressing ACE2 from humans, civets or Chinese horseshoe bats. We found that WIV1 is able to use ACE2 of different origins as an entry receptor and replicated efficiently in the ACE2-expressing cells (Fig. 3). This is, to our knowledge, the first identification of a wild-type bat SL-CoV capable of using ACE2 as an entry receptor.

To assess its cross-species transmission potential, we conducted infectivity assays in cell lines from a range of species. Our results (Fig. 4 and Extended Data Table 5) indicate that bat SL-CoV-WIV1 can grow in human alveolar basal epithelial (A549), pig kidney 15 (PK-15) and *Rhinolophus sinicus* kidney (RSKT) cell lines, but not in human cervix (HeLa), Syrian golden hamster kidney (BHK21), *Myotis davidii* kidney (BK), *Myotis chinensis* kidney (MCKT), *Rousettus leschenaulti* kidney (RLK) or *Pteropus alecto* kidney (PaKi) cell lines. Real-time RT–PCR indicated that WIV1 replicated much less efficiently in A549, PK-15 and RSKT cells than in Vero E6 cells (Fig. 4).
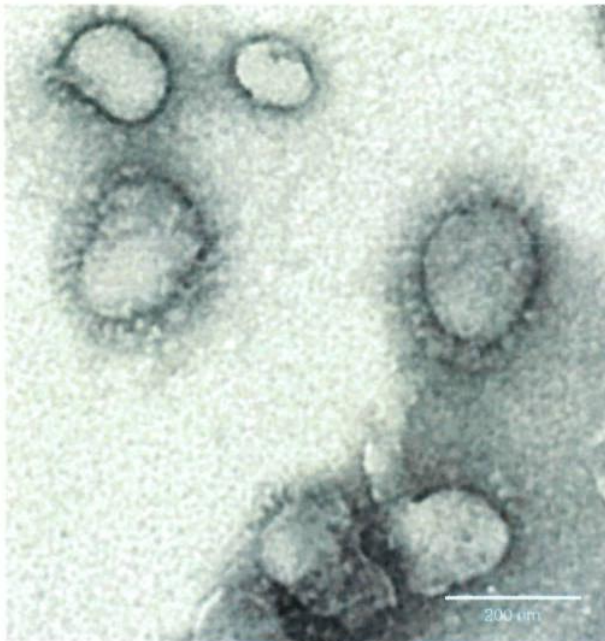
Figure 2 | Electron micrograph of purified virions. Virions from a 10-ml culture were collected, fixed and concentrated/purified by sucrose gradient centrifugation. The pelleted viral particles were suspended in 100 μl PBS, stained with 2% phosphotungstic acid (pH 7.0) and examined directly using a Tecnai transmission electron microscope (FEI) at 200 kV.

To assess the cross-neutralization activity of human SARS-CoV sera against WIV1, we conducted serum-neutralization assays using nine convalescent sera from SARS patients collected in 2003. The results showed that seven of these were able to completely neutralize 100 tissue culture infectious dose 50 ($TCID_{50}$) WIV1 at dilutions of 1:10 to 1:40, further confirming the close relationship between WIV1 and SARS-CoV.

Our findings have important implications for public health. First, they provide the clearest evidence yet that SARS-CoV originated in bats. Our previous work provided phylogenetic evidence of this[5], but the lack of an isolate or evidence that bat SL-CoVs can naturally infect human cells, until now, had cast doubt on this hypothesis. Second, the lack of capacity of SL-CoVs to use of ACE2 receptors has previously been considered as the key barrier for their direct spillover into humans, supporting the suggestion that civets were intermediate hosts for SARS-CoV adaptation to human transmission during the SARS outbreak[24]. However, the ability of SL-CoV-WIV1 to use human ACE2 argues against the necessity of this step for SL-CoV-WIV1 and suggests that direct bat-to-human infection is a plausible scenario for some bat SL-CoVs. This has implications for public health control measures in the face of potential spillover of a diverse and growing pool of recently discovered SARS-like CoVs with a wide geographic distribution.

Our findings suggest that the diversity of bat CoVs is substantially higher than that previously reported. In this study we were able to demonstrate the circulation of at least seven different strains of SL-CoVs within a single colony of *R. sinicus* during a 12-month period. The high genetic diversity of SL-CoVs within this colony was mirrored by high phenotypic diversity in the differential use of ACE2 by different strains. It would therefore not be surprising if further surveillance reveals a broad diversity of bat SL-CoVs that are able to use ACE2, some of which may have even closer homology to SARS-CoV than SL-CoV-WIV1. Our results—in addition to the recent demonstration of MERS-CoV in a Saudi Arabian bat[25], and of bat CoVs closely related to MERS-CoV in China, Africa, Europe and North America[3,26,27]—suggest that bat coronaviruses remain a substantial global threat to public health.

Finally, this study demonstrates the public health importance of pathogen discovery programs targeting wildlife that aim to identify the 'known unknowns'—previously unknown viral strains closely related to known pathogens. These programs, focused on specific high-risk wildlife groups and hotspots of disease emergence, may be a critical part of future global strategies to predict, prepare for, and prevent pandemic emergence[28].
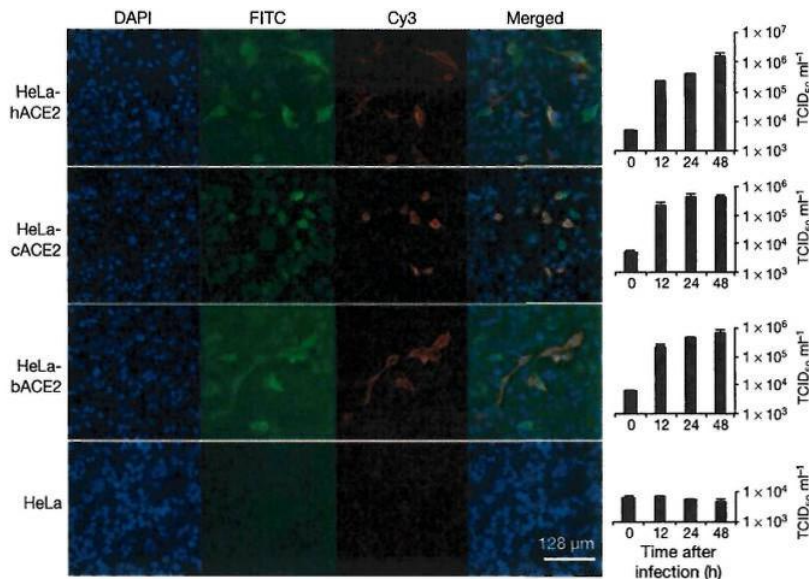
Figure 3 | Analysis of receptor usage of SL-CoV-WIV1 determined by immunofluorescence assay and real-time PCR. Determination of virus infectivity in HeLa cells with and without the expression of ACE2. b, bat; c, civet; h, human. ACE2 expression was detected with goat anti-humanACE2 antibody followed by fluorescein isothiocyanate (FITC)-conjugated donkey anti-goat IgG. Virus replication was detected with rabbit antibody against the SL-CoV Rp3 nucleocapsid protein followed by cyanine 3 (Cy3)-conjugated mouse anti-rabbit IgG. Nuclei were stained with DAPI (4',6-diamidino-2-phenylindole). The columns (from left to right) show staining of nuclei (blue), ACE2 expression (green), virus replication (red), merged triple-stained images and real-time PCR results, respectively. ($n = 3$); error bars represent standard deviation.
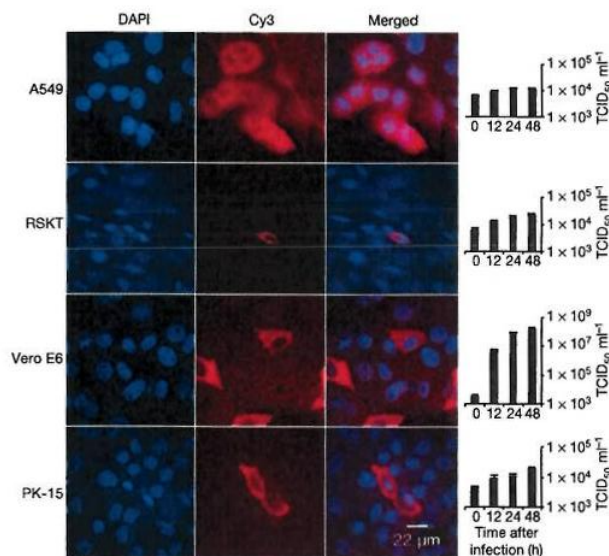
Figure 4 | Analysis of host range of SL-CoV-WIV1 determined by immunofluorescence assay and real-time PCR. Virus infection in A549, RSKT, Vero E6 and PK-15 cells. Virus replication was detected as described for Fig. 3. The columns (from left to right) show staining of nuclei (blue), virus replication (red), merged double-stained images and real-time PCR results, respectively. $n = 3$; error bars represent s.d.

METHODS SUMMARY

Throat and faecal swabs or fresh faecal samples were collected in viral transport medium as described previously[14]. All PCR was conducted with the One-Step RT-PCR kit (Invitrogen). Primers targeting the highly conserved regions of the RdRP gene were used for detection of all alphacoronaviruses and betacoronaviruses as described previously[15]. Degenerate primers were designed on the basis of all available genomic sequences of SARS-CoVs and SL-CoVs and used for amplification of the RBD sequences of S genes or full-length genomic sequences. Degenerate primers were used for amplification of the bat *ACE2* gene as described previously[29]. PCR products were gel purified and cloned into pGEM-T Easy Vector (Promega). At least four independent clones were sequenced to obtain a consensus sequence. PCR-positive faecal samples (in 200 µl buffer) were gradient centrifuged at 3,000–12,000g and supernatant diluted at 1:10 in DMEM before being added to Vero E6 cells. After incubation at 37 °C for 1 h, inocula were removed and replaced with fresh DMEM with 2% FCS. Cells were incubated at 37 °C and checked daily for cytopathic effect. Cell lines from different origins were grown on coverslips in 24-well plates and inoculated with the novel SL-CoV at a multiplicity of infection of 10. Virus replication was detected at 24 h after infection using rabbit antibodies against the SL-CoV Rp3 nucleocapsid protein followed by Cy3-conjugated goat anti-rabbit IgG.

Online Content Any additional Methods, Extended Data display items and Source Data are available in the online version of the paper; references unique to these sections appear only in the online paper.

1. Ksiazek, T. G. *et al.* A novel coronavirus associated with severe acute respiratory syndrome. *N. Engl. J. Med.* **348**, 1953–1966 (2003).
2. Zaki, A. M., van Boheemen, S., Bestebroer, T. M., Osterhaus, A. D. & Fouchier, R. A. Isolation of a novel coronavirus from a man with pneumonia in Saudi Arabia. *N. Engl. J. Med.* **367**, 1814–1820 (2012).
3. Anthony, S. J. *et al.* Coronaviruses in bats from Mexico. *J. Gen. Virol.* **94**, 1028–1038 (2013).
4. Raj, V. S. *et al.* Dipeptidyl peptidase 4 is a functional receptor for the emerging human coronavirus-EMC. *Nature* **495**, 251–254 (2013).
5. Li, W. *et al.* Bats are natural reservoirs of SARS-like coronaviruses. *Science* **310**, 676–679 (2005).
6. Drexler, J. F. *et al.* Genomic characterization of severe acute respiratory syndrome-related coronavirus in European bats and classification of coronaviruses based on partial RNA-dependent RNA polymerase gene sequences. *J. Virol.* **84**, 11336–11349 (2010).
7. Tong, S. *et al.* Detection of novel SARS-like and other coronaviruses in bats from Kenya. *Emerg. Infect. Dis.* **15**, 482–485 (2009).
8. Lau, S. K. P. *et al.* Severe acute respiratory syndrome coronavirus-like virus in Chinese horseshoe bats. *Proc. Natl Acad. Sci. USA* **102**, 14040–14045 (2005).
9. Ren, W. *et al.* Difference in receptor usage between severe acute respiratory syndrome (SARS) coronavirus and SARS-like coronavirus of bat origin. *J. Virol.* **82**, 1899–1907 (2008).
10. Hon, C. C. *et al.* Evidence of the recombinant origin of a bat severe acute respiratory syndrome (SARS)-like coronavirus and its implications on the direct ancestor of SARS coronavirus. *J. Virol.* **82**, 1819–1826 (2008).
11. Li, W. *et al.* Angiotensin-converting enzyme 2 is a functional receptor for the SARS coronavirus. *Nature* **426**, 450–454 (2003).
12. Wong, S. K., Li, W., Moore, M. J., Choe, H. & Farzan, M. A 193-amino acid fragment of the SARS coronavirus S protein efficiently binds angiotensin-converting enzyme 2. *J. Biol. Chem.* **279**, 3197–3201 (2004).
13. Becker, M. M. *et al.* Synthetic recombinant bat SARS-like coronavirus is infectious in cultured cells and in mice. *Proc. Natl Acad. Sci. USA* **105**, 19944–19949 (2008).
14. Li, Y. *et al.* Host range, prevalence, and genetic diversity of adenoviruses in bats. *J. Virol.* **84**, 3889–3897 (2010).
15. De Souza Luna, L. K. *et al.* Generic detection of coronaviruses and differentiation at the prototype strain level by reverse transcription-PCR and nonfluorescent low-density microarray. *J. Clin. Microbiol.* **45**, 1049–1052 (2007).
16. Cui, J. *et al.* Evolutionary relationships between bat coronaviruses and their hosts. *Emerg. Infect. Dis.* **13**, 1526–1532 (2007).
17. Yuan, J. *et al.* Intraspecies diversity of SARS-like coronaviruses in *Rhinolophus sinicus* and its implications for the origin of SARS coronaviruses in humans. *J. Gen. Virol.* **91**, 1058–1062 (2010).
18. Ren, W. *et al.* Full-length genome sequences of two SARS-like coronaviruses in horseshoe bats and genetic variation analysis. *J. Gen. Virol.* **87**, 3355–3359 (2006).
19. Martin, D. P. *et al.* RDP3: a flexible and fast computer program for analyzing recombination. *Bioinformatics* **26**, 2462–2463 (2010).
20. Wu, K., Peng, G., Wilken, M., Geraghty, R. J. & Li, F. Mechanisms of host receptor adaptation by severe acute respiratory syndrome coronavirus. *J. Biol. Chem.* **287**, 8904–8911 (2012).
21. Li, W. *et al.* Receptor and viral determinants of SARS-coronavirus adaptation to human ACE2. *EMBO J.* **24**, 1634–1643 (2005).
22. Lau, S. K. *et al.* Ecoepidemiology and complete genome comparison of different strains of severe acute respiratory syndrome-related *Rhinolophus* bat coronavirus in China reveal bats as a reservoir for acute, self-limiting infection that allows recombination events. *J. Virol.* **84**, 2808–2819 (2010).
23. Lau, S. K. *et al.* Coexistence of different genotypes in the same bat and serological characterization of *Rousettus* bat coronavirus HKU9 belonging to a novel Betacoronavirus subgroup. *J. Virol.* **84**, 11385–11394 (2010).
24. Song, H. D. *et al.* Cross-host evolution of severe acute respiratory syndrome coronavirus in palm civet and human. *Proc. Natl Acad. Sci. USA* **102**, 2430–2435 (2005).
25. Memish, Z. A. *et al.* Middle East respiratory syndrome coronavirus in bats, Saudi Arabia. *Emerg. Infect. Dis.* **19**, 11 (2013).
26. Chan, J. F. *et al.* Is the discovery of the novel human betacoronavirus 2c EMC/2012 (HCoV-EMC) the beginning of another SARS-like pandemic? *J. Infect.* **65**, 477–489 (2012).
27. Ithete, N. L. *et al.* Close relative of human Middle East respiratory syndrome coronavirus in bat, South Africa. *Emerg. Infect. Dis.* **19**, 1697–1699 (2013).
28. Morse, S. S. *et al.* Prediction and prevention of the next pandemic zoonosis. *Lancet* **380**, 1956–1965 (2012).
29. Hou, Y. *et al.* Angiotensin-converting enzyme 2 (ACE2) proteins of different bat species confer variable susceptibility to SARS-CoV entry. *Arch. Virol.* **155**, 1563–1569 (2010).

Author Contributions Z.-L.S. and P.D. designed and coordinated the study. X.-Y.G., J.-L. L. and X.-L.Y. conducted majority of experiments and contributed equally to the study. A.A.C., B.H., W.Z., C.P., Y.-J.Z., C.-M.L., B.T., N.W. and Y.Z. conducted parts of the experiments and analyses. J.H.E., J.K.M. and S.-Y.Z. coordinated the field study. X.-Y.G., J.-L.L., X.-L.Y., B.T. and G.-J.Z. collected the samples. G.C. and L.-F.W. designed and supervised part of the experiments. All authors contributed to the interpretations and conclusions presented. Z.-L.S. and X.-Y.G. wrote the manuscript with significant contributions from P.D. and L-F.W. and input from all authors.

Author Information Sequences of three bat SL-CoV genomes, bat SL-CoV RBD and *R. sinicus* ACE2 genes have been deposited in GenBank under accession numbers KC881005–KC881007 (genomes from SL-CoV RsSHC014, Rs3367 and W1V1, respectively), KC880984–KC881003 (bat SL-CoV RBD genes) and KC881004 (*R. sinicus* ACE2), respectively. Reprints and permissions information is available at www.nature.com/reprints. The authors declare no competing financial interests. Readers are welcome to comment on the online version of the paper. Correspondence and requests for materials should be addressed to P.D. (daszak@ecohealthalliance.org) or Z.-L.S. (zlshi@wh.iov.cn).

METHODS

Sampling. Bats were trapped in their natural habitat as described previously[5]. Throat and faecal swab samples were collected in viral transport medium (VTM) composed of Hank's balanced salt solution, pH 7.4, containing BSA (1%), amphotericin (15 µg ml^{-1}), penicillin G (100 U ml^{-1}) and streptomycin (50 µg ml^{-1}). To collect fresh faecal samples, clean plastic sheets measuring 2.0 by 2.0 m were placed under known bat roosting sites at about 18:00 h each evening. Relatively fresh faecal samples were collected from sheets at approximately 05:30–06:00 the next morning and placed in VTM. Samples were transported to the laboratory and stored at −80 °C until use. All animals trapped for this study were released back to their habitat after sample collection. All sampling processes were performed by veterinarians with approval from Animal Ethics Committee of the Wuhan Institute of Virology (WIVH05210201) and EcoHealth Alliance under an inter-institutional agreement with University of California, Davis (UC Davis protocol no. 16048).

RNA extraction, PCR and sequencing. RNA was extracted from 140 µl of swab or faecal samples with a Viral RNA Mini Kit (Qiagen) following the manufacturer's instructions. RNA was eluted in 60 µl RNAse-free buffer (buffer AVE, Qiagen), then aliquoted and stored at −80 °C. One-step RT–PCR (Invitrogen) was used to detect coronavirus sequences as described previously[15]. First round PCR was conducted in a 25-µl reaction mix containing 12.5 µl PCR 2× reaction mix buffer, 10 pmol of each primer, 2.5 mM MgSO4, 20 U RNase inhibitor, 1 µl SuperScript III/ Platinum Taq Enzyme Mix and 5 µl RNA. Amplification of the RdRP-gene fragment was performed as follows: 50 °C for 30 min, 94 °C for 2 min, followed by 40 cycles consisting of 94 °C for 15 s, 62 °C for 15 s, 68 °C for 40 s, and a final extension of 68 °C for 5 min. Second round PCR was conducted in a 25-µl reaction mix containing 2.5 µl PCR reaction buffer, 5 pmol of each primer, 50 mM MgCl₂, 0.5 mM dNTP, 0.1 µl Platinum Taq Enzyme (Invitrogen) and 1 µl first round PCR product. The amplification of RdRP-gene fragment was performed as follows: 94 °C for 5 min followed by 35 cycles consisting of 94 °C for 30 s, 52 °C for 30 s, 72 °C for 40 s, and a final extension of 72 °C for 5 min.

To amplify the RBD region, one-step RT–PCR was performed with primers designed based on available SARS-CoV or bat SL-CoVs (first round PCR primers; F, forward; R, reverse: CoVS931F-5′-VWGADGTTGTKAGRTTYCCT-3′ and CoVS1909R-5′-TAARACAVCCWGCYTGWGT-3′; second PCR primers: CoVS 951F-5′-TGTKAGRTTYCCTAAYATTAC-3′ and CoVS1805R-5′-ACATCYTG ATANARAACAGC-3′). First-round PCR was conducted in a 25-µl reaction mix as described above except primers specific for the S gene were used. The amplification of the RBD region of the S gene was performed as follows: 50 °C for 30 min, 94 °C for 2 min, followed by 35 cycles consisting of 94 °C for 15 s, 43 °C for 15 s, 68 °C for 90 s, and a final extension of 68 °C for 5 min. Second-round PCR was conducted in a 25-µl reaction mix containing 2.5 µl PCR reaction buffer, 5 pmol of each primer, 50 mM MgCl₂, 0.5 mM dNTP, 0.1 µl Platinum Taq Enzyme (Invitrogen) and 1 µl first round PCR product. Amplification was performed as follows: 94 °C for 5 min followed by 40 cycles consisting of 94 °C for 30 s, 41 °C for 30 s, 72 °C for 60 s, and a final extension of 72 °C for 5 min.

PCR products were gel purified and cloned into pGEM-T Easy Vector (Promega). At least four independent clones were sequenced to obtain a consensus sequence for each of the amplified regions.

Sequencing full-length genomes. Degenerate coronavirus primers were designed based on all available SARS-CoV and bat SL-CoV sequences in GenBank and specific primers were designed from genome sequences generated from previous rounds of sequencing in this study (primer sequences will be provided upon request). All PCRs were conducted using the One-Step RT–PCR kit (Invitrogen). The 5′ and 3′ genomic ends were determined using the 5′ or 3′ RACE kit (Roche), respectively. PCR products were gel purified and sequenced directly or following cloning into pGEM-T Easy Vector (Promega). At least four independent clones were sequenced to obtain a consensus sequence for each of the amplified regions and each region was sequenced at least twice.

Sequence analysis and databank accession numbers. Routine sequence management and analysis was carried out using DNAStar or Geneious. Sequence alignment and editing was conducted using ClustalW, BioEdit or GeneDoc. Maximum Likelihood phylogenetic trees based on the protein sequences were constructed using a Poisson model with bootstrap values determined by 1,000 replicates in the MEGA5 software package.

Sequences obtained in this study have been deposited in GenBank as follows (accession numbers given in parenthesis): full-length genome sequence of SL-CoV RsSHC014 and Rs3367 (KC881005, KC881006); full-length sequence of WIV1 S (KC881007); RBD (KC880984–KC881003); ACE2 (KC8810040). SARS-CoV sequences used in this study: human SARS-CoV strains Tor2 (AY274119), BJ01 (AY278488), GZ02 (AY390556) and civet SARS-CoV strain SZ3 (AY304486). Bat coronavirus sequences used in this study: Rs672 (FJ588686), Rp3 (DQ071615), Rf1 (DQ412042), Rm1 (DQ412043), HKU3-1 (DQ022305), BM48-31 (NC_014470), HKU9-1 (NC_009021), HKU4 (NC_009019), HKU5 (NC_009020), HKU8 (DQ249228),

HKU2 (EF203067), BtCoV512 (NC_009657), 1A (NC_010437). Other coronavirus sequences used in this study: HCoV-229E (AF304460), HCoV-OC43 (AY391777), HCoV-NL63 (AY567487), HKU1 (NC_006577), EMC (JX869059), FIPV (NC_002306), PRCV (DQ811787), BWCoV (NC_010646), MHV (AY700211), IBV (AY851295).

Amplification, cloning and expression of the bat ACE2 gene. Construction of expression clones for human and civet ACE2 in pcDNA3.1 has been described previously[29]. Bat ACE2 was amplified from a *R. sinicus* (sample no. 3357). In brief, total RNA was extracted from bat rectal tissue using the RNeasy Mini Kit (Qiagen). First-strand complementary DNA was synthesized from total RNA by reverse transcription with random hexamers. Full-length bat *ACE2* fragments were amplified using forward primer bAF2 and reverse primer bAR2 (ref. 29). The *ACE2* gene was cloned into pCDNA3.1 with KpnI and XhoI, and verified by sequencing. Purified *ACE2* plasmids were transfected to HeLa cells. After 24 h, lysates of HeLa cells expressing human, civet, or bat ACE2 were confirmed by western blot or immunofluorescence assay.

Western blot analysis. Lysates of cells or filtered supernatants containing pseudoviruses were separated by SDS–PAGE, followed by transfer to a nitrocellulose membrane (Millipore). For detection of S protein, the membrane was incubated with rabbit anti-Rp3 S fragment (amino acids 561–666) polyantibodies (1:200), and the bound antibodies were detected by alkaline phosphatase (AP)-conjugated goat anti-rabbit IgG (1:1,000). For detection of HIV-1 p24 in supernatants, monoclonal antibody against HIV p24 (p24 MAb) was used as the primary antibody at a dilution of 1:1,000, followed by incubation with AP-conjugated goat anti-mouse IgG at the same dilution. To detect the expression of ACE2 in HeLa cells, goat antibody against the human ACE2 ectodomain (1:500) was used as the first antibody, followed by incubation with horseradish peroxidase-conjugated donkey anti-goat IgG (1:1,000).

Virus isolation. Vero E6 cell monolayers were maintained in DMEM supplemented with 10% FCS. PCR-positive samples (in 200 µl buffer) were gradient centrifuged at 3,000–12,000g, and supernatant were diluted 1:10 in DMEM before being added to Vero E6 cells. After incubation at 37 °C for 1 h, inocula were removed and replaced with fresh DMEM with 2% FCS. Cells were incubated at 37 °C for 3 days and checked daily for cytopathic effect. Double-dose triple antibiotics penicillin/streptomycin/amphotericin (Gibco) were included in all tissue culture media (penicillin 200 IU ml^{-1}, streptomycin 0.2 mg ml^{-1}, amphotericin 0.5 µg ml^{-1}). Three blind passages were carried out for each sample. After each passage, both the culture supernatant and cell pellet were examined for presence of virus by RT–PCR using primers targeting the RdRP or S gene. Virions in supernatant (10 ml) were collected and fixed using 0.1% formaldehyde for 4 h, then concentrated by ultracentrifugation through a 20% sucrose cushion (5 ml) at 80,000g for 90 min using a Ty90 rotor (Beckman). The pelleted viral particles were suspended in 100 µl PBS, stained with 2% phosphotungstic acid (pH 7.0) and examined using a Tecnai transmission electron microscope (FEI) at 200 kV.

Virus infectivity detected by immunofluorescence assay. Cell lines used for this study and their culture conditions are summarized in Extended Data Table 5. Virus titre was determined in Vero E6 cells by cytopathic effect (CPE) counts. Cell lines from different origins and HeLa cells expressing ACE2 from human, civet or Chinese horseshoe bat were grown on coverslips in 24-well plates (Corning) incubated with bat SL-CoV-WIV1 at a multiplicity of infection = 10 for 1 h. The inoculum was removed and washed twice with PBS and supplemented with medium. HeLa cells without ACE2 expression and Vero E6 cells were used as negative and positive controls, respectively. At 24 h after infection, cells were washed with PBS and fixed with 4% formaldehyde in PBS (pH 7.4) for 20 min at 4 °C. ACE2 expression was detected using goat anti-human ACE2 immunoglobulin (R&D Systems) followed by FITC-labelled donkey anti-goat immunoglobulin (PTGLab). Virus replication was detected using rabbit antibody against the SL-CoV Rp3 nucleocapsid protein followed by Cy3-conjugated mouse anti-rabbit IgG. Nuclei were stained with DAPI. Staining patterns were examined using a FV1200 confocal microscope (Olympus).

Virus infectivity detected by real-time RT–PCR. Vero E6, A549, PK15, RSKT and HeLa cells with or without expression of ACE2 of different origins were inoculated with 0.1 TCID$_{50}$ WIV-1 and incubated for 1 h at 37 °C. After removing the inoculum, the cells were cultured with medium containing 1% FBS. Supernatants were collected at 0, 12, 24 and 48 h. RNA from 140 µl of each supernatant was extracted with the Viral RNA Mini Kit (Qiagen) following manufacturer's instructions and eluted in 60 µl buffer AVE (Qiagen). RNA was quantified on the ABI StepOne system, with the TaqMan AgPath-ID One-Step RT–PCR Kit (Applied Biosystems) in a 25 µl reaction mix containing 4 µl RNA, 1 × RT–PCR enzyme mix, 1 × RT–PCR buffer, 40 pmol forward primer (5′-GTGGTGGTGACGGCA AAATG-3′), 40 pmol reverse primer (5′-AAGTGAAGCTTCTGGGCCAG-3′) and 12 pmol probe (5′-FAM-AAAGAGCTCAGCCCCAGATG-BHQ1-3′). Amplification parameters were 10 min at 50 °C, 10 min at 95 °C and 50 cycles of 15 s at 95 °C and 20 s at 60 °C. RNA dilutions from purified WIV-1 stock were used as a standard.

Serum neutralization test. SARS patient sera were inactivated at 56 °C for 30 min and then used for virus neutralization testing. Sera were diluted starting with 1:10

and then serially twofold diluted in 96-well cell plates to 1:40. Each 100 μl serum dilution was mixed with 100 μl viral supernatant containing 100 TCID$_{50}$ of WIV1 and incubated at 37 °C for 1 h. The mixture was added in triplicate wells of 96-well cell plates with plated monolayers of Vero E6 cells and further incubated at 37 °C for 2 days. Serum from a healthy blood donor was used as a negative control in each experiment. CPE was observed using an inverted microscope 2 days after inoculation. The neutralizing antibody titre was read as the highest dilution of serum which completely suppressed CPE in infected wells. The neutralization test was repeated twice.

Recombination analysis. Full-length genomic sequences of SL-CoV Rs3367 or RsSHC014 were aligned with those of selected SARS-CoVs and bat SL-CoVs using Clustal X. The aligned sequences were preliminarily scanned for recombination events using Recombination Detection Program (RDP) 4.0 (ref. 19). The potential recombination events suggested by RDP owing to their strong P values ($<10–20$) were investigated further by similarity plot and bootscan analyses implemented in Simplot 3.5.1. Phylogenetic origin of the major and minor parental regions of Rs3367 or RsSHC014 were constructed from the concatenated sequences of the essential ORFs of the major and minor parental regions of selected SARS-CoV and SL-CoVs. Two genome regions between three estimated breakpoints (20,827–26,553 and 26,554–28,685) were aligned independently using ClustalX and generated two alignments of 5,727 base pairs and 2,133 base pairs. The two alignments were used to construct maximum likelihood trees to better infer the fragment parents. All nucleotide numberings in this study are based on Rs3367 genome position.
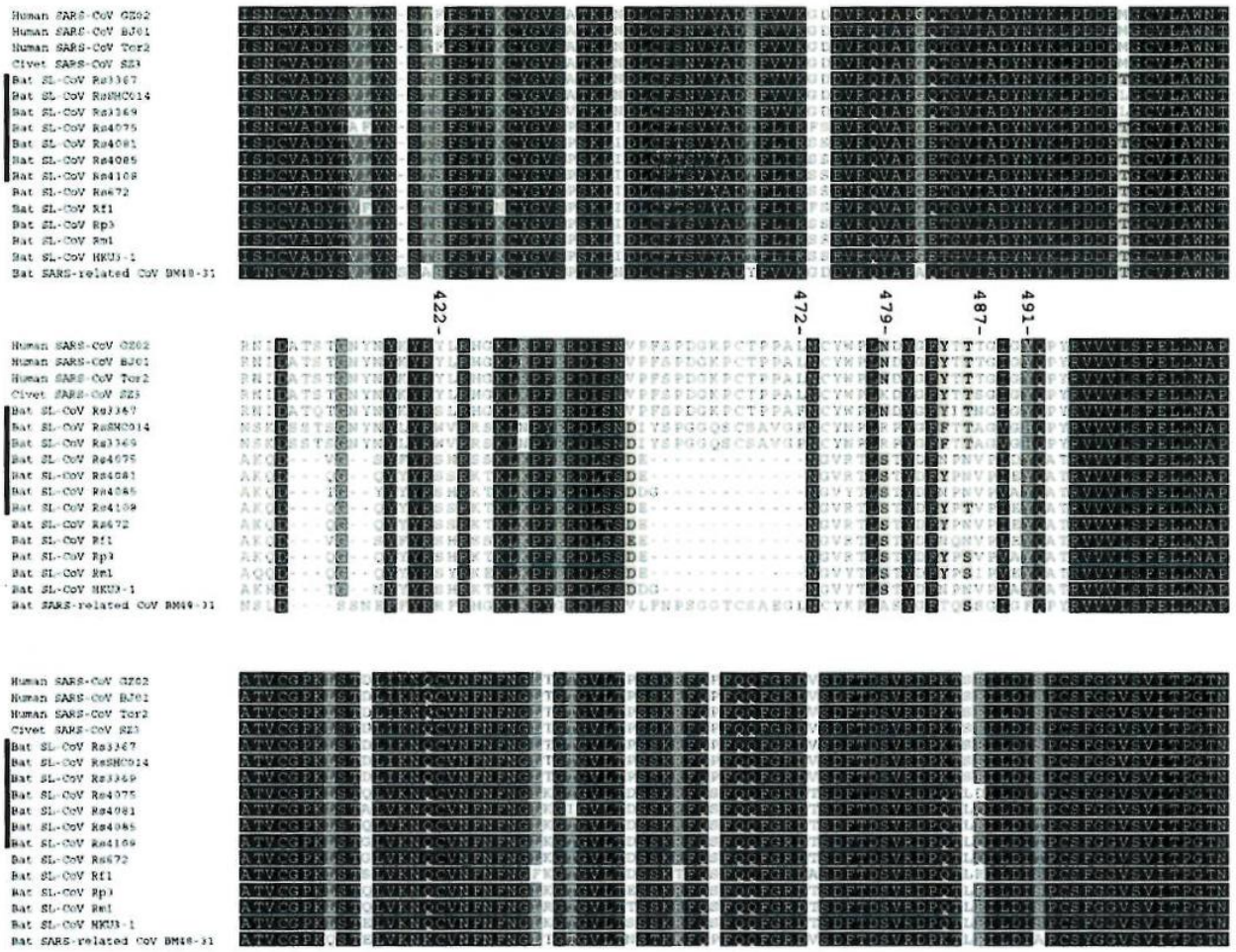
Extended Data Figure 1 | Sequence alignment of CoV S protein RBD.
SARS-CoV S protein (amino acids 310–520) is aligned with homologous regions of bat SL-CoVs using ClustalW. The newly discovered bat SL-CoVs are indicated with a bold vertical line on the left. The key amino acid residues involved in the interaction with human ACE2 are numbered on the top of the aligned sequences.

Extended Data Figure 2 | Alignment of CoV S protein S1 sequences.
Alignment of S1 sequences (amino acids 1–660) of the two novel bat SL-CoV S proteins with those of previously reported bat SL-CoVs and human and civet SARS-CoVs. The newly discovered bat SL-CoVs are boxed in red. SARS-CoV GZ02, BJ01 and Tor2 were isolated from patients in the early, middle and late phase, respectively, of the SARS outbreak in 2003. SARS-CoV SZ3 was identified from *P. larvata* in 2003 collected in Guangdong, China. SL-CoV Rp3, Rs 672 and HKU3-1 were identified from *R. sinicus* collected in Guangxi, Guizhou and Hong Kong, China, respectively. Rf1 and Rm1 were identified from *R. ferrumequinum* and *R. macrotis*, respectively, collected in Hubei Province, China. Bat SARS-related CoV BM48-31 was identified from *R. blasii* collected in Bulgaria.
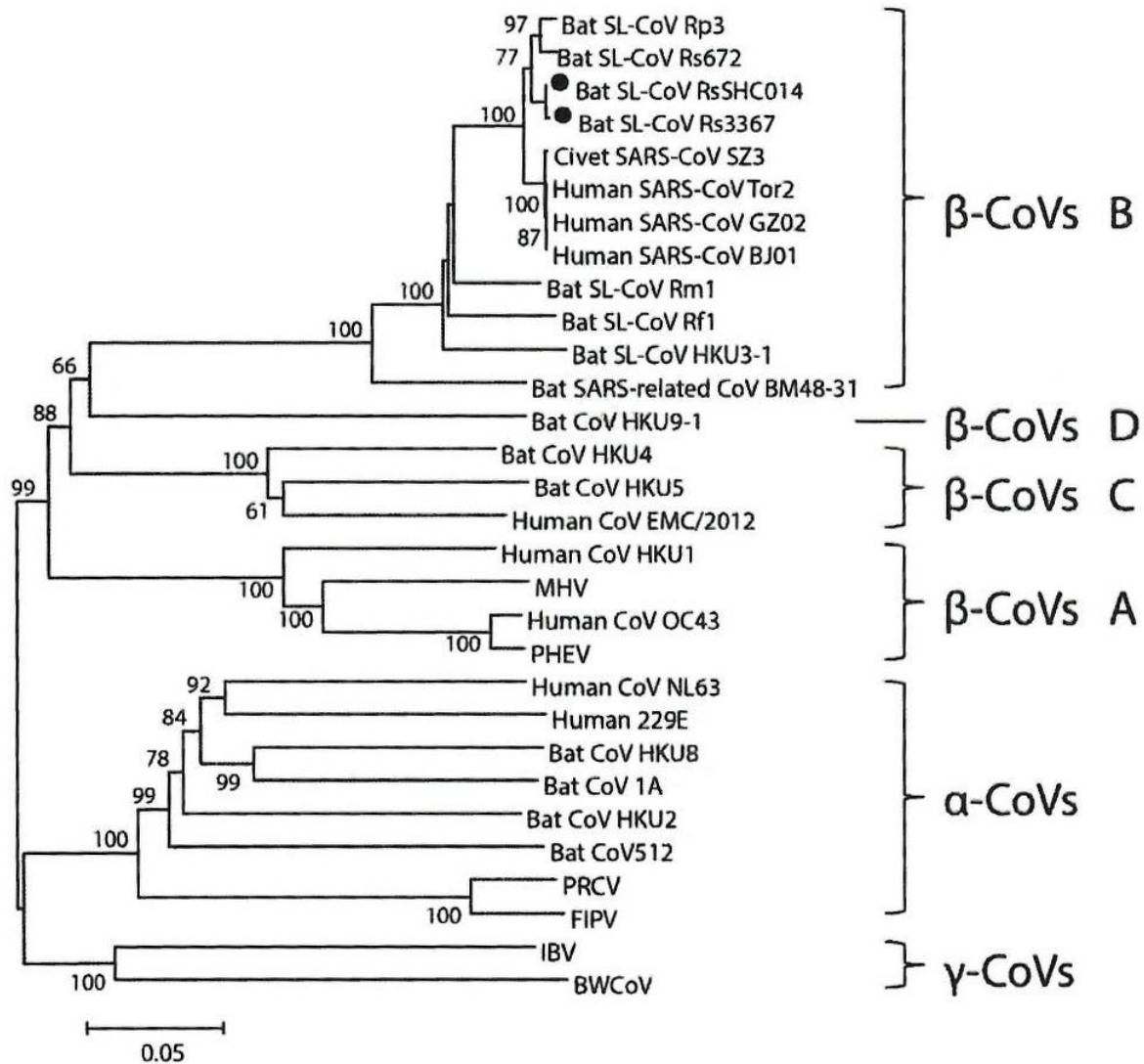
Extended Data Figure 3 | Complete RdRP sequence phylogeny.
Phylogenetic tree of bat SL-CoVs and SARS-CoVs on the basis of complete RdRP sequences (2,796 nucleotides). Bat SL-CoVs RsSHC014 and Rs3367 are highlighted by filled circles. Three established coronaivirus genera, *Alphacoronavirus*, *Betacoronavirus* and *Gammacoronavirus* are marked as α, β and γ, respectively. Four CoV groups in the genus *Betacoronavirus* are indicated as A, B, C and D, respectively. MHV, murine hepatitis virus; PHEV, porcine haemagglutinating encephalomyelitis virus; PRCV, porcine respiratory coronavirus; FIPV, feline infectious peritonitis virus; IBV, infectious bronchitis coronavirus; BW, beluga whale coronavirus.
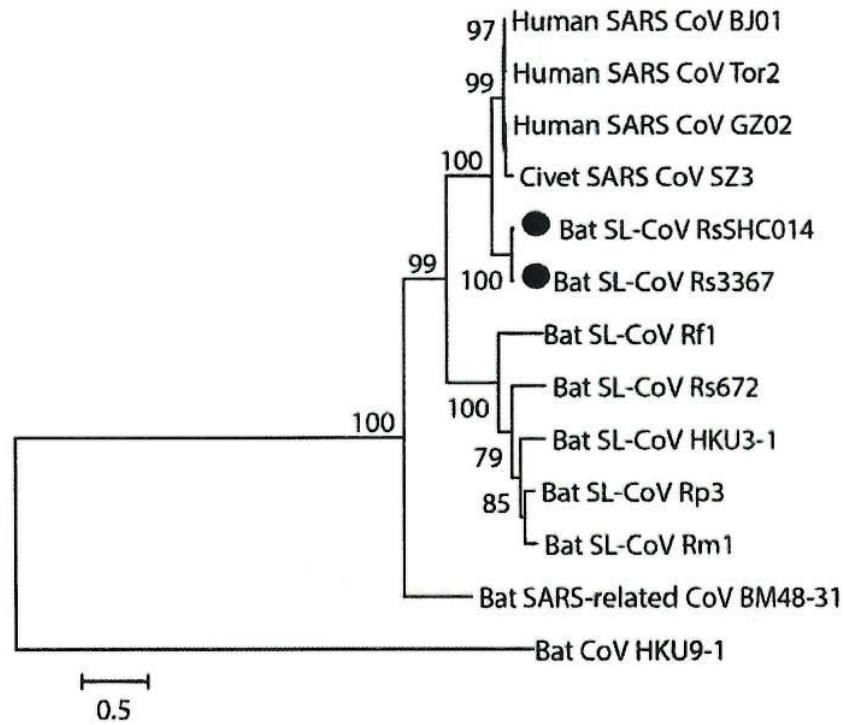
Extended Data Figure 4 | Sequence phylogeny of the complete S protein of SL-CoVs and SARS-CoV. Phylogenetic tree of bat SL-CoVs and SARS-CoVs on the basis of complete S protein sequences (1,256 amino acids). Bat SL-CoVs RsSHC014 and Rs3367 are highlighted by filled circles. Bat CoV HKU9 was used as an outgroup.
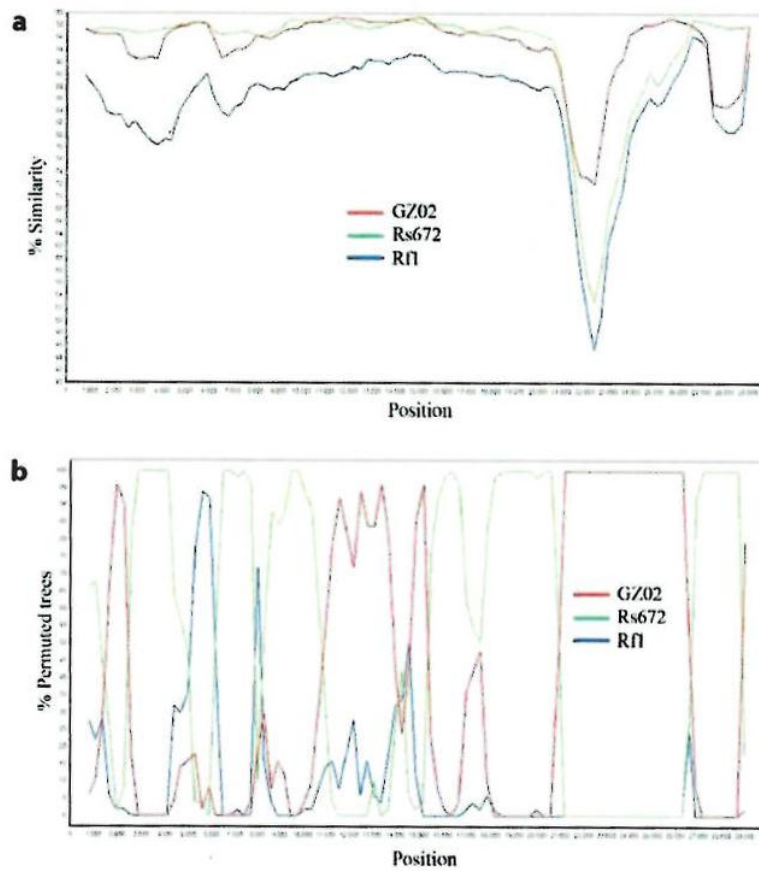
Extended Data Figure 5 | Detection of potential recombination events.
a, b, Similarity plot (**a**) and bootscan analysis (**b**) detected three recombination breakpoints in the bat SL-CoV Rs3367 or SHC014 genome. The three breakpoints were located at the ORF1b (nt 20,827), M (nucleotides 26,553) and N (nucleotides 28,685) genes, respectively. Both analyses were performed with an F84 distance model, a window size of 1,500 base pairs and a step size of 300 base pairs.

Extended Data Table 1 | Summary of sampling detail and CoV prevalence

Sampling time	Total number of swab or fecal samples collected	Number of CoV PCR positive samples (%)
April, 2011	14	1 (7.1)
October, 2011	10	3 (30)
May, 2012	54	4 (7.4)
September, 2012	39	19 (48.7)

Extended Data Table 2 | Genomic sequence identities of bat SL-CoVs with SARS-CoVs

CoVs	Genome size (nt)	Pairwise genomic nucleotide acids identity (%)										
		Bat SARS-Like CoVs							Human and civet SARS-CoVs			
		SHC014	Rs672	Rp3	Rf1	Rm1	HKU3-1	BM48-31	GZ02	BJ01	Tor2	SZ3
3367	29,787	98.8	92.5	93.2	87.3	88.0	87.8	76.9	95.4	95.3	95.4	95.3
SHC014	29,787	-	92.6	93.2	87.3	88.1	87.8	77.0	95.2	95.1	95.1	95.1
Rs672	29,059		-	92.4	86.2	87.4	87.0	75.2	90.9	90.9	90.8	91.0
Rp3	29,736			-	88.3	90.3	89.6	77.0	92.1	92.0	92.1	92.0
Rf1	29,709				-	89.4	88.4	76.6	87.2	87.1	87.2	87.1
Rm1	29,749					-	90.1	76.4	87.6	87.5	87.5	87.5
HKU3-1	29,728						-	76.8	87.4	87.3	87.4	87.3
BM48-31	29,276							-	76.9	77.1	77.0	76.9
GZ02	29,760								-	99.6	99.6	99.7
BJ01	29,725									-	99.8	99.6
Tor2	29,751										-	99.5
SZ3	29,741											-

Extended Data Table 3 | Genomic annotation and comparison of bat SL-CoV Rs3367 with human/civet SARS-CoVs and other bat SL-CoVs

					ORF Identity nt/aa (%)									
					Human and civet SARS-CoVs				Bat SARS-like CoVs					
ORFs	Start-End (nt.)	No. of Nt.	No. of Aa.	TRS	GZ02	BJ01	Tor2	SZ3	Rs672	Rp3	Rf1	Rm1	HKU3-1	BM48-31
P1a	265-13,398	13,134	4,377	ACGAA...	?.7/97.9	96.6/97.9	96.8/97.9	96.8/98.1	93.3/94.2	95.5/96.9	88.1/94.0	87.9/93.3	87.9/94.2	76.3/80.8
P1b	13,398-21,485	8,088	2,695		96.3/99.2	96.3/99.2	96.3/99.2	96.3/99.2	97.2/99.2	97.2/99.2	90.6/98.4	91.0/98.7	90.7/98.5	83.4/93.7
S	21,492-25,262	3,771	1,256	ACGAACAUG	88.3/90.1	88.2/90.0	88.1/89.8	88.2/90.0	76.5/78.2	76.0/79.1	74.0/77.4	76.3/79.1	75.6/78.2	70.2/74.5
(S1)*	21,493-23,535	2,043	681		78.2/81.1	78.2/80.9	78.1/80.6	78.2/81.1	65.1/82.2	63.9/63.0	62.9/62.5	64.7/63.3	65.2/63.4	62.2/64.7
(S2)*	23,536-25,263	1,728	575		98.1/99.3	98.1/99.3	98.?/...	...	...	...	...2.7	87.9/95.4	86/93.5	76.6/88.2
ORF3a	25,271-26,095	825	274	ACGAAC AUG	99.2/98.1	98.6/97.0	98.?/...	...	...	...	...8	83.6/84.3	83.1/82.4	72.1/71.2
ORF3b	25,692-26,036	345	114		99.1/99.1	98.2/98.2	...	...	N/D	...1	N/D	N/D	N/D	
E	26,120-26,350	231	76	ACGAAC AUG	98.7/98.6	98.7/98.6	98.?/...	...	...	...0	...0	96.1/97.3	97.4/98.6	91.3/93.4
M	26,401-27,066	666	221	ACGAAC AUG	97.4/98.1	97.2/98.1	97.?/...	...	...	...6	93.2/95.4	93.9/98.8	78.5/88.1	
ORF6	27,077-27,268	192	63	ACGAAC AUG	97.3/95.2	96.8/93.6	97.?/...	...	...	...0	95.3/92	94.7/90.4	63.5/49.2	
ORF7a	27,276-27,644	369	122	ACGAACAUG	94.5/95.9	94.5/95.9	94.?/...	...	...	...0	93.4/97.5	93.2/97.5	62.3/58.1	
ORF7b	27,641-27,776	135	44		96.2/93.1	96.2/93.1	96.?/...	98.?/...	99.2/100	.../100	.../.7	99.2/100	93.3/95.4	62.9/63.6
ORF8	27,782-28,147	366	121	ACGAACAUG	47.1/46.3	N/A	N/A	47.1/46.3	97.8/100	85.2/90.2	46.2/39.0	85.7/90.2	85.7/85.3	N/A
N	28,162-29,430	1,269	422	ACGAAC AUG	98.3/99.5	98.4/99.5	98.4/99.5	98.4/99.5	98/98.5	96.6/97.8	93.7/95.2	96.2/97.1	95.9/98.2	77.9/87.2
s2m	29,628-29,668	41			97.5	97.5	97.5	97.5	100	100	100	100	100	95.1

*S1, the N-terminal domain of the coronavirus S protein responsible for receptor binding. S2, the S protein C-terminal domain responsible for membrane fusion.

The ORFs in the genome were predicted and potential protein sequences were translated. The pairwise comparisons were conducted for all ORFs at nucleotide acids (nt) and amino acids (aa) levels. The s2m were compared at nt level. TRS: Transcription regulating-sequences; N/D, not done; N/A, not available.

Extended Data Table 4 | Genomic annotation and comparison of bat SL-CoV RsSHC014 with human/civet SARS-CoVs and other bat SL-CoVs

ORFs	Start-End (nt.)	No. of Nt.	No. of Aa.	TRS	ORF Identity nt/aa (%)									
					Human and civet SARS-CoVs				Bat SARS-like CoVs					
					GZ02	BJ01	Tor2	SZ3	Rs672	Rp3	Rf1	Rm1	HKU3-1	BM48-31
P1a	265-13,398	13,134	4,377	ACGAAC	98.7/97.9	96.6/97.9	96.8/97.9	96.8/98.1	93.3/94.2	95.5/96.9	88.1/94.0	87.9/93.3	87.9/94.2	76.3/80.8
P1b	13,398-21,485	8,088	2,695		96.3/99.2	96.3/99.2	96.3/99.2	96.3/99.2	97.2/99.2	97.2/99.2	90.6/98.4	91.0/98.7	90.7/98.5	83.4/93.7
S	21,492-25,262	3,771	1,256	ACGAACAUG	88.3/90.1	88.2/90.0	88.1/89.8	88.2/90.0	76.5/78.2	76.0/79.1	74.0/77.4	76.3/79.1	75.6/78.2	70.2/74.5
(S1)*	21,493-23,535	2,043	681		78.2/81.1	78.2/80.9	78.1/80.6	78.2/81.1	65.1/62.2	63.9/63.0	62.9/62.5	64.7/63.3	65.2/63.4	62.2/64.7
(S2)*	23,536-25,263	1,728	575		98.1/99.3	98.1/99.3	98.1/99.3	98.1/99.3				87.9/95.4	86/93.5	76.6/88.2
ORF3a	25,271-26,095	825	274	ACGAAC AUG	99.2/98.1	98.6/97.0						83.6/84.3	83.1/82.4	72.1/71.2
ORF3b	25,692-26,036	345	114		99.1/99.1	98.2/98.2						N/D	N/D	N/D
E	26,120-26,350	231	76	ACGAAC AUG	98.7/98.6	98.7/98.6						96.1/97.3	97.4/98.6	91.3/93.4
M	26,401-27,066	666	221	ACGAAC AUG	97.4/98.1	97.2/98.1						93.2/95.4	93.9/98.8	78.5/88.1
ORF6	27,077-27,268	192	63	ACGAAC AUG	97.3/95.2	96.8/93.6						95.3/92	94.7/90.4	63.5/49.2
ORF7a	27,276-27,644	369	122	ACGAACAUG	94.5/95.9	94.5/95.9						93.4/97.5	93.2/97.5	62.3/58.1
ORF7b	27,641-27,776	135	44		96.2/93.1	96.2/93.1	96.2/93.1	96.2/93.1				99.2/100	93.3/95.4	62.9/63.6
ORF8	27,782-28,147	366	121	ACGAACAUG	47.1/46.3	N/A	N/A	47.1/46.3	97.8/100	85.2/90.2	45.2/39.0	85.7/90.2	85.7/85.3	N/A
N	28,162-29,430	1,269	422	ACGAAC AUG	98.3/99.5	98.4/99.5	98.4/99.5	98.4/99.5	98/98.5	96.8/97.6	93.7/95.2	96.2/97.1	95.9/96.2	77.9/87.2
s2m	29,628-29,668	41			97.5	97.5	97.5	97.5	100	100	100	100	100	95.1

*S1, the N-terminal domain of the coronavirus S protein responsible for receptor binding. S2, the S protein C-terminal domain responsible for membrane fusion.

The ORFs in the genome were predicted and potential protein sequences were translated. The pairwise comparisons were conducted for all ORFs at nucleotide acids (nt) and amino acids (aa) levels. The s2m were compared at nt level. TRS: Transcription regulating-sequences. N/D, not done. N/A, not available.

Extended Data Table 5 | Cell lines used for virus isolation and susceptibility tests

Cell lines	Species (organ) origin	Medium	Infectivity
293T	Human (kidney)	DMEM+10%FBS	-
Hela	Human (cervix)		-
VeroE6	Monkey (kidney)		+
PK15	Pig (kidney)		+
BHK21	Hamster (kidney)		-
A549	Human (alveolar basal epithelial)		+
BK	*Myotis davidii* (kidney)	RPMI1640+10%FBS	-
RSKT	*Rhinolophus sinicus* (kidney)	DMEM/F12+10%FBS	+
MCKT	*Myotis chinensis* (kidney)		-
PaKi	*Pteropus alecto* (kidney)		-
RLK	*Rousettus leschenaulti* (kidney)		-

* Infectivity was determined by the presence of viral antigen detected by immunofluorescence assay.

SARS-like WIV1-CoV poised for human emergence

Vineet D. Menachery[a], Boyd L. Yount Jr.[a], Amy C. Sims[a], Kari Debbink[a,b], Sudhakar S. Agnihothram[c], Lisa E. Gralinski[a], Rachel L. Graham[a], Trevor Scobey[a], Jessica A. Plante[a], Scott R. Royal[a], Jesica Swanstrom[a], Timothy P. Sheahan[a], Raymond J. Pickles[c,d], Davide Corti[e,f,g], Scott H. Randell[d], Antonio Lanzavecchia[e,f], Wayne A. Marasco[h], and Ralph S. Baric[a,c,1]

[a]Department of Epidemiology, University of North Carolina at Chapel Hill, Chapel Hill, NC 27599; [b]Department of Microbiology and Immunology, University of North Carolina at Chapel Hill, Chapel Hill, NC 27599; [c]Division of Microbiology, National Center for Toxicological Research, Food and Drug Administration, Jefferson, AR 72079; [d]Department of Cell Biology and Physiology and Marsico Lung Institute/Cystic Fibrosis Center, University of North Carolina at Chapel Hill, Chapel Hill, NC 27599; [e]Institute for Research in Biomedicine, Bellinzona, Switzerland; [f]Institute of Microbiology, Eidgenössische Technische Hochschule Zurich, Zurich, Switzerland; [g]Humabs BioMed SA, Bellinzona, Switzerland; and [h]Department of Cancer Immunology and AIDS, Dana-Farber Cancer Institute–Department of Medicine, Harvard Medical School, Boston MA 02215

Outbreaks from zoonotic sources represent a threat to both human disease as well as the global economy. Despite a wealth of metagenomics studies, methods to leverage these datasets to identify future threats are underdeveloped. In this study, we describe an approach that combines existing metagenomics data with reverse genetics to engineer reagents to evaluate emergence and pathogenic potential of circulating zoonotic viruses. Focusing on the severe acute respiratory syndrome (SARS)-like viruses, the results indicate that the WIV1-coronavirus (CoV) cluster has the ability to directly infect and may undergo limited transmission in human populations. However, in vivo attenuation suggests additional adaptation is required for epidemic disease. Importantly, available SARS monoclonal antibodies offered success in limiting viral infection absent from available vaccine approaches. Together, the data highlight the utility of a platform to identify and prioritize prepandemic strains harbored in animal reservoirs and document the threat posed by WIV1-CoV for emergence in human populations.

SARS | CoV | emergence | Spike | WIV1

Although previously associated with upper respiratory infections, the emergence of severe acute respiratory coronavirus (SARS-CoV) in 2002–2003, and more recently, Middle East respiratory syndrome (MERS)-CoV underscores the threat of cross-species transmission leading to virulent pandemic viral infections (1, 2). Whereas prevailing research suggests that SARS-CoV emerged from viruses in the Chinese horseshoe bat, identifying a progenitor strain that used human angiotensin converting enzyme 2 (ACE2) had proven elusive (3, 4). However, recent metagenomics studies isolated several SARS-like virus sequences that share ≥90% genome-wide homology and represented the closest sequences to the epidemic strains (5, 6). Importantly, researchers also isolated replication competent virus; WIV1-CoV, part of the Rs3306 cluster, could use ACE2 orthologs and mediated low-level replication in human cells (5). Overall, the evidence indicates that SARS-CoV likely emerged from Chinese horseshoe bats and that similar viruses are still harbored in these populations.

The identification of WIV1-CoV and its capacity to use ACE2 orthologs offers a warning for possible reemergence and provides an opportunity to prepare for a future CoV outbreak. To achieve this goal, a new platform is required to translate metagenomics findings; the approach must generate critical diagnostic reagents, define emergence potential of novel strains, and determine efficacy of current therapeutics. Building on this premise, we developed a framework to examine circulating CoVs using reverse genetic systems to construct full-length and chimeric viruses. The results indicate that viruses using WIV1-CoV spike are poised to emerge in human populations due to efficient replication in primary human airway epithelial cell cultures. However, additional adaptation, potentially independent of the spike protein receptor-binding domain, is required for pathogenesis and epidemic disease. Importantly, monoclonal antibody

strategies against SARS were effective against WIV1-CoV spike unlike available vaccine approaches. Together, the results highlight the utility of developing platforms to evaluate circulating zoonotic viruses as threats for future emergence and epidemic potential.

Results

The discovery of SARS-like virus clusters that bridge the gap between the epidemic strains and related precursor CoV strain HKU3 virus provided the best evidence for emergence of SARS-CoV from Chinese horseshoe bats (5). Comparing the receptor binding domain (RBD), SARS-CoV Urbani and WIV1 share homology at 11 of the 14 contact residues with human ACE2 (Fig. 1A); importantly, the three amino acid changes represent relatively conservative substitution not predicted to ablate binding (Fig. 1B). Therefore, exploring WIV1 strains allows examination of emergence, pathogenesis potential, and adaptation requirements. Using the SARS-CoV infectious clone as a template (7), we designed and synthesized a full-length infectious clone of WIV1-CoV consisting of six plasmids that could be enzymatically cut, ligated together, and electroporated into cells to rescue replication competent progeny virions (Fig. S1A). In addition to the full-length clone, we also produced WIV1-CoV

Significance

The emergence of severe acute respiratory syndrome coronavirus (SARS-CoV) and Middle East respiratory syndrome (MERS)-CoV highlights the continued risk of cross-species transmission leading to epidemic disease. This manuscript describes efforts to extend surveillance beyond sequence analysis, constructing chimeric and full-length zoonotic coronaviruses to evaluate emergence potential. Focusing on SARS-like virus sequences isolated from Chinese horseshoe bats, the results indicate a significant threat posed by WIV1-CoV. Both full-length and chimeric WIV1-CoV readily replicated efficiently in human airway cultures and in vivo, suggesting capability of direct transmission to humans. In addition, while monoclonal antibody treatments prove effective, the SARS-based vaccine approach failed to confer protection. Together, the study indicates an ongoing threat posed by WIV1-related viruses and the need for continued study and surveillance.
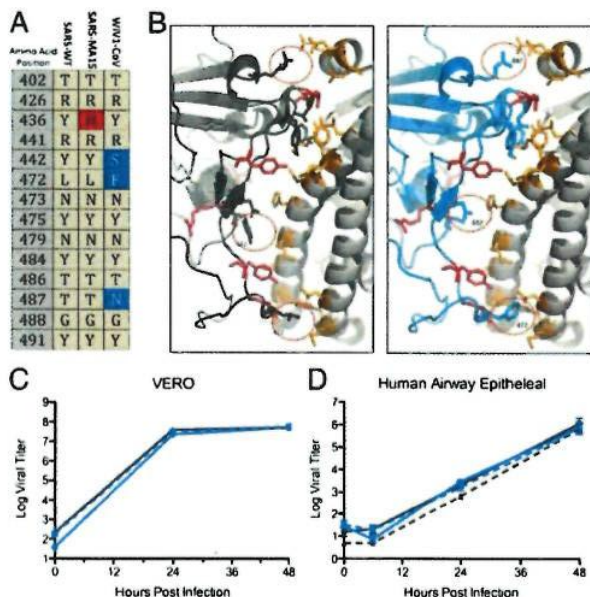
Fig. 1. Full-length and chimeric WIV1 infectious clones produce viruses that replicate in primary human airway epithelial cell cultures. (*A*) Spike amino acid residues that interact directly with human ACE2 from SARS-CoV, SARS-MA15, and WIV1-CoV spike proteins. Residue changes are highlighted by color. (*B*) Interaction between S1 domain of SARS-Urbani spike (black) and WIV1 spike (blue) with human ACE2 (gray). Contact residues highlighted with consensus amino acids (red) and differences (circled) between SARS and WIV1 spike proteins; human ACE2 contact residues are also highlighted (orange). (*C*) Viral replication of WIV1-CoV (blue), WIV1-MA15 (blue hatched), and SARS-CoV Urbani (black) following infection of Vero cells at a multiplicity of infection (MOI) of 0.01. (*D*) Well-differentiated air–liquid interface primary human airway epithelial cell cultures were infected with SARS-CoV Urbani (black), SARS-CoV MA15 (black hatched), WIV1-MA15 (blue-white hatched), and WIV-CoV (blue) at (*E*) MOI of 0.01 in cells from the same donor at an MOI of 0.01. Samples were collected at individual time points with biological replicates (*n* = 3) for all experiments for both *C* and *D*.

chimeric virus that replaced the SARS spike with the WIV1 spike within the mouse-adapted backbone (WIV1-MA15, Fig. S1*B*). WIV1-MA15 incorporates the original binding and entry capabilities of WIV1-CoV, but maintains the backbone changes to mouse-adapted SARS-CoV. Importantly, WIV1-MA15 does not incorporate the Y436H mutation in spike that is required for SARS-MA15 pathogenesis (8). Following electroporation into Vero cells, robust stock titers were recovered from both chimeric WIV1-MA15 and WIV1-CoV. To confirm growth kinetics and replication, Vero cells were infected with SARS-CoV Urbani, WIV1-MA15, and WIV1-CoV (Fig. 1*C*); the results indicate similar replication kinetics and overall titers between the CoVs. However, Western blot analysis suggests potential differences in spike cleavage/processing of WIV1 and SARS-CoV spike proteins (Fig. S1*C*); the ratio of full-length to cleaved spike varied between SARS spikes (Urbani, 1.21; MA15, 1.44) and WIV1 (full length, 0.61; WIV1-MA15, 0.25) signaling possible variation in host proteolytic processing (Fig. S1*D*). Overall, the results indicate comparable viral replication, but possible biochemical differences in processing.

Replication in Primary Human Epithelial Cells. Next, we wanted to determine WIV-CoV replication potential in models of the human lung. Previous examination of WIV1-CoV recovered from bat samples demonstrated poor replication in A549 cells (5); however, replication of epidemic SARS-CoV is also poor in

this cell type, potentially due to ACE2 expression levels (9). Therefore, well-differentiated primary human airway epithelial cell (HAE) air–liquid interface cultures were infected with WIV1-MA15, WIV1-CoV, SARS-CoV Urbani, or SARS-CoV MA15. At 24 and 48 h postinfection, both WIV1-MA15 and WIV1-CoV produce robust infection in HAE cultures equivalent to the epidemic strain and mouse-adapted strains (Fig. 1*D*). Together, the data demonstrate that the WIV1-CoV spike can mediate infection of human airway cultures with no significant adaptation required.

WIV1 Spike in Vivo. To extend analysis to pathogenesis, we next evaluated in vivo infection following WIV1-MA15 and WIV1-CoV challenge. Initial studies compared WIV1-MA15 to mouse-adapted SARS-CoV (MA15) to determine spike-dependent pathogenesis. Ten-week-old BALB/c mice were infected with 10^4 plaque forming units (pfu) of WIV1-MA15 or SARS-CoV MA15 and followed over a 4-d time course. As expected, animals infected with SARS-CoV MA15 experienced rapid weight loss and lethality by day 4 postinfection (Fig. 2*A* and Fig. S2*A*) (10). In contrast, WIV1-MA15 induced neither lethality nor notable changes in body weight, indicating limited disease in vivo. Viral titer in the lung also revealed reduced replication following WIV1-MA15 challenge compared with control (Fig. 2*B*). Similarly, lung antigen staining indicated distinct attenuation of the WIV1-MA15, with most staining occurring in the airways and absent from large regions of the lungs (Fig. S2 *B–D*). Together, these data indicate that WIV1 spike substitution does not program pathogenesis in the mouse-adapted SARS-CoV backbone.

Although chimeric studies suggest minimal pathogenesis potential for WIV1 spike, SARS-CoV Urbani spike within the mouse-adapted backbone yielded similar results (8). Therefore, we examined the full-length WIV1-CoV versus the epidemic SARS-CoV Urbani strain in vivo. Ten-week-old BALB/c mice
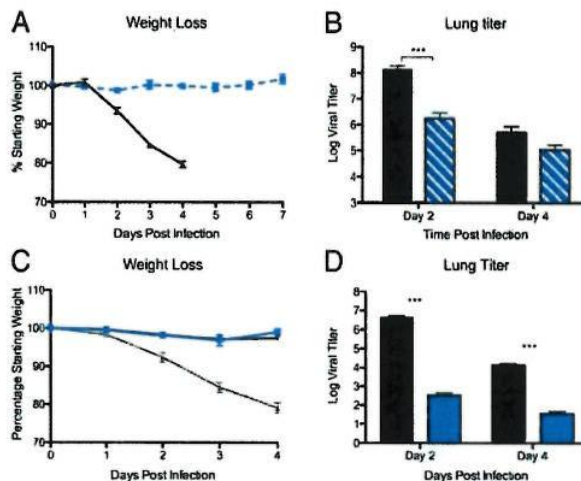

Fig. 2. Viruses using WIV1 spike attenuated relative to SARS spike in vivo. (*A* and *B*) Ten-week-old BALB/c mice were infected with 10^4 pfu of either SARS-CoV MA15 (black) or WIV1-MA15 (blue hatched) via the i.n. route and examined over a 7-d time course. (*A*) Weight loss (*n* = 17 for WIV1-MA15, *n* = 9 for SARS-CoV MA15) and (*B*) lung titer (*n* = 3 for MA15, *n* = 4 for WIV1-MA15. (*C* and *D*) Ten-week-old BALB/c mice were infected with 1 × 10^5 pfu of either SARS-CoV Urbani (black), WIV1-CoV (blue), or SARS-CoV MA15 (gray) and examined over a 4-d time course. (*C*) Weight loss (*n* = 6 for WIV1-CoV, *n* = 6 for SARS-CoV Urbani) and (*D*) lung titer (*n* = 3 for WIV1-CoV, *n* = 3 for SARS-CoV Urbani) were examined. For each bar graph, center value is representative of group mean and error bars are defined by SEM. *P* values based on two-tailed Student's *t* test of individual time points are marked as indicated: ***P* < 0.001.

were infected with 10^5 pfu of WIV1-CoV or SARS-CoV Urbani and followed over a 4-d time course. As expected, neither infection condition resulted in significant weight loss compared with MA15 (Fig. 2C). However, viral replication was significantly attenuated for WIV1-CoV compared with SARS-CoV Urbani (Fig. 2D); at both days 2 and 4 postinfection, WIV1-CoV titer was reduced nearly 10,000- and 1,000-fold, respectively. Similarly, only minor antigen staining was observed following WIV1-CoV infection, contrasting antigen staining throughout the parenchyma 2-d post–SARS-CoV Urbani infection (Fig. S2 *E* and *F*). Together, the data indicate significant attenuation of WIV1-CoV relative to the epidemic SARS-CoV in wild-type mice.

WIV1-CoV in Human ACE2 Expressing Mice. Whereas studies in wild-type mice provide insight into pathogenesis potential, the absence of clinical disease in the epidemic strains of SARS-CoV suggests that the mouse model may not be adequate to access human disease potential. To test a model more relevant to humans, we generated a mouse that expresses human ACE2 receptor under control of HFH4, a lung ciliated epithelial cell promoter (11). However, whereas robust expression was observed in the lung, other tissues including brain, liver, kidney, and gastrointestinal tract had varying levels of human ACE2 expression, indicating greater tissue distribution of HFH4-mediated expression than initially expected (Fig. S3*A*). In addition, examination of individual HFH4-ACE2–expressing progeny revealed the occasional absence of the human ACE2 gene, suggesting possible selection against human receptor (Fig. S3*B*). Therefore, PCR-positive, 10- to 20-wk-old HFH4-ACE2–expressing mice were infected with 10^5 pfu of WIV1-CoV or SARS-CoV Urbani and then followed for a 7-d time course to determine pathogenesis. The results indicated that WIV1-CoV infection was augmented, but remained attenuated relative to SARS-CoV Urbani in the presence of human *ACE2*. Following SARS-CoV Urbani challenge, HFH4-hACE2–expressing mice lost no weight, but then, experienced rapid weight loss and death between days 4 and 5 (Fig. 3*A* and Fig. S3*C*). In contrast, WIV1-CoV produce minimal changes in weight loss until late times where animals fell into distinct categories either losing less than or more than 10% of their body weight. Whereas day-2 lung titers were still attenuated relative to SARS-CoV Urbani, titers for WIV1-CoV were 100-fold higher in the presence of human ACE2 compared with wild-type BALB/c, with no similar augmentation observed with the epidemic SARS-CoV strain (Fig. 3*B*). Based on pilot studies and previous studies with ACE2 transgenic animals (12), mice experiencing rapid weight loss were predicted to have lethal encephalitis and were humanely killed and harvested for lung and brain titer if weight loss approached >20% of starting body weight. All HFH4-ACE2 mice infected with SARS-CoV Urbani lost >20% body weight and maintained robust replication in the lung and brain following infection (Fig. 3 *C* and *D*). Similarly, mice with >10% weight loss following WIV1-CoV infection produced robust viral replication in the brain, but significantly lower titers in the lung. In contrast, mice that maintained minimal weight loss (<10%) following WIV1-CoV infection after 7 d had minimal titers in both the lung and brain, suggesting a sufficient adaptive immune response was generated to clear virus and survive infection. Together, the data indicate that WIV1-CoV maintains attenuation relative to SARS-CoV Urbani despite the availability of human *ACE2*. In addition, augmented replication suggests that WIV1-CoV may bind the human ACE2 receptor more efficiently that the mouse ACE2, indicating potential inadequacies in the current mouse models of SARS pathogenesis.

Therapeutics Against WIV1 Emergence. Having established a potential threat based on replication in primary human cells and preference for the human ACE2 receptor in vivo, we next sought
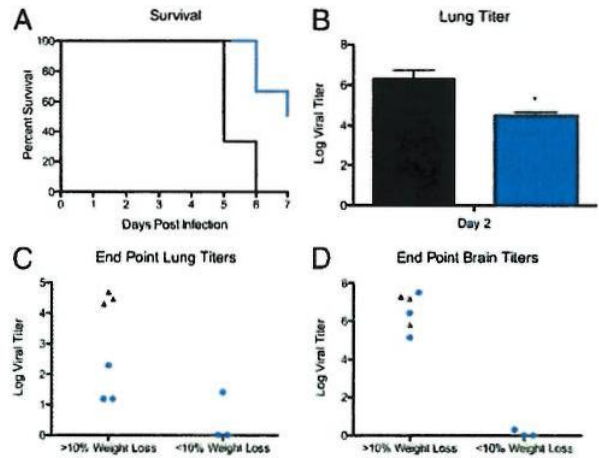

Fig. 3. WIV1-Cov still attenuated despite human ACE2 expression in vivo. (*A*) Ten- to twenty-week-old HFH4 ACE2-expressing mice were infected with 10^5 pfu of SARS-CoV Urbani (black) or WIV1-CoV (blue) and examined over a 7-d time course for (*A*) survival and (*B*) day-2 lung titer ($n = 3$ for WIV1-CoV, $n = 3$ for SARS-CoV Urbani). (*C* and *D*) Upon reaching thresholds for humane sacrifice (>20% weight loss) or 7 d postinfection (DPI), endpoint titers were determined in the (*C*) lung and (*D*) brain following infection. *P* values based on two-tailed Student's *t* test of individual time points are marked as indicated: *$P < 0.05$.

to determine if monoclonal antibody therapies could be used to lessen disease similar to ZMApp for Ebola (13). We first tested a SARS-CoV monoclonal derived via phage display and antibody escape (Fm6) (14) and found both wild-type SARS-CoV Urbani and WIV1-MA15 were strongly neutralized at low antibody concentrations (Fig. 4*A*). Similarly, a panel of monoclonal antibodies derived from B cells from SARS-CoV–infected patients also prevented virus infection via WIV1-CoV spike (15, 16). Both antibodies 230.15 and 227.14 robustly inhibited WIV1-MA15 replication with kinetics similar to or exceeding SARS-CoV Urbani (Fig. 4 *B* and *C*). In contrast, antibody 109.8, which maps outside the receptor binding domain, produced only marginal neutralization of WIV1-MA15 (Fig. 4*D*). Whereas the residue associated with prior escape mutants was conserved at position 332, the adjacent residue had a significant change (K332T) in WIV1-CoV, possibly contributing to reduced efficacy of this antibody.

To further extend these findings, in vivo studies with antibody 227.14 were initiated in HFH4-ACE2–expressing mice. One day before infection, HFH4-ACE2–expressing mice were injected with 200 µg of antibody 227.14 or PBS control as previously described (17); mice were subsequently challenged with either SARS-CoV Urbani or WIV1-CoV and monitored for 7 d. The results indicate that antibody 227.14 protected mice from both lethal SARS-CoV Urbani and WIV-CoV challenge (Fig. 4*E*); in addition, lung titers revealed no detectable virus in either SARS-CoV or WIV1-CoV–infected HFH4-ACE2–expressing mouse lungs following antibody treatment (Fig. 4*F*). Together, the in vitro and in vivo data indicate that a mixture of broadly neutralizing antibodies against SARS-CoV would likely provide significant protection if WIV1-CoV–like viruses successfully transmitted to humans.

Vaccine Efficacy Limited Against WIV1 Spike. Previously, whole virion SARS-CoV inactivated by both formalin and UV irradiation (double inactivated virus, DIV) was demonstrated as a potential vaccination candidate based on robust neutralization and protection following homologous SARS-CoV challenge in young mice (18). However, both aged animal and heterologous
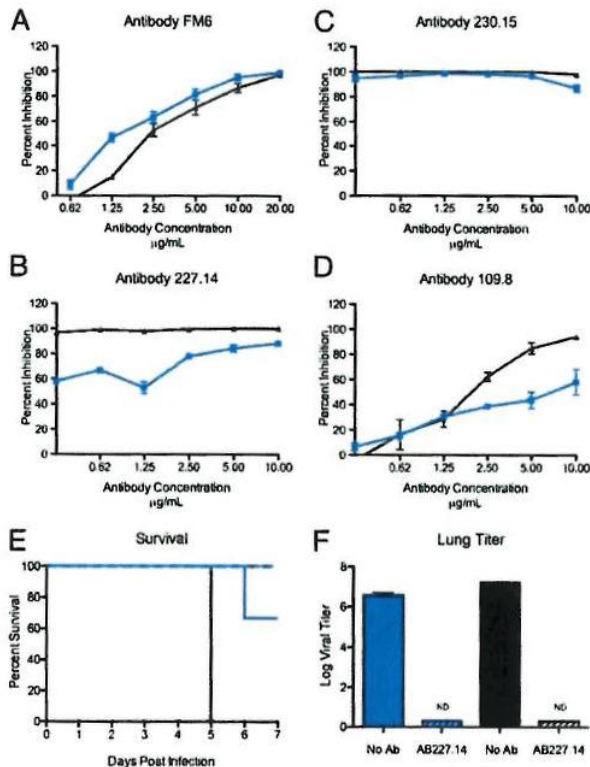
Discussion

The recent outbreaks of Ebola, influenza, and MERS-CoV underscore the threat posed by viruses emerging from zoonotic sources. Coupled with air travel and uneven public health infrastructures, it is critical to develop approaches to mitigate these and future outbreaks. In this paper, we outline a platform that leverages metagenomics data, synthetic genome design, transgenic mouse models, and therapeutic human antibodies to identify and treat potential prepandemic viruses. Focusing on SARS-like CoVs, the approach indicates that viruses using the WIV1-CoV spike protein are capable of infecting HAE cultures directly without further spike adaptation. Whereas in vivo data indicate attenuation relative to SARS-CoV, the augmented replication in the presence of human *ACE2* in vivo suggests that the virus has significant pathogenic potential not captured by current small animal models. Importantly, therapeutic treatment with monoclonal antibodies suggests a Zmapp-based approach would be effective against a WIV1-CoV spike-mediated outbreak. However, failure of SARS DIV vaccine to induce protection highlights the need for continued development of additional therapeutics. Overall, the characterization of WIV1-CoV and its pathogenic potential highlight the utility of this platform in evaluating currently circulating zoonotic viruses.

Primary human airway epithelial cell cultures derived from human donors and grown at an air–liquid interface represent the
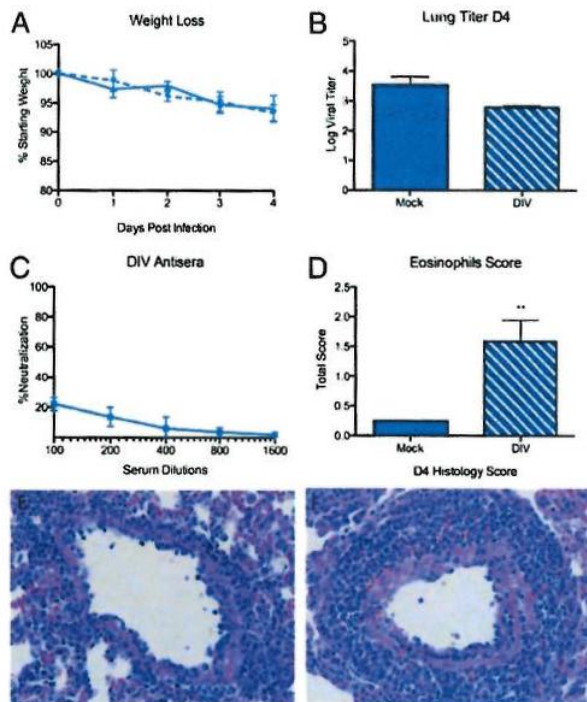
Fig. 4. SARS-CoV monoclonal antibodies have robust neutralization against WIV1 spike-mediated infection. Neutralization efficacy was evaluated using percent neutralization assays against SARS-CoV Urbani (black) or WIV1-MA15 (blue) with a panel of monoclonal antibodies: (*A*) fm6, (*B*) 230.15, (*C*) 227.15, and (*D*) 109.8, all originally generated against epidemic SARS-CoV. Each data point is representative of two or more independent neutralization wells. (*E* and *F*) Twenty- to twenty-four-week-old HFH4 ACE2-expressing mice were injected with 200 μg of anti-SARS human antibody 227.15 (hatched line) or mock (solid line) 1 d before infection with 1 × 10^5 pfu of SARS-CoV Urbani (black) or WIV1-CoV (blue) and examined over a 7-d time course for (*E*) survival (*n* = 3 for both antibody-treated groups and mock PBS control WIV1-CoV, *n* = 2 for mock-treated SARS-CoV Urbani), (*F*) day-2 lung titer (*n* = 3 for all groups). ND signifies no titers detected. For each bar graph, center value is representative of group mean and error bars are defined by SEM.

challenge studies revealed incomplete protection, increased immune pathology, and eosinophilia, indicating the possibility of adverse affects following DIV vaccination (19). To determine if heterologous challenge with WIV1-CoV spike produced a similar affect, 1-y-old BALB/c mice were vaccinated and boosted with DIV or PBS mock control. Mice were then challenged 6 wk postinitial vaccination with WIV1-MA15 and examined over a 4-d time course. Similar to previous experiments, mice infected with WIV1-MA15 had only marginal weight loss and showed no clinical signs of disease with either vaccination group (Fig. 5*A*). However, viral replication at day 4 was not significantly reduced in DIV-vaccinated groups compared with control (Fig. 5*B*). In addition, plaque reduction neutralization titers from the serum of aged DIV-vaccinated mice indicated no neutralization of WIV1-MA15, suggesting inadequate protection (Fig. 5*C*). Importantly, examination of histopathology revealed increased eosinophilia in DIV-vaccinated mice compared with PBS controls, indicating the potential for immune induced pathology due to vaccination. Together, the data indicate that DIV vaccination would not provide significant protection and may cause adverse effects in the context of WIV1-CoV spike-mediated outbreak.

Fig. 5. Double-inactivated whole SARS-CoV vaccine fails to protect aged animals from chimeric WIV1-CoV infection. Twelve-month-old mice were vaccinated and boosted with DIV (dotted line) or PBS (solid line) and infected 21 d postboost with 10^4 pfu of WIV1-MA15 via the i.n. route. (*A*) Weight loss following WIV1-MA15 challenge and (*B*) viral replication in the lung 4 DPI. (*C*) Neutralization of WIV1-MA15 (blue) with serum from aged, DIV-vaccinated mice. (*D*–*H*) Histopathology lung sections stained for H&E from DIV- and mock-vaccinated mice. (*D*) Eosinophil score (scale 0–4) following DIV or mock vaccination 4 DPI. (*E* and *F*) Representative H&E lung sections for (*E*) mock- and (*F*) DIV-vaccinated mice infected with WIV-MA15. Red arrows indicate individual eosinophil locations. *P* values based on two-tailed Student's *t* test of individual time points are marked as indicated: **$P < 0.01$.

closest model to the human lung. Therefore, the ability of both WIV1-CoV and WIV1-MA15 to grow equivalently to the epidemic SARS-CoV in these cultures is a major concern for emergence. However, pathogenesis studies in mice suggest that further adaptation may be required for epidemic disease. Compared with SARS equivalents, both full-length and chimeric WIV1 viruses had significant attenuation even with the presence of human *ACE2* in the mouse model. Together, the data suggest that despite using ACE2 and robust replication in primary human airway epithelial cultures, WIV1-CoV likely maintains deficits that impact pathogenesis in mice; therefore, WIV1-mediated infection may have diminished epidemic potential in humans relative to SARS-CoV.

A number of factors may contribute to reduced mouse pathogenesis observed following WIV1-CoV spike-mediated infection. In the context of both the SARS-CoV and MERS-CoV outbreaks, focus had been primarily directed to spike binding as the key component of emergence and pandemic potential. Supported by adaption at Y436H in mouse-adapted SARS spike (10), improved binding to host receptor cannot be discounted as a crucial component in emergence. This fact is supported by improved replication of WIV1-CoV in mice expressing human ACE2 compared with control (Fig. 2D versus Fig. 3B). However, in vivo attenuation of WIV1-CoV relative to SARS-CoV Urbani despite efficient infection in primary human airway cultures suggests that additional factors contribute to epidemic emergence. One possibility is that adaptation outside of spike protein may lead to emergence via altered host–virus interactions. Whereas WIV1-MA15 was attenuated relative to SARS-MA15 in vivo, overall titers in the lung were similar to the epidemic SARS-CoV Urbani in BALB/c mice (Figs. 3 and 4). These data suggest that CoV backbone changes may account for or compensate for deficits in WIV1-CoV replication compared with SARS-CoV Urbani in vivo. Another possible factor accounting for attenuation is changes to spike that are independent of receptor binding. Whereas the receptor binding domain had garnered the most interest, changes in the remaining portion of S1 as well as the S2 portion of spike may also play a critical role in facilitating CoV infection, transmission, and/or pathogenesis (20). Differences in these regions of spike may yield increased protease targeting, enhanced spike cleavage, and/or expanded tropism leading to more robust infection for the epidemic SARS strains. Globally, the in vivo results suggest that any of these areas may have contributed to SARS-CoV emergence. However, even these interpretations must be tempered due to the robust differences between mouse and human models; further studies in nonhuman primates are required to confirm these results and derive further insight into CoV emergence from zoonotic sources.

Despite the differences in the backbone genome sequences, therapeutics developed against SARS-CoV provide some measure of protection in the context of a future outbreak. Testing the four most broadly neutralizing SARS-CoV antibodies revealed effective control of WIV1-MA15 at relatively low concentrations of antibody (14, 15, 21). For two of the four antibodies tested (Fm6 and 230.15), WIV1-CoV spike-expressing virus was neutralized equivalently or better than SARS-CoV Urbani. Similarly, only minimal differences at the low end of the neutralization curve were noted for antibody 227.14. Whereas antibody 109.8 produced only marginal neutralization of WIV1-MA15, the overall antibody neutralization data argue that multivalent monoclonal antibody approaches could limit a WIV1-CoV spike-mediated outbreak. As such, a "ZMapp"-based approach could have great potential in stemming or preventing a future SARS-CoV–like outbreak.

In contrast to the success of monoclonal antibodies, vaccine failure indicated further development and refinement are necessary. The development of a DIV SARS-CoV vaccine was buoyed as a possible means to control SARS-CoV outbreaks based on robust neutralization and protection in young mice (18). However, studies with DIV in aged animals revealed incomplete protection, significant immune pathology, and eosinophilia (19). Despite these prior results, the efficacy of monoclonal antibody treatments made further testing of DIV seemingly worthwhile against WIV1-CoV spike-mediated infection. However, the results remained the same, as vaccination of aged mice resulted in no protection from WIV1-MA15 replication in vivo (Fig. 5). Importantly, increased immune pathology and observed eosinophilia indicate that broad-based vaccination efforts against SARS-CoV–like viruses must consider heterologous viruses as well as failure due to senescence in the aged host. A number of novel platforms including Venezuelan Equine Encephalitis Virus Replicon Particle (VRP) and live-attenuated vaccine approaches show great promise in these areas, but require further testing and development before deployment in an outbreak setting (22, 23).

Overall, the results from these studies highlight the utility of a platform that leverages metagenomics findings and reverse genetics to identify prepandemic threats. For SARS-like WIV1-CoV, the data can inform surveillance programs, improve diagnostic reagents, and facilitate effective treatments to mitigate future emergence events. However, building new and chimeric reagents must be carefully weighed against potential gain-of-function (GOF) concerns. Whereas not generally expected to increase pathogenicity, studies that build reagents based on viruses from animal sources cannot exclude the possibility of increased virulence or altered immunogenicity that promote escape from current countermeasures. As such, the potential of a threat, real or perceived, may cause similar exploratory studies to be limited out of an "abundance of caution." Importantly, the government pause on GOF studies may have already impacted the scope and direction of these studies. Whereas previous adaption of the epidemic SARS-CoV strain provided insights into species-specific changes, bat-derived WIV1 adaptation may identify elements critical for pathogenesis and transition from reservoir to human host; targets include viral proteins that interact with host machinery or host immunity like NSP1, envelope, or ORF6 (22, 24, 25). Similarly, WIV1-CoV could be used to drive improved therapeutics, including escape mutants for improved monoclonal antibodies or more broadly neutralizing vaccine approaches. However, it remains unclear from the current policies and GOF environment if these types of studies will be permissible. Although limits and standards for these types of experiments must be established, erring on the side of caution is not without its own risks and balancing the benefits of these types of studies must also be weighed against the potential hazards.

Using a novel platform to translate metagenomics findings, the WIV1-CoV cluster has been identified as a threat for future emergence in human populations due to robust replication in primary human airway epithelial cell cultures. However, based on in vivo mouse data, additional adaptations will likely be required to produce epidemic disease. Notably, whereas current antibody-based therapies hold great promise in treating WIV1-CoV spike-mediated infection, failure of SARS-CoV vaccination approaches presents a major challenge for any efforts to protect against future emergent viruses. Together, the data illustrate the utility of the platform and highlight the need to build and maintain preparations for future emergence events.

Materials and Methods

Viruses, Cells, and Infection. Wild-type and chimeric CoVs were cultured on Vero E6 cells, grown in DMEM (Gibco) and 5% fetal clone serum (HyClone) along with anti/anti (Gibco). Growth curves in Vero and primary human airway epithelial cells were performed as previously described (26, 27). Human lungs were procured under University of North Carolina at Chapel Hill (UNC) Institutional Review Board-approved protocols.

Construction of Chimeric SARS-Like Viruses. Both wild-type and chimeric WIV-CoV infectious clones were designed using published sequences and based on the SARS-CoV infectious clone (10). Synthetic construction of chimeric mutant and full-length WIV1-CoV were approved by the UNC Institutional Biosafety Committee and the Dual Use Research of Concern Committee.

Ethics Statement. The study was carried out in accordance with the recommendations for care and use of animals by the Office of Laboratory Animal Welfare (OLAW), National Institutes of Health. The Institutional Animal Care and Use Committee (IACUC) of University of North Carolina (UNC permit no. A-3410-01) approved the animal study protocol (IACUC no. 13–033).

Mice and in Vivo Infection. Female 10-wk- and 12-mo-old Balb/cAnNHsD mice ordered from the Harlan Labs were infected as previously described (23). For vaccination, young and aged mice were vaccinated and boosted by footpad injection with a 20-μL volume of either 0.2 μg of double-inactivated SARS-CoV vaccine (DIV) with alum or mock PBS as previously described (19).

Generation and Infection of ACE2 Tissue-Specific Transgenic Mice. Transgenic mice with airway-targeted overexpression of human *ACE2* were generated by microinjection of fertilized C3H × C57BL/6 (C3B6) F₁ hybrid oocytes with an expression cassette consisting of the HFH4/FOXJ1 lung ciliated epithelial cell-specific promoter elements and the coding region of *ACE2* cDNA in a pTG1 vector (11) (UNC Animal Model Core). Founder mice were crossed to C3B6, producing human ACE2-transgenic mice that were each previously tested for transgene expression as described in *SI Materials and Methods*. ACE2-transgenic mice given i.p. injection of 200 μg of human Ab S227.14 or PBS control (0.20 mL total volume, five to six mice per group) 1 d before infection as previously described (17).

Histological Analysis. Lung tissues for histological analysis were fixed in buffered formalin phosphate 10% (4–5% wt/wt formaldehyde) (Fisher #SF100-20) for at least 7 d, tissues were embedded in paraffin, and 5-μm sections were prepared by the UNC histopathology core facility as previous described (23). Images were captured using an Olympus BX41 microscope with an Olympus DP71 camera.

Virus Neutralization Assays. Plaque reduction neutralization titer assays were preformed with previously characterized antibodies against SARS-CoV as previously described (14, 15, 21). Briefly, neutralizing antibodies or serum were serially diluted twofold and incubated with 100 pfu of the different virus strains for 1 h at 37 °C. The virus and antibodies were then added to a six-well plate with 5×10^5 Vero E6 cells per well with $n \geq 2$. After a 1-h incubation at 37 °C, cells were overlaid with 3 mL of 0.8% agarose in media. Plates were incubated for 2 d at 37 °C and then stained with neutral red for 3 h, and plaques were counted. The percentage of plaque reduction was calculated as [1 − (no. of plaques with antibody/no. of plaques without antibody)] × 100.

Statistical Analysis. All experiments were conducted contrasting two experimental groups (either two viruses or vaccinated and unvaccinated cohorts). Therefore, significant differences in viral titer and histology scoring were determined by a two-tailed Student's *t* test at individual time points. Data were normally distributed in each group being compared and had similar variance.

1. Peiris JS, Guan Y, Yuen KY (2004) Severe acute respiratory syndrome. *Nat Med* 10(12, Suppl):S88–S97.
2. Al-Tawfiq JA, et al. (2014) Surveillance for emerging respiratory viruses. *Lancet Infect Dis* 14(10):992–1000.
3. Graham RL, Baric RS (2010) Recombination, reservoirs, and the modular spike: Mechanisms of coronavirus cross-species transmission. *J Virol* 84(7):3134–3146.
4. Graham RL, Donaldson EF, Baric RS (2013) A decade after SARS: Strategies for controlling emerging coronaviruses. *Nat Rev Microbiol* 11(12):836–848.
5. Ge XY, et al. (2013) Isolation and characterization of a bat SARS-like coronavirus that uses the ACE2 receptor. *Nature* 503(7477):535–538.
6. He B, et al. (2014) Identification of diverse alphacoronaviruses and genomic characterization of a novel severe acute respiratory syndrome-like coronavirus from bats in China. *J Virol* 88(12):7070–7082.
7. Yount B, et al. (2003) Reverse genetics with a full-length infectious cDNA of severe acute respiratory syndrome coronavirus. *Proc Natl Acad Sci USA* 100(22):12995–13000.
8. Frieman M, et al. (2012) Molecular determinants of severe acute respiratory syndrome coronavirus pathogenesis and virulence in young and aged mouse models of human disease. *J Virol* 86(2):884–897.
9. Gillim-Ross L, et al. (2004) Discovery of novel human and animal cells infected by the severe acute respiratory syndrome coronavirus by replication-specific multiplex reverse transcription-PCR. *J Clin Microbiol* 42(7):3196–3206.
10. Roberts A, et al. (2007) A mouse-adapted SARS-coronavirus causes disease and mortality in BALB/c mice. *PLoS Pathog* 3(1):e5.
11. Ostrowski LE, Hutchins JR, Zakel K, O'Neal WK (2003) Targeting expression of a transgene to the airway surface epithelium using a ciliated cell-specific promoter. *Mol Ther* 8(4):637–645.
12. Netland J, Meyerholz DK, Moore S, Cassell M, Perlman S (2008) Severe acute respiratory syndrome coronavirus infection causes neuronal death in the absence of encephalitis in mice transgenic for human ACE2. *J Virol* 82(15):7264–7275.
13. Qiu X, et al. (2014) Reversion of advanced Ebola virus disease in nonhuman primates with ZMapp. *Nature* 514(7520):47–53.
14. Sui J, et al. (2008) Broadening of neutralization activity to directly block a dominant antibody-driven SARS-coronavirus evolution pathway. *PLoS Pathog* 4(11):e1000197.
15. Rockx B, et al. (2010) Escape from human monoclonal antibody neutralization affects in vitro and in vivo fitness of severe acute respiratory syndrome coronavirus. *J Infect Dis* 201(6):946–955.
16. Traggiai E, et al. (2004) An efficient method to make human monoclonal antibodies from memory B cells: Potent neutralization of SARS coronavirus. *Nat Med* 10(8):871–875.
17. Zhu Z, et al. (2007) Potent cross-reactive neutralization of SARS coronavirus isolates by human monoclonal antibodies. *Proc Natl Acad Sci USA* 104(29):12123–12128.
18. Spruth M, et al. (2006) A double-inactivated whole virus candidate SARS coronavirus vaccine stimulates neutralising and protective antibody responses. *Vaccine* 24(5):652–661.
19. Bolles M, et al. (2011) A double-inactivated severe acute respiratory syndrome coronavirus vaccine provides incomplete protection in mice and induces increased eosinophilic proinflammatory pulmonary response upon challenge. *J Virol* 85(23):12201–12215.
20. McRoy WC, Baric RS (2008) Amino acid substitutions in the S2 subunit of mouse hepatitis virus variant V51 encode determinants of host range expansion. *J Virol* 82(3):1414–1424.
21. Sui J, et al. (2014) Effects of human anti-spike protein receptor binding domain antibodies on severe acute respiratory syndrome coronavirus neutralization escape and fitness. *J Virol* 88(23):13769–13780.
22. DeDiego ML, et al. (2014) Coronavirus virulence genes with main focus on SARS-CoV envelope gene. *Virus Res* 194:124–137.
23. Agnihothram S, et al. (2014) A mouse model for Betacoronavirus subgroup 2c using a bat coronavirus strain HKU5 variant. *MBio* 5(2):e00047–e14.
24. Narayanan K, Ramirez SI, Lokugamage KG, Makino S (2015) Coronavirus nonstructural protein 1: Common and distinct functions in the regulation of host and viral gene expression. *Virus Res* 202:89–100.
25. Bolles M, Donaldson E, Baric R (2011) SARS-CoV and emergent coronaviruses: Viral determinants of interspecies transmission. *Curr Opin Virol* 1(6):624–634.
26. Sheahan T, Rockx B, Donaldson E, Corti D, Baric R (2008) Pathways of cross-species transmission of synthetically reconstructed zoonotic severe acute respiratory syndrome coronavirus. *J Virol* 82(17):8721–8732.
27. Sims AC, et al. (2013) Release of severe acute respiratory syndrome coronavirus nuclear import block enhances host transcription in human lung cells. *J Virol* 87(7):3885–3902.

SEE COMMENTARY

MICROBIOLOGY

Fatal swine acute diarrhoea syndrome caused by an HKU2-related coronavirus of bat origin

Peng Zhou[1,11], Hang Pan[2,11], Tian Lan[3,11], Xing-Lou Yang[1], Wei-Feng Shi[4], Wei Zhang[1], Yan Zhu[1], Ya-Wei Zhang[2], Qing-Mei Xie[3], Shailendra Mani[5], Xiao-Shuang Zheng[1], Bei Li[1], Jin-Man Li[2], Hua Guo[1], Guang-Qian Pei[2], Xiao-Ping An[2], Jun-Wei Chen[3], Ling Zhou[3], Kai-Jie Mai[3], Zi-Xian Wu[3], Di Li[3], Danielle E. Anderson[5], Li-Biao Zhang[6], Shi-Yue Li[7], Zhi-Qiang Mi[2], Tong-Tong He[2], Feng Cong[8], Peng-Ju Guo[8], Ren Huang[8], Yun Luo[1], Xiang-Ling Liu[1], Jing Chen[1], Yong Huang[2], Qiang Sun[2], Xiang-Li-Lan Zhang[2], Yuan-Yuan Wang[2], Shao-Zhen Xing[2], Yan-Shan Chen[3], Yuan Sun[3], Juan Li[4], Peter Daszak[9]*, Lin-Fa Wang[5]*, Zheng-Li Shi[1]*, Yi-Gang Tong[2,10]* & Jing-Yun Ma[3]*

[1]CAS Key Laboratory of Special Pathogens and Biosafety, Wuhan Institute of Virology, Chinese Academy of Sciences, Wuhan, China.

[2]Beijing Institute of Microbiology and Epidemiology, Beijing, China.

[3]College of Animal Science, South China Agricultural University and Key Laboratory of Animal Health Aquaculture and Environmental Control, Guangdong, Guangzhou, China

[4]Shandong Universities Key Laboratory of Etiology and Epidemiology of Emerging Infectious Diseases, Taishan Medical College, Taian, China.

[5]Programme in Emerging Infectious Diseases, Duke-NUS Medical School, Singapore, Singapore.

[6]Guangdong Key Laboratory of Animal Conservation and Resource Utilization, Guangdong Public Laboratory of Wild Animal Conservation and Utilization, Guangdong Institute of Applied Biological Resources, Guangzhou, China.

[7]School of Public Health, Wuhan University, Wuhan, China.

[8]Guangdong Key Laboratory of Laboratory Animals, Guangdong Laboratory Animals Monitoring Institute, Guangzhou, China.

[9]EcoHealth Alliance, New York, NY, USA.

[10]School of Life Sciences, North China University of Science and Technology, Tangshan, China.

[11]These authors contributed equally: Peng Zhou, Hang Fan, Tian Lan.

*e-mail: daszak@ecohealthalliance.org; linfa.wang@duke-nus.edu.sg; zlshi@wh.iov.cn; tong.yigang@gmail.com; majy2400@scau.edu.cn

Cross-species transmission of viruses from wildlife animal reservoirs poses a marked threat to human and animal health[1]. Bats have been recognized as one of the most important reservoirs for emerging viruses and the transmission of a coronavirus that originated in bats to humans via intermediate hosts was responsible for the high-impact

emerging zoonosis, severe acute respiratory syndrome (SARS)[2-10]. Here we provide virological, epidemiological, evolutionary and experimental-infection evidence that a novel HKU2-related bat coronavirus, swine acute diarrhoea syndrome coronavirus (SADS-CoV), is the aetiological agent that is responsible for a large scale outbreak of fatal disease in pigs in China that has caused the death of 24,693 piglets across four farms. Notably, the outbreak began in Guangdong Province in the vicinity of the origin of the SARS pandemic. Furthermore, we identified SADS-related CoVs with 96–98% sequence identity in 11.9% (71 out of 596) of anal swabs collected from bats in Guangdong Province during 2013–16, predominantly in horseshoe bats (*Rhinolophus* spp.) that are known reservoirs of SARS-related CoVs. We found that there are striking similarities between the SADS and SARS outbreaks in geographical, temporal, ecological and aetiological settingsThis study highlights the importance of identifying coronavirus diversity and distribution in bats to mitigate future outbreaks that could threaten livestock, public health and economic growth.

The emergence of SARS in southern China in 2002, which was caused by a previously unknown coronavirus (SARS-CoV)[11-15] and has led to more than 8,000 human infections and 774 deaths (http://www.who.int/csr/sars/en/), highlights two new frontiers in emerging infectious diseases. First, it demonstrates that coronaviruses are capable of causing fatal diseases in humans. Second, the identification of bats as the reservoir for SARS-related coronaviruses, and the fact that SARS-CoV[3-10] probably originated in bats, firmly establishes that bats are an important source of highly lethal zoonotic viruses, such as Hendra, Nipah, Ebola and Marburg viruses[16].

Here we report on a series of fatal swine disease outbreaks in Guangdong Province, China, approximately 100 km from the location of the purported index case of SARS. Most strikingly, we found that the causative agent of this swine acute diarrhoea syndrome (SADS) is a novel HKU2-related coronavirus that is 98.48% identical in genome sequence to a bat coronavirus, which we detected in 2016 in bats in a cave in the vicinity of the index pig farm. This new virus (SADS-CoV) originated from the same genus of horseshoe bats (*Rhinolophus*) as SARS-CoV.

From 28 October 2016 onwards, a fatal swine disease outbreak was observed in a pig farm in Qingyuan, Guangdong Province, China, very close to the location of the first known index case of SARS in 2002, who lived in Foshan (Extended Data Fig. 1a). Porcine epidemic diarrhoea virus (PEDV, a coronavirus) had caused prior outbreaks at this farm, and was detected in the intestine of deceased piglets at the start of the outbreak. However, PEDV could no longer be detected in deceased piglets after 12 January 2017, despite accelerating mortality (Fig. 1a), and extensive testing for other common swine viruses yielded no results (Extended Data Table 1). These findings suggested that this was an outbreak of a novel disease. Clinical signs are similar to those caused by other known swine enteric coronaviruses[17,18] and include

severe and acute diarrhoea and acute vomiting, leading to death due to rapid weight loss in newborn piglets that are less than five days of age. Infected piglets died 2–6 days after disease onset, whereas infected sows suffered only mild diarrhoea and most sows recovered within two days. The disease caused no signs of febrile illness in piglets or sows. The mortality rate was as high as 90% in piglets that were five days or younger, whereas in piglets that were older than eight days, the mortality dropped to 5%. Subsequently, SADS-related outbreaks were found in three additional pig farms within 20–150 km of the index farm (Extended Data Fig. 1a) and, by 2 May 2017, the disease had caused the death of 24,693 piglets at these four farms (Fig. 1a). In farm A alone, 64% (4,659 out of 7,268) of all piglets that were born in February died. The outbreak has abated, and measures that were taken to control SADS included separation of sick sows and piglets from the rest of the herd. A qPCR test described below was used as the main diagnostic tool to confirm SADS-CoV infection.

A sample collected from the small intestine of a diseased piglet was analysed by metagenomics analysis using next-generation sequencing (NGS) to identify potential aetiological agents. Of the 15,256,565 total reads obtained, 4,225 matched sequences of the bat CoV HKU2, which was first detected in Chinese horseshoe bats in Hong Kong and Guangdong Province, China[19]. By de novo assembly and targeted PCR, we obtained a 27,173-bp CoV genome that shared 95% sequence identity to HKU2-CoV (GenBank accession number NC009988). Thirty-three full genome sequences of SADS-CoV were subsequently obtained (8 from farm A, 5 from farm B, 11 from farm C and 9 from farm D), and these were 99.9% identical to each other (Supplementary Table 1).

Using qPCR targeting the nucleocapsid gene (Supplementary Table 2), we detected SADS-CoV in acutely sick piglets and sows, but not in recovered or healthy pigs on the four farms, nor in nearby farms that showed no evidence of SADS. The virus replicated to higher titres in piglets than in sows (Fig. 1b). SADS-CoV displayed tissue tropism of the small intestine (Fig. 1c), as observed for other swine enteric coronaviruses[20]. Retrospective PCR analysis revealed that SADS-CoV was present on farm A during the PEDV epidemic, where the first strongly positive SADS-CoV sample was detected on 6 December 2016. From mid-January onwards, SADS-CoV was the dominant viral agent detected in diseased animals (Extended Data Fig. 1b). It is possible that the presence of PEDV early in the SADS-CoV outbreak may have somehow facilitated or enhanced spillover and amplification of SADS. However the fact that the vast majority of piglet mortality occurred after PEDV infection had become undetectable suggests that SADS-CoV itself causes a lethal infection in pigs that was responsible for these large-scale outbreaks, and that PEDV does not directly contribute to its severity in individual pigs. This was supported by the absence of PEDV and other known swine diarrhoea viruses during the peak and later phases of the SADS outbreaks in the four farms (Extended Data Table 1).

We rapidly developed an antibody assay based on the S1 domain of the spike (S) protein using a luciferase immunoprecipitation system[21]. Because SADS occurs acutely and has a rapid onset in piglets, serological investigation was conducted only in sows. Among 46 recovered sows tested, 12 were seropositive for SADS-CoV within three weeks of infection (Fig. 1d). To investigate possible zoonotic transmission, serum samples from 35 farm workers who had close contact with sick pigs were also analysed using the same luciferase immunoprecipitation system approach and none were positive for SADS-CoV.

Although the overall genome identity of SADS-CoV and HKU2-CoV is 95%, the S gene sequence identity is only 86%, suggesting that the previously reported HKU2-CoV is not the direct progenitor of SADS-CoV, but that they may have originated from a common ancestor. To test this hypothesis, we developed a SADS-CoV-specific qPCR assay based on its RNA-dependent RNA polymerase (*RdRp*) gene (Supplementary Table 2) and screened 596 bat anal swabs collected between 2013 and 2016 from seven different locations in Guangdong Province (Extended Data Fig. 1a). A total of 71 samples (11.9%) tested positive (Extended Data Table 2), the majority (94.3%) were from *Rhinolophus* spp. bats that are also the natural reservoir hosts of SARS-related coronaviruses[3–10]. Four complete genome sequences with the highest *RdRp* PCR-fragment sequence identity to that of SADS-CoV were determined by NGS. They are very similar in size (27.2 kb) compared to SADS-CoV (Fig. 2a) and we tentatively call them SADS-related coronaviruses (SADSr-CoV). Overall sequence identity between SADSr-CoV and SADS-CoV ranges from 96–98%. Most importantly, the S protein of SADS-CoV shared more than 98% sequence identity with sequences of two of the SADSr-CoVs (samples 162149 and 141388), compared to 86% with HKU2-CoV. The major sequence differences among the four SADSr-CoV genomes were found in the predicted coding regions of the *S* and *NS7a* and *NS7b* genes (Fig. 2a). In addition, the coding region of the S protein N-terminal (S1) domain was determined from 19 bat SADSr-CoVs to enable more detailed phylogenetic analysis.

The phylogeny of S1 and the full-length genome revealed a high genetic diversity of alphacoronaviruses among bats and strong coevolutionary relationships with their hosts (Fig. 2b and Extended Data Fig. 2), and showed that SADS-CoVs were more closely related to SADSr-CoVs from *Rhinolophus affinis* than from *Rhinolophus sinicus*, in which HKU2-CoV was foundBoth phylogenetic and haplotype network analyses demonstrated that the viruses from the four farms probably originated from their reservoir hosts independently (Extended Data Fig. 3), and that a few viruses might have undergone further genetic recombination (Extended Data Fig. 4). However, molecular clock analysis of the 33 SADS-CoV genome sequences failed to establish a positive association between sequence divergence and sampling date. Therefore, we speculate that either the virus was introduced into pigs from bats multiple times, or that the virus was introduced into pigs once, but subsequent genetic recombination disturbed the molecular clock.

For viral isolation, we tried to culture the virus in a variety of cell lines (see Methods for details) using intestinal tissue homogenates as starting material. Cytopathogeniceffects were observed in Vero cells only after five passages (Extended Data Fig. 5a, b). The identity of SADS-CoV was verified in Vero cells by immunofluorescence microscopy (Extended Data Fig. 5c, d) and by whole-genome sequencing (GenBank accession number MG557844). Similar results were obtained by other groups[22,23].

Known coronavirus host cell receptors include angiotensin-converting enzyme 2 (ACE2) for SARS-related CoV, aminopeptidase N (APN) for certain alphacoronaviruses, such as human (H)CoV-229E, and dipeptidyl peptidase 4 (DPP4) for Middle East respiratory syndrome (MERS)-CoV[24–26]. To investigate the receptor usage of SADS-CoV, we tested live or pseudotyped SADS-CoV infection on HeLa cells that expressed each of the three molecules. Whereas the positive control worked for SL-CoVand MERS-CoV pseudoviruses, we found no evidence of enhanced infection or entry for SADS-CoV, suggesting that none of these receptors functions as a receptor for virus entry for SADS-CoV (Extended Data Table 3).

To fulfill Koch's postulates for SADS-CoV, two different types of animal challenge experiments were conducted (see Methods for details). The first challenge experiment was conducted with specific pathogen-free piglets that were infected with a tissue homogenate of SADS-CoV-positive intestines. Two days after infection, 3 out of 7 animals died in the challenge group whereas 4 out of 5 survived in the control group. Incidentally, the one piglet that died in the control group was the only individual that did not receive colostrum due to a shortage in the supply. It is thus highly likely that lack of nursing and inability to access colostrum was responsible for the death (Extended Data Table 4). For the second challenge, healthy piglets were acquired from a farm in Guangdong that had been free of diarrheal disease for a number of weeks before the experiment, and were infected with the cultured isolate of SADS-CoV or tissue-culture medium as control. Of those inoculated with SADS-CoV, 50% (3 out of 6) died between 2 and 4 days after infection, whereas all control animals survived (Extended Data Table 5). All animals in the infected group suffered watery diarrhoea, rapid weight loss and intestinal lesions (determined after euthanasia upon experiment termination, Extended Data Tables 4, 5). Histopathological examination revealed marked villus atrophy in SADS-CoV inoculated farm piglets four days after inoculation but not in control piglets (Fig. 3a, b) and viral N protein-specific staining was observed mainly in small intestine epithelial cells of the inoculated piglets (Fig. 3c, d).

The current study highlights the value of proactive viral discovery in wildlife, and targeted surveillance in response to an emerging infectious disease event, as well as the disproportionate importance of bats as reservoirs of viruses that threaten veterinary and public health[1]. It also demonstrates that by using modern technological platforms, such as NGS, luciferase immunoprecipitation system serology and phylogenic analysis, key experiments that traditionally rely on the isolation of live virus can be performed rapidly before virus isolation.

<jrn>1. Olival, K. J. et al. Host and viral traits predict zoonotic spillover from mammals. *Nature* **546**, 646–650 (2017). </jrn>

<jrn>2. Guan, Y. et al. Isolation and characterization of viruses related to the SARS coronavirus from animals in southern China. *Science* **302**, 276–278 (2003). </jrn>

<jrn>3. Lau, S. K. et al. Severe acute respiratory syndrome coronavirus-like virus in Chinese horseshoe bats. *Proc. Natl Acad. Sci. USA* **102**, 14040–14045 (2005). </jrn>

<jrn>4. Li, W. et al. Bats are natural reservoirs of SARS-like coronaviruses. *Science* **310**, 676–679 (2005). </jrn>

<jrn>5. Ge, X. Y. et al. Isolation and characterization of a bat SARS-like coronavirus that uses the ACE2 receptor. *Nature* **503**, 535–538 (2013). </jrn>

<jrn>6. He, B. et al. Identification of diverse alphacoronaviruses and genomic characterization of a novel severe acute respiratory syndrome-like coronavirus from bats in China. *J. Virol.* **88**, 7070–7082 (2014). </jrn>

<jrn>7. Yang, X. L. et al. Isolation and characterization of a novel bat coronavirus closely related to the direct progenitor of severe acute respiratory syndrome coronavirus. *J. Virol.* **90**, 3253–3256 (2016). </jrn>

<jrn>8. Wu, Z. et al. ORF8-related genetic evidence for Chinese horseshoe bats as the source of human severe acute respiratory syndrome coronavirus. *J. Infect. Dis.* **213**, 579–583 (2016). </jrn>

<jrn>9. Wang, L. et al. Discovery and genetic analysis of novel coronaviruses in least horseshoe bats in southwestern China. *Emerg. Microbes Infect.* **6**, e14 (2017). </jrn>

<jrn>10. Hu, B. et al. Discovery of a rich gene pool of bat SARS-related coronaviruses provides new insights into the origin of SARS coronavirus. *PLoS Pathog.* **13**, e1006698 (2017). </jrn>

<jrn>11. Drosten, C. et al. Identification of a novel coronavirus in patients with severe acute respiratory syndrome. *N. Engl. J. Med.* **348**, 1967–1976 (2003). </jrn>

<jrn>12. Ksiazek, T. G. et al. A novel coronavirus associated with severe acute respiratory syndrome. *N. Engl. J. Med.* **348**, 1953–1966 (2003). </jrn>

<jrn>13. Marra, M. A. et al. The genome sequence of the SARS-associated coronavirus. *Science* **300**, 1399–1404 (2003). </jrn>

<jrn>14. Peiris, J. S. et al. Coronavirus as a possible cause of severe acute respiratory syndrome. *Lancet* **361**, 1319–1325 (2003). </jrn>

<jrn>15. Rota, P. A. et al. Characterization of a novel coronavirus associated with severe acute respiratory syndrome. *Science* **300**, 1394–1399 (2003). </jrn>

<bok>16. Wang, L.-F. & Cowled, C. (eds) *Bats and Viruses: A New Frontier of Emerging Infectious Diseases* 1st edn (John Wiley & Sons, New Jersey, 2015).</bok>

<jrn>17. Dong, N. et al. Porcine deltacoronavirus in mainland China. *Emerg. Infect. Dis.* **21**, 2254–2255 (2015). </jrn>

<jrn>18. Sun, D., Wang, X., Wei, S., Chen, J. & Feng, L. Epidemiology and vaccine of porcine epidemic diarrhea virus in China: a mini-review. *J. Vet. Med. Sci.* **78**, 355–363 (2016). </jrn>

<jrn>19. Lau, S. K. et al. Complete genome sequence of bat coronavirus HKU2 from Chinese horseshoe bats revealed a much smaller spike gene with a different evolutionary lineage from the rest of the genome. *Virology* **367**, 428–439 (2007). </jrn>

<jrn>20. Chen, J. et al. Molecular epidemiology of porcine epidemic diarrhea virus in China. *Arch. Virol.* **155**, 1471–1476 (2010). </jrn>

<jrn>21. Burbelo, P. D. et al. Serological diagnosis of human herpes simplex virus type 1 and 2 infections by luciferase immunoprecipitation system assay. *Clin. Vaccine Immunol.* **16**, 366–371 (2009). </jrn>

<jrn>22. Gong, L. et al. A new bat-HKU2-like coronavirus in swine, China, 2017. *Emerg. Infect. Dis.* **23**, 1607–1609 (2017). </jrn>

<jrn>23. Pan, Y. et al. Discovery of a novel swine enteric alphacoronavirus (SeACoV) in southern China. *Vet. Microbiol.* **211**, 15–21 (2017). </jrn>

<jrn>24. Li, W. et al. Angiotensin-converting enzyme 2 is a functional receptor for the SARS coronavirus. *Nature* **426**, 450–454 (2003). </jrn>

<edb>25. Masters, P. S. & Perlman, S. in *Fields Virology* Vol. 2 (eds Knipe, D. M. & Howley, P. M.) 825–858 (Lippincott Williams & Wilkins, 2013).</edb>

<jrn>26. Raj, V. S. et al. Dipeptidyl peptidase 4 is a functional receptor for the emerging human coronavirus-EMC. *Nature* **495**, 251–254 (2013). </jrn>